·

DYNAMICAL PROPERTIES OF HADRONIC MATTER EXCITED IN RELATIVISTIC NUCLEAR COLLISIONS

Ina Sarcevic

Department of Physics, University of Arizona

Prepared for

THE U.S. DEPARTMENT OF ENERGY
AGREEMENT NO. DE-FG03-93ER40792

The main focus of the research supported by the nuclear theory grant DE-FG03-93ER40792 has been on studying parton dynamics in high-energy nuclear collisions, of relevance to the possible formation of quark-gluon plasma, such as the nuclear shadowing effect, the energy loss of the parton in a dense medium and its detection, the formation and detection of the disoriented chiral condensate and dilepton production from heavy quark decays at RHIC.

In addition to Professor Sarcevic, the grant currently also supports a Senior Research Scientist, Dr. Sean Gavin. Dr. Gavin was an Associate Scientist at Brookhaven from 1991 to 1996 and Visiting Scientist at Columbia University in 1996/1997. Dr. Zheng Huang, who was a Postdoctoral Fellow in our group from 1995 to 1997, has received a postdoctoral offer from RIKEN/BNL for 1997-1999, but has decided to take up a permanent position at the BNP/Cooper Neff, Inc. in Randor, Pensylvania instead. Graduate student, Peter Valerio, who has been partially supported by this grant from 1993 to 1996 has successfully completed his Ph.D. Thesis in November 1996 and is currently teaching at Kantner School in North Carolina.

In this document we summarize progress made on this project during two-year grant period, and we outline proposed activities of the theoretical nuclear physics group at the University of Arizona, under Grant DE-FG03-93ER40792. Some of these projects have been completed; others are in progress. First we simply list the research topics, then we provide a discussion of each.

RESEARCH TOPICS

1. Dilepton Production from Heavy Quark Decays at RHIC, *Ina Sarcevic, Zheng Huang, David Fein and Peter Valerio*
2. Partonic Picture of Nuclear Shadowing at Small x, *Ina Sarcevic, Zheng Huang and Hung Jung Lu*
3. Jet Quenching in High-Energy Heavy-Ion Collisions, *Ina Sarcevic, Zheng Huang and Xin-Nian Wang*
4. Testing for QCD Energy Loss at High x_F, *Sean Gavin and Miklos Gyulassy*
5. Disoriented Chiral Condensate, *Sean Gavin and Ina Sarcevic*
6. Wavelet analysis of Disoriented Chiral Condensate in Heavy-Ion Collisions, *Ina Sarcevic, Zheng Huang, Xin-Nian Wang and Robert Thews*
7. Event Structure of Disoriented Chiral Condensates at RHIC, *Sean Gavin*
8. Hanbury-Brown Twiss Correlations from Disoriented Chiral Condensate, *Sean Gavin and Ina Sarcevic*
9. Dynamics of Chiral Condensate Formation, *Sean Gavin*
10. Dilepton and Photon Production from a Coherent Pion Oscillations, *Zheng Huang and Xin-Nian Wang*
11. Charmonium Suppression, *Sean Gavin and Ina Sarcevic*
12. Interpreting CERN and RHIC J/ψ Suppression Experiments, *Sean Gavin and Ina Sarcevic*
13. Perturbative Contribution to Comover Scattering at RHIC and LHC, *Sean Gavin and Ina Sarcevic*
14. Correlated Antiproton and Deuteron Measurements, *Sean Gavin, S.V. Greene and T. Miller*
15. Superevents at RHIC, *Sean Gavin, S.V. Greene and T. Miller*
16. Collins-Soper-Sterman Approach to the Drell Yan p_T Distribution in Nuclear Collisions, *Sean Gavin, P.V. Ruuskanen, D.K. Srivastava and R.L. Thews*
17. PHENIX Experiment at RHIC, *Sean Gavin*

INA SARCEVIC

Publications (1995-1997)

1. "Charm Production in Hadronic and Heavy-Ion Collisions at RHIC and LHC Energies to $O(\alpha_s^3)$" (with P. Valerio), *Phys. Rev.* **C51**, 1433 (1995).

2. "Charm Production at RHIC and LHC to $O(\alpha_s^3)$", *Nucl. Phys.* **A590** (1995) 499.

3. "Towards a Field Theoretical Description of Multiparticle Production in High-Energy Collisions", in Proceedings of the *NATO Workshop on Hot Hadronic Matter*, eds. H.H. Gutbrod, J. Letessier and J. Rafelski (Plenum Pub. Co., New York, 1995) p. 283.

4. "Charm Production at RHIC and LHC to $O(\alpha_s^3)$", in Proceedings of the *Annual Meeting of the American Physical Society, Division of Particles and Fields*, (DPF '94), ed. S. Seidel (World Scientific, Singapore, 1995) p. 1243.

5. "Ultrahigh-Energy Neutrino Interactions", (with R. Gandhi, C. Quigg, and M.H. Reno), *Astropart. Phys.* **5**, 81 (1996).

6. "Small-x Parton Densities from HERA and the Ultrahigh Energy Neutrino-Nucleon Cross Sections" (with R. Gandhi, C. Quigg and M. H. Reno), in *Frontiers in Strong Interactions*, eds. P. Chiappetta, M. Haguenauer and J. Tran Thanh Van (Editions Frontiers, 1996), p. 215.

7. "Ultrahigh Energy Neutrino-Nucleon Cross Sections" (with R. Gandhi, C. Quigg and M. H. Reno), in Proceedings of the *IVth International Workshop on Theoretical and Phenomenological Aspects of Underground Physics (TAUP '95)*, Toledo, Spain, September 17-23, 1995.

8. "Domain Structure of a Disoriented Chiral Condensate from a Wavelet Prospective" (with Z. Huang, R. Thews and X. N. Wang), *Phys. Rev.* **D54**, 750 (1996).

9. "New Predictions for Neutrino Telescope Event Rates" (with R. Gandhi, C. Quigg and M.H. Reno), *Nucl. Phys.* **B78**, 475 (1996).

10. "Jet Quenching in the Opposite Direction of a Tagged Photon in High-Energy Heavy-Ion Collisions", (with X. N. Wang and Z. Huang), *Phys. Rev. Lett.* **77**, 23 (1996).

11. "Detecting Neutrinos from AGNS and Topological Defects with Neutrino Telescope" (with R. Gandhi, C. Quigg and M.H. Reno), AZPH-TH-96/25, to appear in the Proceedings of the *1996 Annual Meeting of the American Physical Society, Division of Particles and Fields* (DPF'96), Minneapolis, MN, 10-15 Aug. 1996.

12. “Wavelet Perspective of a Disoriented Chiral Condensate”, (with Z. Huang, R. Thews and X. N. Wang), AZPH-TH-96-27, to appear in the Proceedings of the *1996 Annual Meeting of the American Physical Society, Division of Particles and Fields* (DPF’96), Minneapolis, MN, 10-15 Aug. 1996.

13. “Wavelet View of a Disoriented Chiral Condensate”, (with Z. Huang, R. Thews and X. N. Wang), AZPH-TH-96-20, to appear in the Proceedings of the *14th International Conference on Particles and Nuclei* (PANIC 96), Williamsburg, VA, 22-28 May 1996.

14. “Wavelet Analysis of a Disoriented Chiral Condensate”, (with Z. Huang, R. Thews and X. N. Wang), in Proceedings of the *VIIth International Workshop on Multiparticle Production, Correlations and Fluctuations*, eds. R.C. Hwa, W. Kittel, W.J. Metzger and D.J. Schotanus (World Scientific, 1997), p. 145.

15. “Ultrahigh-Energy Neutrino Interactions and Neutrino Telescope Event Rates”, (with R. Gandhi, C. Quigg and M.H. Reno), in Proceedings of the *International Conference on Orbis Scientiae 1996: Neutrino Mass , Dark Matter, Gravitational Waves, Condensation of Atoms and Monopoles, Light-Cone Quantization*, eds. B. N. Kursunoglu, S. L. Mintz and A. Perlmutter (Plenum Pub.Co., New York, 1996) p. 115.

16. “What is the Brightest Source for Dilepton Emissions at RHIC?” (with D. Fein, Z. Huang and P. Valerio), *Phys. Rev.* **C56** 1637 (1997).

17. “On the Nature of the EGRET Source at the Galactic Center”, (with S. Markoff and F. Melia), *Astrophys. J. (Letters)* **47** 489 (1997).

18. “Partonic Picture of Nuclear Shadowing at Small X”, (with Z. Huang and H.J. Lu), hep-ph/9705250, submitted to *Nucl. Phys.* **A**.

19. “Secondary Decays in Atmospheric Charm Contributions to the Flux of Muon Neutrinos”, hep-ph/9710363 (with L. Pasquali and M. H. Reno), submitted to *Phys. Rev.* **D**.

20. “Physics at RHIC; the Search for the Quark Gluon Plasma”, to appear in the Proceedings of the *XXVII International Symposium on Multiparticle Dynamics* (Nucl. Phys. B, Proc. Suppl.), 1998.

21. “Ultrahigh Energy Neutrino Interactions”, to appear in the Proceedings of the *Workshop on Observing Giant Cosmic Ray Airshowers for $E > 10^{20} eV$ Particles from Space* (AIP, 1998).

22. “Muon and Muon Neutrino Fluxes from Atmospheric Charm”, (with L. Pasquali and M. H. Reno), hep-ph/9711457, to appear in the Proceedings of the *5th International Workshop on Topics in Astroparticle and Underground Physics (TAUP 97)*, Gran Sasso, Italy, 7-11 Sep 1997.

23. "Partonic Picture of Nuclear Shadowing at Small x", to appear in the Proceedings of the *Quark Matter '97* (Nucl. Phys. A, Proc. Suppl.), 1998.

EDITED VOLUMES

1. Proceedings of the Workshop on the *State of Physics at the End of the 20th Century*, eds. F. Cooper, I. Sarcevic and G. West (World Scientific, Singapore), to be published.

INVITED TALKS (1995-1997)

1. "Charm Production at RHIC and LHC to $O(\alpha_s^3)$", presented at *Quark Matter '95*, Monterey, California, January 9-13, 1995.

2. "The Ultrahigh Energy Neutrino Interactions", Physics Department, UCLA, Los Angeles, May 1995.

3. "Ultrahigh Energy Neutrino Interactions: How to Search for AGN Neutrinos", Theoretical Division, T-8, Los Alamos National Laboratory, Los Alamos, June 1995.

4. "Small-x Parton Densities from HERA and the Ultrahigh Energy Neutrino-Nucleon Cross Sections", presented at the *VIth International Workshop on Elastic and Diffractive Scatterings, Frontiers in Strong Interactions*, Recontres de Blois, Chateaue de Blois, France, June 1995.

5. "Open Charm Production in Hadronic and Heavy Ion Collisions at RHIC and LHC Energies to $O(\alpha_s^3)$", Nuclear and Particles Colloquium, Los Alamos National Laboratory, Los Alamos, June 1995.

6. "The Ultrahigh Energy Neutrino Interactions: Implications for AGN Neutrino Searches", Astronomy Department, UCLA, Los Angelos, June 1995.

7. "Ultrahigh Energy Neutrino Interactions", LPTHE Universite Paris XI, Orsay, France, June 1995.

8. "Small-x Parton Densities from HERA and the Ultrahigh Energy Neutrino-Nucleon Cross Sections", presented at the *IVth International Workshop on Theoretical and Phenomenological Aspect of Underground Physics (TAUP '95)*, Toledo, Spain, September 1995.

9. "Ultrahigh Energy Neutrinos from Active Galactic Nuclei," presented at *XXIV Coral Gables Conference on Elementary Particle Physics and Cosmology*, Coral Gables, Florida, January 1996.

10. "Ultrahigh Energy Neutrino Interactions", presented at the Aspen Winter Conference on Particle Physics, Aspen, Colorado, January 1996.

11. "New Predictions for Neutrino Telescope Event Rates", presented at the Aspen Workshop on *Neutrino Astrophysics*, Aspen, Colorado, May 1996.

12. "On Detection of Neutrinos from AGNs and Topological Defects Formed in the Early Universe", Colloquium, Aspen Center for Physics, Aspen, Colorado, June 1996.

13. "Detecting Neutrinos from AGNS and Topological Defects with Neutrino Telescope", presented at the *1996 Annual Meeting of the American Physical Society, Division of Particles and Fields* (DPF'96), Minneapolis, MN, 10-15 Aug. 1996.

14. "Wavelet Perspective of a Disoriented Chiral Condensate", presented at the *1996 Annual Meeting of the American Physical Society, Division of Particles and Fields* (DPF'96), Minneapolis, MN, 10-15 Aug. 1996.

15. "Wavelet Analysis of a Disoriented Chiral Condensate", presented at the *VIIth Workshop on Multiparticle Production, Correlations and Fluctuations*, Nijmegen, Netherlands, July 1-7, 1996.

16. "Prospects of Physics at RHIC: the Search for the Quark-Gluon Plasma", University of Arizona, January 1997.

17. "Heavy-Ion Physics at RHIC", review talk, presented at the Aspen Winter Conference on Particle Physics, *Particle Physics Enters its Second Century*, January 19-25, 1997.

18. "Prospects of Physics at RHIC: the Search for the Quark-Gluon Plasma", CEBAF, Newport News, January 1997.

19. "Neutrinos from Topological Defects Formed in the Early Universe", presented at the *Celebration of 25 Coral Gables Conferences and Their Impact on High Energy Physics and Cosmology Since 1964*, Miami Beach, Florida, January 23-26, 1997.

20. "Detection of Ultrahigh Energy Neutrinos from AGNs and from Topological Defects Formed in the Early Universe", Colloquium, College of William and Mary, Williamsburg, February 1997.

21. "Prospects for the Detection of Extragalactic Neutrinos", Department of Physics and Astronomy and Bartol Institute, University of Delaware, May 1997.

22. "QCD Physics at RHIC", presented at the Aspen Workshop on *Lattice, Perturbative QCD and Heavy Quarks*, Aspen Center for Physics, Aspen, Colorado, July 1997.

23. "Search for the Quark Gluon Plasma", review talk, presented at the *XXVII International Workshop on Multiparticle Dynamics*, September 8-12, 1997, Frascati, Italy.

24. "Prospects of Physics at RHIC: the Search for the Quark Gluon Plasma", seminar, LPTHE Universite Paris XI, Orsay, France, September 1997.

25. "Particle Astrophysics with High Energy Neutrinos", Colloquium, Auburn University, Alabama, October 1997.

26. "Ultrahigh Energy Neutrino Interactions", review talk, presented at the Workshop on *Observing Giant Cosmic Ray Airshowers for* $E > 10^{20}\,eV$ *Particles from Space*, College Park, Maryland, November 1997.

27. "Partonic Picture of Nuclear Shadowing at Small x", *Quark Matter '97*, Tsukuba, Japan, December 1997.

Invited talks in Sring 1998: LBL, Berkeley; University of Delaware (colloquium); IVth Workshop on QCD (review talk), Paris (June 1998); Nonlinear Phenomena in Complex Systems (review talk), Minsk, Belarus (April 1998); Correlations and Fluctuations '98, Matrahaza, Hungary (June 1998); Erice Summer School (July 1998).

CONFERENCES AND WORKSHOPS ORGANIZED 1995-1997

1. "Frontiers in Particle Physics", Aspen Winter Conference on Particle Physics, January 25-31, 1998 (organizers: I. Sarcevic and W. C. Louis).

2. "Interface of Soft and Hard Processes in QCD", Aspen Center for Physics, June 2-23, 1996 (organizers: I. Sarcevic, L. Durand and Chung-I Tan).

3. "The State of Physics at the End of the 20th Century", Santa Fe, NM, October 23-26, 1996 (organizers: F. Cooper, I. Sarcevic and G. West).

Sean Gavin

Publications (1995-1997)

1. "Transverse Momentum of ψ and Drell-Yan Dimuon Production in Pb+Pb Collisions," (with R. Vogt) CU-TP-791, hep-ph/9609470.

2. "ψ and ψ' Suppression by Comovers in Nuclear Collisions," in Proc. RHIC Summer Studies '96, Upton, USA, D. Kahana et al. eds. (1996), hep-ph/9609470.

3. "Discovering Disoriented Chiral Condensates at RHIC," in Proc. RHIC Summer Studies '96, Upton, USA, D. Kahana et al. eds. (1996).

4. "Charmonium Suppression by Comovers in Pb+Pb Collisions," (with R. Vogt) Phys. Rev. Lett. **78**, 1006 (1997).

5. "Dilepton Production from Charm Decay in Nuclear Collisions at 200 AGeV and 5.5 ATeV," (with P. L. McGaughey, P. V. Ruuskanen and R. Vogt) Phys. Rev. **C54**, 2606 (1996).

6. "ψ Suppression from Comovers in Pb+Pb," (with R. Vogt) Nucl. Phys. **A610**, 442c (1996).

7. "Summary of Heavy Ion Theory," in Proc. of the Four Seas Conference: Physics Without Frontiers, G. Charpak, ed., in press (1996).

8. "Disoriented Chiral Condensates," Nucl. Phys. **A590**, 163c (1995).

9. "Production of Drell-Yan Pairs in High Energy Nucleon-Nucleon Collisions," (with R. Kauffman, P.V. Ruuskanen, D.K. Srivastava, and R.L. Thews) Int. J. Mod. Phys. **A10**, 2961 (1995).

10. "Summary of Heavy Ion Theory," in Proc. 8th Meeting of the Division of Particles and Fields of the American Physical Society, Albuquerque, NM, S. Seidel ed., (World Scientific, Singapore, 1995) 1353.

11. "Dynamics of the Chiral Transition," in Proc. 5th Conf. on the Intersections Between Particle and Nuclear Physics, St. Petersburg, May 31 – June 6, 1994, S. Seestrom, ed., AIP Conf. Proc. **338** 928 (1995).

12. "Dynamics of Chiral Symmetry Breaking in Nuclear Collisions," in Proc. 3rd Int'l. Workshop on Relativistic Aspects of Nuclear Physics, 24-27 August 1993, Rio de Janeiro, Brazil, eds. K. C. Chung, Y. Hama and T. Kodama, (World Scientific, 1995) 203.

Edited Volumes

1. S. Gavin and M. Strikman, eds., "Nuclei At HERA and Heavy Ion Physics," Proc. Workshop at Brookhaven National Laboratory, 17-18 November 1995, BNL-62634.

Invited Talks (1995-1997)

1. "Charmonium Suppression," Gordon Research Conference on QCD in Nuclear Physics, Newport, RI, Jul. 1997

2. "J/ψ Suppression – Plasma or What?" RHIC Summer Study '97, Brookhaven National Laboratory, Upton, NY, Jul. 1997.

3. "Comover Model of J/ψ Suppression," *Hirschegg '97*, 25th Int. Workshop on Gross Properties of Nuclei and Nuclear Excitation: QCD Phase Transitions, Hirschegg, Austria, 13-18 Jan. 1997.

4. "Parton Scattering in Nuclear Collisions," and "J/psi Suppression from Comovers," INT Workshop on Strong Interactions at High Temperature, Seattle, WA, Dec. 1996.

5. "Disoriented Chiral Condensates: Your Eye On the Chiral Transition at RHIC," American Physical Society 1996 Meeting of the Division of Nuclear Physics, Boston, MA. Workshop on Relativistic Heavy Ion Collisions, Oct. 1996.

6. "Summary of RHIC Summer Study '96." STAR Collaboration meeting, Brookhaven National Laboratory, Upton, NY, Aug. 1996.

7. "J/ψ Suppression," and "Discovering Disoriented Chiral Condensates." RHIC Summer Study '96, Upton, NY, Jul. 1996.

8. "J/ψ Suppression from SPS to RHIC," Collaboration Meeting of the PHENIX Experiment at RHIC, Santa Fe, NM, July 1996.

9. "J/ψ Suppression from Comovers in Pb+Pb," *Quark Matter '96*, 12^{th} International Conference on Ultrarelativistic Nucleus-Nucleus Collisions, Heidelberg, Germany, May 1996.

10. "J/ψ Suppression in Pb+Pb Collisions," AGS Users Group Meeting, Brookhaven National Laboratory, NY, May 1996.

11. "Parton Scattering in Nuclear Collisions," NA44 Collaboration Meeting, Nevis Laboratories, Irvington, NY, Apr. 1996.

12. "Nuclear Effects in the Drell Yan Process," 2^{nd} INT/RHIC Workshop, Electromagnetic Probes of Quark Gluon Plasma, Seattle, WA, Jan. 1996.

13. "Discovering DCC's with PHENIX," Collaboration Meeting of the PHENIX Experiment at RHIC, Upton, NY, Jan. 1996.

14. "Summary Talk: HERA Tomorrow," Nuclei at HERA and Heavy Ion Physics, Upton, NY, Nov. 1995.

15. "Physics from Heavy Ion Collisions," LP'95: 17^{th} International Symposium on Lepton-Photon Interactions, Beijing, China, Aug. 1995.

16. "Summary of Heavy Ion Theory," The Four Seas Conference: Physics Without Frontiers, Trieste, Italy, Jul. 1995.

17. "Energy Loss in Hard Processes," Workshop on QCD and Relativistic Heavy Ion Collisions, European Center for Theoretical Nuclear Physics (ECT*), Trento, Italy, Jun. 1995.

18. "Progress of the Drell Yan Group," Workshop on Hard Probes of Relativistic Heavy Ion Collisions, ECT*, Trento, Italy, May 1995.
19. "Discovering Disoriented Chiral Condensates," Collaboration Meeting of the STAR Experiment at RHIC, Monterey, CA, Jan. 1995.
20. "Disoriented Chiral Condensates," *Quark Matter '95*, 11^{th} International Conference on Ultrarelativistic Nucleus-Nucleus Collisions, Monterey, CA, Jan. 1995.

Honors and Affiliations 1995-1997

1. McMinn Distinguished Lecturer, Vanderbilt University, Spring 1997.
2. Elected, Executive Committee, New York State Section of the American Physical Society, Fall 1995; Reelected Fall 1997.

Conferences and Workshops Organized 1995-1997

1. Theory session at PHENIX Collaboration Meeting, Tsukuba, Japan, Dec. 1997.
2. Fall Symposium on Space Science (with Executive Committee), New York State Section of the American Physical Society, Ithaca, NY, Oct. 1997.
3. Spring Symposium on Computers in Science and Education (with Executive Committee), New York State Section of the American Physical Society, Yorktown Heights, NY, Apr. 1997.
4. Theory session at PHENIX Collaboration Meeting, Costa Mesa, CA, Mar. 1997.
5. Fall Symposium on the Physics of Medical Imaging (with Executive Committee), New York State Section of the American Physical Society, Schenectady, NY, Oct. 1996.
6. Theory Session at PHENIX Collaboration Meeting of the PHENIX, Santa Fe, NM Jul. 1996.
7. Fall Symposium on Space Science (with Executive Committee), New York State Section of the American Physical Society, Oct. 1996.
8. Workshop on Nuclei At HERA and Heavy Ion Physics (with Mark Strikman), Brookhaven National Laboratory, 17-18 Nov. 1995.
9. Workshop on Hard Probes of Relativistic Heavy Ion Collisions, (with H. Satz and X.-N. Wang), ECT*, Trento, Italy, Mar. 1995.

Colloquia and Seminars (1995-1997)

1. Seminar, University of Connecticut, Storrs, CT, Apr. 1997.
2. Seminar, Wayne State University, Detroit, MI, Nov. 1997
3. Colloquium, University of Michigan, Ann Arbor, MI, Nov. 1996.
4. Seminar, University of Texas, Austin, TX, Nov. 1996.
5. Seminar, Columbia University, New York, NY, Nov. 1996.
6. Seminar, Lawrence Berkeley National Laboratory, Berkeley, CA, June 1996.
7. Seminars (2), Los Alamos National Laboratory, May 1996.
8. Seminar, Ohio State University, Columbus, OH, Mar. 1996.
9. Seminars (2), Lawrence Berkeley National Laboratory, Berkeley, CA, Nov. 1995.
10. Seminar, Columbia University, New York, NY, Nov. 1995.
11. Seminar, Nevis Laboratories, Irvington, NY, Mar. 1995.
12. Seminar, SUNY Stony Brook, Stony Brook, NY, Mar. 1995.
13. Colloquium, Brookhaven National Laboratory, Feb. 1995

Zheng Huang

Publications (1995-1997)

1. X.-N. Wang and **Z. Huang**, *Study Medium-induced Parton Energy Loss in Gamma+jet Events of High-Energy Heavy-Ion Collisions*, submitted to Physical Review C, hep-ph/9701227
2. D. Fein, **Z. Huang**, P. Valerio and I. Sarcevic, *What is the Brightest Source for Dilepton Emissions at RHIC?*, submitted to Nucl. Phys. A, hep-ph/9607264 (1996)
3. **Z. Huang** and X.-N. Wang, *Dilepton and Photon Production from a Coherent Pion Oscillation*, Physics Letters **B383**, 457 (1996)
4. X.-N. Wang, **Z. Huang** and I. Sarcevic, *Jet Quenching in the Opposite Direction of a Tagged Photon in High-Energy Heavy-Ion Collisions*, Physical Review Letters **77**, 231 (1996).
5. **Z. Huang**, *Wavelet View of Disoriented Chiral Condensate*, Proceedings of 14th International Conference on Particles and Nuclei (PANIC 96)

6. T. Han, **Z. Huang** and P.Q. Hung, *A Model of Low-lying States in Strongly Interacting Electroweak Symmetry Breaking Sector*, Modern Physics Letters **A11**, 1131 (1996)

7. L.-Z. Fang, **Z. Huang** and X.-P. Wu, *Phase Randomization and Doppler Peaks in the CMB Angular Power Spectrum*, International Journal of Modern Physics **D5**, 495 (1996)

8. **Z. Huang**, I. Sarcevic, R. Thews and X.-N. Wang, *Domain Structure of Disoriented Chiral Condensate from a Wavelet Perspective*, Physical Review **D54**, 750 (1996).

9. **Z. Huang** and X.-N. Wang, *Partial $U(1)_A$ Restoration and η Enhancement in High Energy Collisions*, Physical Review **D53**, 5034 (1996).

10. **Z. Huang** and M. Suzuki, *General Classical Solutions of Nonlinear σ Model and Pion Charge Distribution of Disoriented Chiral Condensate*, Physical Review **D53**, 891 (1996).

11. **Z. Huang**, *Thermal Dilepton Production in Heavy-Ion Collisions*, Physics Letters **B361**, 131 (1995).

12. **Z. Huang** and M. Suzuki, *Isospin Coherence and Final-State Quantum Scattering of Disoriented Chiral Condensate*, Physical Review **D52**, 2610 (1995)

13. **Z. Huang**, *Disoriented Chiral Condensate*, in Proceedings of 4th International Conference on Physics Beyond the Standard Model, eds. J. Gunion, T. Han and J. Ohnemus (World Scientific, Singapore, 1995), p.422.

14. M. Asakawa, **Z. Huang** and X.-N. Wang, *How Disoriented Chiral Condensates Form: Quenching vs. Annealing*, Physical Review Letters **74**, (1995) 3126-3129.

PROJECT DESCRIPTIONS

Dilepton Production from Heavy Quark Decays at RHIC

(I. Sarcevic, Z. Huang, D. Fein and P. Valerio)

Dilepton emission in high energy heavy-ion collisions provides an excellent probe of the property of dense hadronic matter such as the quark-gluon plasma and the hot hadronic gas. Due to the small cross sections of electromagnetic interactions, these dileptons once produced can escape the strong interacting volume of sizes which might be produced in heavy-ion collisions. The dilepton invariant mass spectrum holds the most promising signatures of the quark-gluon plasma such as thermal dileptons [1] and the J/ψ suppression [2]. However, the use of the dilepton probe is difficult for an obvious reason: it is sensitive to many different sources. In the low mass region, the resonance decays from the light hadrons constitute the main background. In the intermediate and high mass regions, the Drell-Yan dilepton production from the initial hard scattering is important. In high energy heavy-ion colliders such as RHIC and LHC, the heavy flavor quark production can be quite substantial and its subsequent decay can lead to a large combinatorial background for the dilepton spectrum. Therefore it is crucial to make a solid theoretical prediction on the contribution from heavy quark decays.

We have studied the dimuon emission as the decay product of the heavy quarks (charm and bottom) produced in an initial hard scattering and in a thermalized quark-gluon plasma at RHIC energy [3]. In our calculation we have included the next-to-leading order radiative corrections and nuclear shadowing effects and we have examined various components of the heavy quark spectra and their role in the dilepton production in an extended dilepton mass region. We have also studied the sensitivities of the perturbative calculation on the choices of the relevant physical scale and the heavy quark fragmentation function. The heavy parton production was calculated using the explicit next-to-leading order matrix elements, while the parton fragmentation and the heavy hadron decay are handled by the ISAJET Monte Carlo model [4]. The cascade decay of the bottom quark, $b \to c \to s$ is included in this model [3].

Theoretical calculations of heavy quark differential and total cross sections to the next-to-leading order $O(\alpha_s^3)$ at RHIC and LHC energies for the initial hard scattering indicate that higher order radiative corrections are important and the theoretical K-factor ranging from $1 \sim 3$ has strong transverse momentum dependence [5]. The nuclear shadowing effect is also non-negligible even at RHIC energy. Therefore, it is crucial to include full next-to-leading order corrections when one evaluates the dilepton production from heavy-quark decay.

The production of heavy hadrons is based on the factorization theorem, which states that the cross section for the production process of a hadron with an energy-momentum $(E, \mathbf{k})$ can be written in a factorized form

$$E\frac{d\sigma}{d^3k} = \sum_i \int E' \frac{d\sigma_i}{d^3k'}(k', \mu) D_i^{(h)}(z, \mu) \frac{E}{E'} \frac{dz}{z^3} \,, \tag{1}$$

where $k' = k/z$, $D_i^{(h)}(z, \mu)$ is the fragmentation function for producing the hadron h from the parton i and $d\sigma_i$ is the short-distance cross section for producing the parton i from the colliding hadrons. Clearly if i is a light parton, the cross section $d\sigma_i$ is not finite and the prescription for subtracting the collinear singularity has to be employed. However, in the case of heavy quark production, $d\sigma_i$ is an infrared safe quantity because the heavy quark mass acts as a cutoff for final state collinear singularities. Thus, the heavy quark mass sets the scale for a perturbative expansion in the strong coupling constant. In the limit when the mass can be considered much larger than the typical hadronic scale, the fragmentation function $D_i^{(h)}(z,\mu)$ is also calculable in perturbation theory. As long as the transverse momentum of the produced heavy quark is not much larger than its mass, perturbation theory predicts $D_i^{(h)}(z) \sim \delta(1-z)$. On the other hand, the finite mass and energy transfer (ΔE) in the fragmentation process suggests that the breakup amplitude $\sim 1/\Delta E$, where

$$\begin{aligned} \Delta E &= (m_Q^2 + z^2k^2)^{1/2} + (m_q^2 + (1-z)^2k^2)^{1/2} - (m_Q^2 + k^2)^{1/2} \\ &\propto 1 - 1/z - \epsilon_Q/(1-z) \; . \end{aligned} \tag{2}$$

This leads to a Peterson form [6]

$$D_Q^{(H)} = \frac{N}{z[1-(1/z)-\epsilon_Q/(1-z)]^2} \; , \tag{3}$$

where $\epsilon_c = 0.15$ and $\epsilon_b = 0.016$. The normalization constant N is fixed by the sum rule $\int dz D_Q^H(z) = 1$: $N = 1.28,\ 0.25$ for c and b respectively. Such a parameterization has been shown to be appropriate in e^+e^- reactions and fit well the MARK-II data [6]. For hadronic collisions or an even heavier quark decay, it is known that there are no universal fragmentation functions. The double differential cross sections for (all) charmed hadrons (mainly D-mesons) as well as (all) b-hadrons (mainly B-mesons) are calculated (assuming that there is no energy loss for the produced parton before hadronization) and the results are plotted in Fig. 1 in Ref. 3 against the distributions for the heavy partons.

The initial parton differential distributions are calculated using the next-to-leading-order (NLO) matrix elements provided by Nason, Dawson and Ellis in [7]. We have taken $m_c = 1.5$ GeV, $m_b = 4.7$ GeV, the factorization and renormalization scale μ to be the transverse mass $2m_t$. The nucleon structure function is parameterized by MRS A and the nuclear shadowing parametrization fits the EMC, NMC and E665 data [8]. The total cross sections (per initial nucleon) are $\sigma_{c\bar{c}}^{\rm tot} = 153\mu$b and $\sigma_{b\bar{b}}^{\rm tot} = 1.5\mu$b for Au+Au collisions at $\sqrt{s} = 200$ GeV/n. The choice of a smaller charm quark mass $m_c = 1.2$ GeV increases the total cross section by a factor of 2 (see Vogt in [5]). As is evident from Fig. 1 in Ref. 3, the leading order (in heavy quark mass) fragmentation function $D(z) \sim \delta(1-z)$ seems to be a reasonable approximation for heavy quarks. There is some noticeable softening of heavy mesons at large p_t and an enhancement of B-meson at very small p_t due to the finite heavy quark mass and the heavy quark-hadron mass splitting. The semileptonic decay of the heavy meson can be conveniently handled by Monte Carlo simulations such as ISAJET or JETSET.

Thermal Charm Production

At sufficiently high temperatures, a thermal system of light partons can create a charm pair which will decay into leptons and should also be included. The thermal charm production has been calculated so far at the leading order matrix element level [9]. To estimate the reliability of the leading-order result, one has to perform a full NLO calculation. At the next-to-leading order, there are additional $2 \to 3$ processes and loop diagrams. Formally, the differential production rate is given by the convolution of the parton level differential cross sections with the initial light parton phase space densities (distribution functions) $f_i(p)$

$$E\frac{dR}{d^3k} = \int \frac{d^3p_1}{(2\pi)^3 2E_1}\frac{d^3p_2}{(2\pi)^3 2E_2}F(p_1,p_1)\left[\frac{g_{gg}}{2}f_g(p_1)f_g(p_2)E\frac{d\hat{\sigma}_{gg}}{d^3k}+ g_{q\bar{q}}f_q(p_1)f_{\bar{q}}(p_2)E\frac{d\hat{\sigma}_{q\bar{q}}}{d^3k}+g_{qg}f_q(p_1)f_g(p_2)E\frac{d\hat{\sigma}_{qg}}{d^3k}\right] , \quad (4)$$

where $g_{gg}=16^2$, $g_{q\bar{q}}=6^2N_f$ and $g_{qg}=6\cdot 16N_f$ are the degeneracy factors, and $F(p_1,p_2)=4p_1p_2$ is the inverse flux factor.

At the leading order, the $d\hat{\sigma}_{qg}$ term is absent. At the next-to-leading order, these parton level differential cross sections contain $2\to 3$ processes and loop diagrams and they are not infrared finite quantities. Braaten and Pisarski [10] have shown that a resummation technique has to be employed to take into account the so-called "hard thermal loops" which give the same order of magnitude contributions as the leading order terms when the external momenta of the amplitude are soft. As a result of the resummation, the infrared singularities are shielded by a Debye screening effect, and the screening masses of gluons and quarks provide an infrared cutoff. The perturbative resummation can only regularize the electric part of the propagators and so far the magnetic screening mass has to come from the unknown nonperturbative effect. To obtain a qualitative result for the NLO thermal charm production, we use the Debye screening mass [11]

$$\mu_D^2=\frac{6g^2}{\pi^2}\int pf(p)dp=4\pi\alpha_s T^2 , \quad (5)$$

to regularize all singularities in the radiative cross sections. This amounts to a "massive gluon scheme" where the μ_D^2 sets the scale for the parton level cross sections in Eq.(4). Certainly, this calculation is not entirely consistent, and the results thus obtained can only be taken as an qualitative indication on the reliability of the leading-order result. We have evaluated the thermal charm yield at RHIC energy by integrating over the space-time evolution of the quark-gluon plasma. We assume a fully equilibrated thermal system with an initial temperature $T_0=0.55$ GeV and a Bjorken ideal-fluid scaling $T(\tau)/T_0=(\tau_0/\tau)^{1/3}$ with $\tau_0=0.7$ fm/c and $T_c=0.2$ GeV. A spatial rapidity cutoff $\eta_{\rm max}=3$ is assumed. The differential distributions are plotted in Fig. 2 in Ref. 3 for the leading order and the next-to-leading order calculations using the Debye screening scale in (5). We also compare the result for a choice of the scale $\mu=m_t$. As in the initial hard scattering case, the higher order corrections are sizable with an effective K-factor ranging from 1.7 to 2.5 as p_t varies from 1 GeV to 10 GeV. We use the leading order kinematics to generate the heavy quark momenta and multiply the weights uniformly by an average value $K=2$ to account for the radiative corrections. The calculated dimuon spectra from the decay of heavy quarks produced in a hard scattering and in an idealized quark-gluon plasma are plotted in Fig. 1. The dimuon spectrum from thermal charm quark production is considerably softer than the initial hard scattering results as can be inferred from the p_t distribution in Fig. 2 in Ref. 3. However, it dominates the dilepton production in the low mass region ($M<2$ GeV). This can be a important background at RHIC for the dilepton signature for the low lying vector resonances such as ρ and ϕ. It is important to note that the calculated thermal charm contribution corresponds to a very ideal case where the quarks and gluons are fully

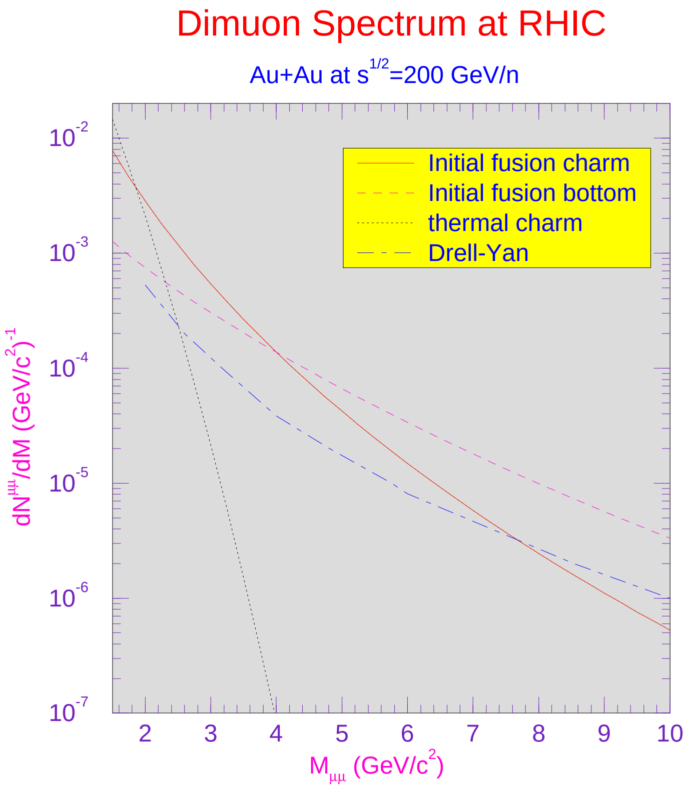

Figure 1: The dimuon invariant mass spectra from the correlated heavy quark decays.

equilibrated. The result may be considerably smaller in the plasma where the chemical process is not in equilibrium [9]. The thermal production of the bottom quark is negligible and is not included. The cascade decay of B-mesons, $b \to c \to s$ is also included in the curve for the initial fusion bottom production. We have not assumed any secondary interactions in the medium produced in the collision. Although the production rate for the initial bottom quark is much smaller than the charm, the dilepton production from B-meson decay is non-negligible in the large invariant mass region due to the large rest mass of the B-meson. It becomes the dominant contribution when the dimuon invariant mass is above ~ 4 GeV. If the fast charm suffers the significant energy loss before it hadronizes, the dimuon spectrum from the initial fusion charm can be considerably softened. In fact, it becomes very similar to that of the thermal charm and falls off rapidly as M gets bigger than 2 GeV, as demonstrated by Shuryak [12]. In this case, the bottom dominance is more prominent and starts at a smaller value of $M \sim 2$ GeV because two B-mesons at rest can produce an energetic lepton pair. In Fig. 2 in Ref. 3 we include the Drell-Yan dimuon production from [13] for comparison. The thermal charm from an ideal quark-gluon plasma dominates the dilepton emission in the low dilepton invariant mass region (< 2 GeV). The correlated heavy mesons produced from the initial hard scattering constitutes the major contribution to the intermediate and high mass dileptons. If there is significant energy loss for the fast charm, the bottom decay is by far the dominant component in the intermediate and high dimuon mass regions. In any case, we are likely to find more bottom than charm in the high mass dilepton channel in central Au+Au collisions at RHIC.

Future Plans: We plan to improve calculation of the thermal charm production by performing self-consistent next-to-leading order calculation. The result should be free of infrared singularities. Current results for thermal charm have the infrared cut off put in by hand and the predictions are very sensitive to its values. This calculation is crucial in order to have firm predictions for charm and/or dilepton enhancement as a signal for the quark-gluon plasma formation at RHIC.

We will also calculate the energy loss of the charm quark in a dense medium similar to the light-quark case done by Baier et al. [14]. We discuss this topic further in a section on QCD Energy Loss. Currently there are interesting phenomenological studies of this effect for heavy quarks [12].

References

[1] E. Shuryak, Phys. Lett. **B78**, 150 (1978)

[2] T. Matsui and H. Satz, Phys. Lett. **B178**, 416 (1986)

[3] D. Fein, Z. Huang, P. Valerio and I. Sarcevic, Phys. Rev. **C56** 1637 (1997).

[4] F.E. Paige, S.D. Protopopescu, Snowmass Summer Study 1986, pg. 320.

[5] I. Sarcevic and P. Valerio, Phys. Lett. **B338**, 426 (1994); Phys. Rev. **C51**, 1433 (1995); R. Vogt, Z. Phys. **C71**, 475 (1996).

[6] C. Peterson, D. Schlatter, I. Schmitt and P.M. Zerwas, Phys. Rev. **D27**, 105 (1983)

[7] P. Nason, S. Dawson and R.K. Ellis, Nucl. Phys. **B327**, 49 (1989); **B303**, 607 (1988); M.L. Mangano, P. Nason and G. Ridolfi, Nucl. Phys. **B373**, 295 (1992)

[8] C.J. Benesh, J. Qiu and J.P. Vary, Phys. Rev. **C50**, 1015 (1994)

[9] P. Levai, B. Müller and X.-N. Wang, Phys. Rev. **C51**, 3326 (1995); Z. Lin and M. Gyulassy, Phys. Rev. **C51**, 2177 (1995)

[10] E. Braaten and R.D. Pisarski, Nucl. Phys. **B337**, 569 (1990)

[11] T.S. Biro, B. Müller and X.-N. Wang, Phys. Lett. **B283**, 171 (1992)

[12] E. Shuryak, Phys. Rev. **C55**, 961 (1997); Z. Lin, R. Vogt and X.-N. Wang, nucl-th/9705006.

[13] S. Gavin, P.L. McGaughey, P.V. Ruuskanen and R. Vogt, Phys. Rev. **C54**, 2606 (1996).

[14] R. Baier, Yu. L. Dokshitser, S. Peigne, D. Schiff, Phys. Lett. **B345**, 277 (1995).

Partonic Picture of Nuclear Shadowing at Small x

(Ina Sarcevic, Zheng Huang and Hung Jung Lu)

The theoretical studies of semihard processes play a increasingly important role in ultrarelativistic heavy-ion collisions at $\sqrt{s} \geq 200$ GeV in describing the global collision features such as particle multiplicities and transverse energy distributions. These semihard processes can be reliably calculated in the framework of perturbative QCD and they are crucial for determining the initial condition for the possible formation of a quark-gluon plasma. Assuming the validity of the factorization theorem in perturbation theory, it is essential to know the parton distributions in nuclei in order to compute these processes. For example, to calculate the minijet production for $p_T \sim 2$ GeV or the charm quark production in the central rapidity region ($y = 0$), one needs to know the nuclear gluon structure function $xg_A(x, Q^2)$ at $Q \sim p_T$ or m_c and $x = x_{\mathrm{Bj}} = 2p_T/\sqrt{s}$ or $2m_c/\sqrt{s}$. For $\sqrt{s} \geq 200$ GeV, the corresponding value of x is $x \leq 10^{-2}$. Similarly, the nuclear quark density $xf_A(x, Q^2)$ is needed for the Drell-Yan lepton-pair production process.

The attenuation of quark density in a nucleus has been firmly established experimentally at CERN [1] and Fermilab [2] in the region of small values of the Bjorken variable $x = Q^2/2m\nu$ in deeply-inelastic lepton scatterings (DIS) off nuclei, where Q^2 is the four-momentum transfer squared, ν is the energy loss of the lepton and m is the nucleon mass. The data, taken over a wide kinematic range, $10^{-5} < x < 0.1$ and $0.05\ \mathrm{GeV}^2 < Q^2 < 100\ \mathrm{GeV}^2$, show a systematic reduction of nuclear structure function $F_2^A(x, Q^2)/A$ with respect to the free nucleon structure function $F_2^N(x, Q^2)$. There are also some indications of nuclear gluon shadowing from the analysis of J/Ψ suppression in hadron-nucleus experiments [3]. Unfortunately, the extraction of nuclear gluon density is not unambiguous since it involves the evaluation of the initial parton energy loss and final state interactions [4].

The partonic description of nuclear shadowing phenomenon has been extensively investigated in literatures in the context of a recombination model [5, 6, 7] and in a Glauber multiple scattering theory [8, 9, 10, 11, 12]. These approaches predict different scale (Q^2) dependence of the nuclear structure function than the conventional Gribov-Lipatov-Altarelli-Parisi (GLAP) evolution equation [13]. Qualitatively, the scale evolution of the nuclear structure function is slower than the nucleon case, leading to a perturbative mechanism for the depletion of the parton density at large momentum transfer. The quantitative prediction of nuclear shadowing at large Q^2 in general depends on the initial value of shadowing at a small momentum transfer where a perturbative calculation breaks down and some non-perturbative model or experimental input is needed. The so-called vector-meson-dominance (VMD) model [14] has been quite successful in predicting the quark shadowing at small Q^2 where the experimental data is rich [1, 2]. Presently there is no viable non-perturbative model for the gluon case and there is very little experimental information on the initial gluon shadowing value at some small Q_0^2. This, in principle, could make the prediction on gluon shadowing very uncertain.

We suggest that these exists a typical scale $Q^2_{\mathrm{SH}} \simeq 3\ \mathrm{GeV}^2$ in the perturbative evolution of the nuclear gluon density beyond which the nuclear gluon shadowing can be unambiguously predicted in the context of perturbative QCD [15]. The so-called "semihard" scale Q^2_{SH} is determined by the strength of the scaling violation of the nucleon gluon density in the small-x region at which the anomalous dimension $\gamma \equiv \partial \ln xg_N / \ln Q^2$ is of $O(1)$. We demonstrate that as Q^2 approaches $Q^2_{\rm SH}$, the gluon shadowing ratio rapidly approaches a unique perturbative value determined by the Glauber multiple scattering theory. At $Q^2 > Q^2_{\rm SH}$, the nuclear gluon density, in contrast to the quark case, is almost independent of the initial distribution at Q_0^2 and its evolution is mainly governed by a GLAP equation. The suggested phenomenon is intimately related to the singular growth of the gluon density in the small-x region and the perturbative shadowing caused by the coherent parton multiple scattering.

We have studied the x-dependence of the shadowing ratio and the non-saturating feature of the perturbative shadowing. As a by-product of the Glauber approach, we have also considered the nuclear geometry dependence of the shadowing ratio, which cannot be addressed in the recombination model such as the GLR equation. Since the shadowing effect is intimately related to the effective number of scatterings, it should vary strongly as one changes the impact parameter. This leads to the breakdown of the conventional factorization of the nuclear parton density into the product of an impact parameter averaged parton distribution and the nuclear thickness function.

At low Q^2, $Q^2 < 1$ GeV^2, in the deeply-inelastic scattering, the interaction of the virtual photon with the nucleons in the rest frame of the target is most naturally described by a vector-meson-dominance (VMD) model [14], in which the virtual photon interacts with the nucleons via its hadronic fluctuations, namely the ρ, ω and ϕ mesons. The shadowing of the (sea) quark density is caused by the coherent multiple scatterings of the vector meson off the nucleons with a large hadronic cross section σ_{VN}, which can be most conveniently handled by the Glauber diffractive approximation model [16]. The x-dependence of the shadowing ratio $R(x,Q^2) = F_2^A(x,Q^2)/AF_2^N(x,Q^2)$ is explained by the coherent length of the virtual photon $l_c \simeq 1/2mx$. For $x < 10^{-2}$, $l_c > R_A = 4 \sim 5$ fm for large nuclei, the vector meson interacts coherently all nucleons inside the nucleus resulting in a uniform (in x) reduction of the total cross section, while for $x > 10^{-2}$, $l_c < R_A$ the vector meson can only interact coherently with a fraction of all the nucleons and shadowing is reduced. However, the VMD model in general predicts much less scaling violation of $F_2^N(x,Q^2)$ than it is observed in the small x region and a rapid disappearance of the nuclear shadowing as $Q^2 \gg m_V^2$. Although a generalized VMD model which includes higher resonances may improve the situation somewhat, it is generally believed that the nuclear shadowing in the VMD model is a higher twist effect, which is in contraction with the experimental evidence that the $R(x,Q^2)$ has a rather weak Q^2 dependence [1, 2].

At $Q^2 > 1 \sim 2$ GeV^2, the virtual photon can penetrate the nucleon and probe the partonic degrees of freedom where a partonic interpretation based on perturbative QCD is most relevant in the infinite momentum frame. It is well known that the Q^2-dependence, the so-called scaling violation of the nucleon structure function $F_2^N(x,Q^2)$ can be well accounted for by the GLAP evolution equation given some non-perturbative initial condition $F_2^N(x,Q_0^2)$ [17]. In the small x region, the GLAP predicts a strong scaling violation of $F_2^N(x,Q^2)$ due to the strong growth of the gluon density in the nucleon. In fact, a dominant perturbative evolution implies that the growth of $F_2^N(x,Q^2)$ in $\ln Q^2$ at fixed, small x is closely related to the growth in $\ln 1/x$ at fixed Q^2, i.e. the so-called double scaling violation observed in the DIS experiments for nucleon, most transparent in the Double Leading-Logarithm Approximation (DLA) of the gluon structure function. At extremely small x, the resummation of large $\ln 1/x$ is necessary leading to the BFKL evolution equation [18] which may also be derived in a Weiszacker-Williams classical field approximation [19]. It is not clear when the BFKL hard pomeron will become relevant since the GLAP evolution seems able to describe most of kinematical region that current experiments have probed so far. As we show, the main feature of the Q^2-dependence of the nuclear shadowing is intimately related to this strong scaling violation in the small-x region. In the target rest frame, the virtual photon interacts with nucleons via its quark-antiquark pair ($q\bar{q}$) color-singlet fluctuation [9]. If the coherence length of the virtual photon is larger than the radius of the nucleus, $l_c > R_A$, the $q\bar{q}$ configuration interacts coherently with all nucleon with a cross section given by the color transparency mechanism for a point-like color-singlet configuration [20]. That is, the cross section is proportional to the transverse separation squared, r_t^2, of the q and $\bar{q}$. In the double logarithm approximation (DLA), the cross section can be expressed through the gluon structure function for a nucleon [21]

$$\sigma_{q\bar{q}N} = \frac{4\pi^2}{3} r_t^2 \alpha_s x' g_{\mathrm{DLA}}(x', 1/r_t^2) \ , \tag{6}$$

where $x' = M^2/2m\nu$ and M is the invariant mass of $q\bar{q}$ pair.

The Glauber multiple-scattering theory [16] treats nuclear collision as a succession of collisions of the probe with individual nucleons within nucleus. A partonic system (h), being a $q\bar{q}$ or a gg fluctuation, can scatter coherently from several or all nucleons during its passage through the target nucleus. The interference between the multiple scattering amplitudes causes a reduction of the hA cross section compared to the naive scaling result of A times the respective hN cross section, the origin of the nuclear shadowing. In the high-energy eikonal limit, the phase shift of the elastic hA scattering amplitude is just the sum of the individual hN scatterings. The total hA cross section is determined by the imaginary part of the forward elastic scattering amplitude as governed by the unitarity relation or the optical theorem. The unitarity of the total cross section is thus built-in within the Glauber theory.

The total hA cross section is given by

$$\sigma_{hA} = \int d^2\mathbf{b} 2 \left[1 - e^{-\sigma_{hN} T_A(\mathbf{b})/2}\right] \ . \tag{7}$$

For a Gaussian parametrization of $T_A(\mathbf{b})$, the integration on the impact parameter can be done exactly leading to

$$\begin{aligned} \sigma_{hA} &= 2\pi R_A^2 \left[\kappa_h - \frac{1}{4}\kappa_h^2 + \cdots + (-1)^{n-1}\frac{\kappa_h^n}{n n!} + \cdots\right] \\ &= 2\pi R_A^2 \left[\gamma + \ln \kappa_h + E_1(\kappa_h)\right] \ , \end{aligned} \tag{8}$$

where $\kappa_h = A\sigma_{hN}/(2\pi R_A^2)$, $\gamma = 0.5772$ is Euler's constant and $E_n(x)$ is the exponential integral function of rank n. The dimensionless quantity κ_h serves as an impact parameter averaged effective number of scatterings. For small value of κ_h, $\sigma_{hA} \to 2\pi R_A^2 \kappa_h = A\sigma_{hN}$, the total hA cross section is proportional to A. In the limit $\kappa_h \to \infty$, the destructive interference between multiple scattering amplitudes reduces the cross section, $\sigma_{hA} \to 2\pi R_A^2(\gamma + \ln \kappa_h)$. Namely, the effective number of scatterings is large and the total cross section approaches the geometric limit $2\pi R_A^2$, a surface term which varies roughly as $A^{2/3}$. In the kinematical region that we are interested in none of these limits are actually approached. The shadowing effect is determined by the strength of κ_h, which is different for a $h = q\bar{q}$ than for a $h = gg$ case.

In the Glauber eikonal approximation, the total cross section $\sigma(\gamma^\star A)$ is given by

$$\sigma(\gamma^\star A) = \int d^2b \int_0^1 dz \int d^2\mathbf{r} |\psi(z,\mathbf{r})|^2 2(1 - e^{-\sigma_{q\bar{q}N}(\mathbf{r},z)T_A(b)/2}), \tag{9}$$

where

$$|\psi(z,\mathbf{r})|^2 = \frac{6\alpha_{\rm em}}{(2\pi)^2} \sum_1^{N_f} e_i^2 P(z) a^2 K_1(a\mathbf{r})^2 \rightarrow \frac{6\alpha_{\rm em}}{(2\pi)^2} \sum_1^{N_f} e_i^2 \frac{1}{\mathbf{r^2}} , \tag{10}$$

is the photon wave function, $\sigma_{q\bar{q}N}$ is given by (6), z is the fraction of the energy carried by the quark (antiquark), b is the impact parameter and $T_A(b)$ is the nuclear thickness function. The nuclear cross section is therefore reduced when compared to the simple addition of free nucleon cross sections.

For a given Q^2, all $q\bar{q}$ configurations with the separation size $r_t^2 > 1/Q^2$ are possible, but the virtual photon wavefunction $|\psi_{\gamma^*}| \sim 1/r_t^4$ favors the smallest value of $r_t^2 \simeq 1/Q^2$ where the cross section is small and no significant shadowing is expected. The solution to this problem comes from the fact that the nucleon structure function exhibits a strong scaling violation in the small x region at the moderate (semihard) momentum transfer 0.8 $\text{GeV}^2 < Q^2 < Q^2_{\rm SH}$ where $Q^2_{\rm SH} \simeq 3$ GeV^2. As we show, the strong scaling violation in this region can be understood in the context of perturbative QCD. The gluon density grows rapidly with $1/r_t^2$ in the small x region, which can compensate the inherent "smallness" of the cross sections of "hard" QCD processes. As a consequence, the semihard processes can compete successfully with the "soft" processes as described in the VMD model and continue to provide the shadowing mechanism up to some moderately high value of $Q^2 \sim Q^2_{\rm SH}$. In terms of the anomalous dimension, $\gamma(Q^2) = d\ln xg_N/d\ln Q^2$, the cross section in (6) can be written as

$$\sigma_{q\bar{q}N} \propto \frac{(Q^2)^\gamma}{Q^2} . \tag{11}$$

At large Q^2, the anomalous dimension becomes greater than 1 and it delays the rapid decrease of the cross section due to the "smallness" of the configuration size, as first argued by Gribov, Levin and Ryskin in [5]. We refer to this as the perturbative shadowing mechanism as it can be computed in perturbative QCD. At even higher values of Q^2, $Q^2 > Q^2_{\rm SH}$, the scaling violation becomes weak (logarithmic), and the perturbative shadowing mechanism ceases to be effective. In this case, both the nucleon and the nuclear structure function evolve slowly at the same rate. The shadowing ratio developed by both perturbative and non-perturbative mechanisms in the relatively low-Q^2 region persists in the high Q^2 region but tends to 1 rather slowly as $Q^2 \rightarrow \infty$.

In contrast to the VMD model, the x-dependent cross section $\sigma_{q\bar{q}N}$ predicts an additional x-dependence of the shadowing ratio apart from the coherence length dependence in the perturbative region. As a result, one does not in general expects a saturation of the shadowing ratio as x decreases below the coherence limit $x < 10^{-2}$. On the other hand, as Q^2

decreases, the gluon distribution changes from a singular small-x behavior (hard pomeron regime) to the less singular one (soft pomeron regime). The shadowing ratio becomes flatter as Q^2 decreases. The observed saturation of the shadowing ratio in the small-x region [2] is thus a non-perturbative, low-Q^2 feature.

Similarly, the nuclear gluon density can be studied by considering a deeply-inelastic scattering of a virtual colorless probe (e.g. the virtual "Higgs boson") with the nucleus where the interaction proceeds via a gluon pair gg component of the virtual probe. This has been considered by Mueller [11] and recently by Ayala F, Gay Ducati and Levin (AGL) [12]. In contrast to the quark distribution, the gluon structure functions for both a nucleon and a nucleus are poorly known, especially in the small-x regime though they are of extreme importance for the semihard QCD processes at high energies. Most of our knowledge on the gluon distribution comes from the theoretical expectations based on perturbative QCD constrained by the scaling violation of F_2^N and the prompt photon experiments [17]. The nuclear gluon density may also be studied in the Glauber multiple scattering model where $\sigma_{q\bar{q}N}$ in (6) is to be replaced by σ_{ggN}. Simple color group representation argument relates these two cross sections by $\sigma_{ggN} = 9\sigma_{q\bar{q}N}/4$. However, what makes the gluon case very different from the quark case is the unknown initial (non-perturbative) gluon density in the nucleus. There is very little experimental information on the gluon shadowing at low Q^2 and small x. The VMD model is not applicable here since the low-lying meson spectroscopy for gg-like states is poorly known. This would make this approach very uncertain in predicting the amount of gluon shadowing in the nucleus.

However, the large σ_{ggN} implies an even stronger scaling violation of gluon density than in the case of quarks making the perturbative shadowing a dominant mechanism. As a consequence, the shadowing ratio is largely determined by the perturbative calculation at $Q^2 = Q^2_{\rm SH}$. That is, the large anomalous dimension of gluon distribution function for a nucleon drives the shadowing ratio rapidly to approach the perturbative value at moderately large Q^2, $Q^2 = Q^2_{\rm SH}$, and the initial shadowing (at low Q^2) becomes relatively unimportant. For $Q^2 > Q^2_{\rm SH}$, the scaling violation becomes weaker and the shadowing ratio determined by the perturbative shadowing mechanism at the semihard scale persists and evolves slowly. The x-dependence of the shadowing ratio can be also predicted to be non-saturating, a generic feature of the perturbative shadowing. We therefore suggest that the nuclear gluon shadowing at $Q^2 > Q^2_{\rm SH} \simeq 3$ GeV^2 and at small x can be predicted in the context of perturbative QCD. The prediction is based on the scaling violation of the gluon structure function and the existence of the perturbative shadowing in the Glauber multiple scattering model.

At small x, the structure function of a nucleus can be written in terms of the virtual photon-nucleus cross section

$$F_2^A(x,Q^2) = \sum_i e_i^2 x f_A(x,Q^2) = \frac{Q^2}{4\pi^2\alpha_{\rm em}}\sigma(\gamma^* A) \ , \tag{12}$$

where $xf_A(x,Q^2)$ is the (sea) quark distribution function. Using (12) and substituting integration over $(z,\mathbf{r_t})$ to (x',Q'^2) in (9), one obtains for (sea)quarks [15]

$$xf_A(x,Q^2) \;\; = \;\; xf_A(x,Q_0^2) + \frac{3R_A^2}{8\pi^2}x\int_x^1 \frac{dx'}{x'^2}\int_{Q_0^2}^{Q^2} dQ'^2 \left[\gamma + \ln(\kappa_q) + E_1(\kappa_q)\right] \ , \tag{13}$$

where the effective number of scatterings κ_q is given

$$\kappa_q(x, Q^2) = \frac{2A\pi}{3R_A^2 Q^2}\alpha_s(Q^2) x g_N^{\rm DLA}(x, Q^2) \ , \tag{14}$$

Expanding $[\cdots]$ and keeping only the first term which is proportional to κ_q, one recovers the result for the nucleon in the same DLA approximation. We find our result for $F_2^N(x, Q^2)$ to be in excellent agreement with the recent HERA data for a broad range of x and Q^2 (see Figs. 2 and 3 in Ref. 15).

In principle, the initial condition $xf_A(x, Q_0^2)$ in (13) may be calculated in the vector-meson-dominance (VMD) model. Fortunately, there have been some experimental measurements on the nuclear quark shadowing in the low-Q^2 region so that the initial condition can be expressed in terms of the production of the initial nucleon structure function and the shadowing ratio $R_0^q(x)$

$$F_2^A(x, Q_0^2) = AR_0^q(x) F_2^N(x, Q_0^2) \ , \tag{15}$$

where $F_2^N(x, Q_0^2)$ is nucleon structure function. Recently E665 Collaboration has measured the nuclear shadowing effect in muon scatterings off ^{40}Ca and ^{208}Pb at low x [2]. In general, the small x data are measured at low Q^2, e.g., for $x = 6 \times 10^{-4}$ the average $\langle Q^2 \rangle = 0.26$ GeV^2 while $x = 6 \times 10^{-3}$ corresponds to $\langle Q^2 \rangle = 1.35$ GeV^2. We parametrize the initial shadowing ratio $R_0^q(x)$ at $Q_0^2 = 0.4$ GeV^2 and we calculate the nuclear structure function at the measured $\langle Q^2 \rangle$ values at different x values. The nuclear shadowing ratio is defined by

$$\begin{aligned} R_q(x, Q^2) &= \frac{F_2^A(x, Q^2)}{AF_2^N(x, Q^2)} \\ &= \frac{R_q^0(x) F_2^N(x, Q_0^2) + \Delta F_2^A(x; Q^2, Q_0^2)}{F_2^N(x, Q_0^2) + \Delta F_2^N(x; Q^2, Q_0^2)} \ , \end{aligned} \tag{16}$$

where $\Delta F_2 \equiv F_2 - F_2(Q_0^2)$ can be explicitly calculated by performing the double integration over x' and Q'^2 in (13). The results for ^{40}Ca and ^{208}Pb are shown in Fig. 2.

The x-dependence of nuclear quark shadowing ratio $R_q = F_2^A/(AF_2^N)$ at various Q^2 for ^{208}Pb and ^{40}Ca. The lower panels represent the parameterizations of initial shadowing ratios evolved to the experimental $\langle Q^2 \rangle_{\rm exp}$ values. The non-saturation of $R_q(x)$ as x decreases at large Q^2 is the feature of the perturbative shadowing mechanism.

The lower panels of Fig. 2 show our parametrizations of initial shadowing ratio at Q_0^2 evolved to the measured $\langle Q^2 \rangle$ compared to the experimental data from E665. For $\langle Q^2 \rangle < Q_0^2$, we take it to be at the minimal scale Q_0^2. As is evident from the comparison, our parametrizations faithfully represent the experimental data at small x. The shadowing ratio, $R_q(x, Q^2)$, at high values of Q^2 are shown in the upper panels of Fig. 2.

We note that at large Q^2 the nuclear shadowing effect is reduced but does not diminish, i.e. it is not a higher twist effect. This can be understood as the interplay between the perturbative and the non-perturbative shadowing mechanisms. The nuclear quark density is initially shadowed by R_q^0 at Q_0^2 compared to the free nucleon case due to some non-perturbative mechanism such as coherent scatterings of the ρ-meson as discussed in the VMD model [14]. As Q^2 increases from Q_0^2, the nucleon structure function increases by

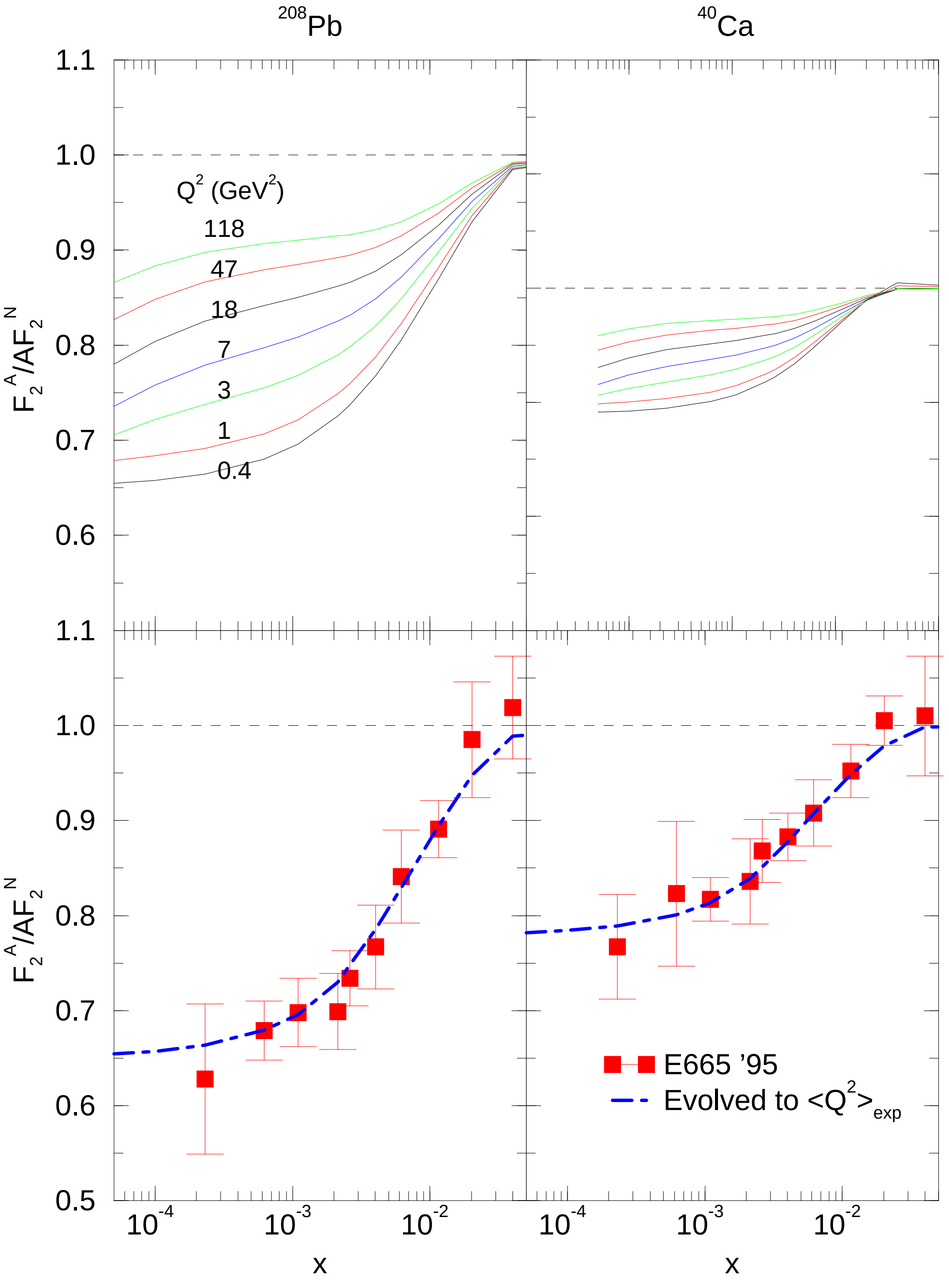

Figure 2:

$\Delta F_2^N(x; Q^2, Q_0^2)$ as governed by the GLAP evolution equation in the DLA. If the nuclear F_2^A increases by the same amount (times A), i.e., we neglect the multiple scattering effect and evolve it according to the same GLAP equation, the initial shadowing effect in (16) decreases quickly due to the strong scaling violation at low Q^2 ($\Delta F_2^N(x; Q^2, Q_0^2)$ is not small compared to $F_2^N(x, Q_0^2)$). This is illustrated in Fig.5 in Ref. 15 where the shadowing ratio is calculated by taking the first term in the expansion $[\cdots]$ in (13) and plotted as function of Q^2 at a fixed $x = 10^{-4}$. The shadowing effect disappears quickly when both the nucleon and nuclear structure functions evolve according to the GLAP equation. Also plotted in Fig. 5

in Ref. 15 is the double scattering case where we take the first two terms in the expansion

$$[\gamma + \ln \kappa_q + E_1(\kappa_q)] \simeq \kappa_q - \frac{1}{4}\kappa_q^2 \, . \tag{17}$$

As it is evident from Fig. 5 in Ref. 15, the double scattering overestimates the amount of shadowing. Nevertheless, it accounts for most of the multiple scattering effect.

The interplay between soft physics and the partonic picture of the nuclear shadowing is also evident in the x-dependence of R_q in Fig. 4. in Ref. 15. The apparent flatness of the shadowing ratio at low Q^2 in the small-x region is altered by the perturbative evolution. This is due to the singular behavior of $xg_N^{\rm DLA}$ as $x \to 0$ at large Q^2 leading to the strong x-dependence of the effective number of scatterings, $\kappa_q(x)$. Thus, the saturation of the R_q as x decreases is a feature only at low Q^2, $Q^2 < 2$ GeV^2 where the gluon density is not so singular, and we do not expect the saturation to happen for higher values of Q^2.

In the previous section, we emphasized the importance of the interplay between the non-perturbative and perturbative shadowing mechanisms in order to predict the nuclear quark shadowing at large Q^2. In principle, the prediction for the nuclear gluon shadowing could be uncertain because there is no experimental information on the gluon shadowing at low Q^2. However, as we demonstrate below that this is not the case and the gluon shadowing can be unambiguously predicted for large Q^2 in the context of perturbative QCD.

The gluon distribution in a nucleus can be calculated in the Glauber model similarly to the quarks [12]

$$xg_A(x,Q^2) \;=\; xg_A(x,Q_0^2) + \frac{2R_A^2}{\pi^2}\int_x^1 \frac{dx'}{x'}\int_{Q_0^2}^{Q^2} dQ'^2\,[\gamma + \ln(\kappa_g \tau) + E_1(\kappa_g \tau)] \;, \tag{18}$$

The essential difference between the quark and gluon cases is different splitting functions and the effective number of scatterings, $\kappa_g = 9\kappa_q/4$ due to different color representations that the quark and the gluon belong to. These two effects combined result in the 12 times faster increase of the gluon density with Q^2 than in the case of the sea quarks in the region of small x. The two important effects which make the gluon shadowing quite different from the quark shadowing are the stronger scaling violation in the semihard scale region and a larger perturbative shadowing effect. This can be seen by considering the shadowing ratio

$$\begin{aligned} R_g(x,Q^2) &= \frac{xg_A(x,Q^2)}{Axg_N(x,Q^2)} \\ &= \frac{xg_N(x,Q_0^2)R_g^0(x) + \Delta xg_A(x;Q^2,Q_0^2)}{xg_N(x,Q_0^2) + \Delta xg_N(x;Q^2,Q_0^2)} \;, \end{aligned} \tag{19}$$

where $R_g^0(x)$ is the initial shadowing ratio at Q_0^2 and $\Delta xg(x;Q^2,Q_0^2)$ is the change of the gluon distribution as the scale changes from Q_0^2 to Q^2. The strong scaling violation due to a larger κ_g at small x causes $\Delta xg_N(x;Q^2,Q_0^2) \gg xg_N(x,Q_0^2)$ as Q^2 is greater than $1 \sim 2$ GeV^2. The dependence of $R_g(x,Q^2)$ on the initial condition $R_g^0(x)$ diminishes and the perturbative shadowing mechanism takes over, i.e.

$$R_g(x,Q^2) \to \frac{\Delta xg_A(x;Q^2,Q_0^2)}{\Delta xg_N(x;Q^2,Q_0^2)} \;, \tag{20}$$

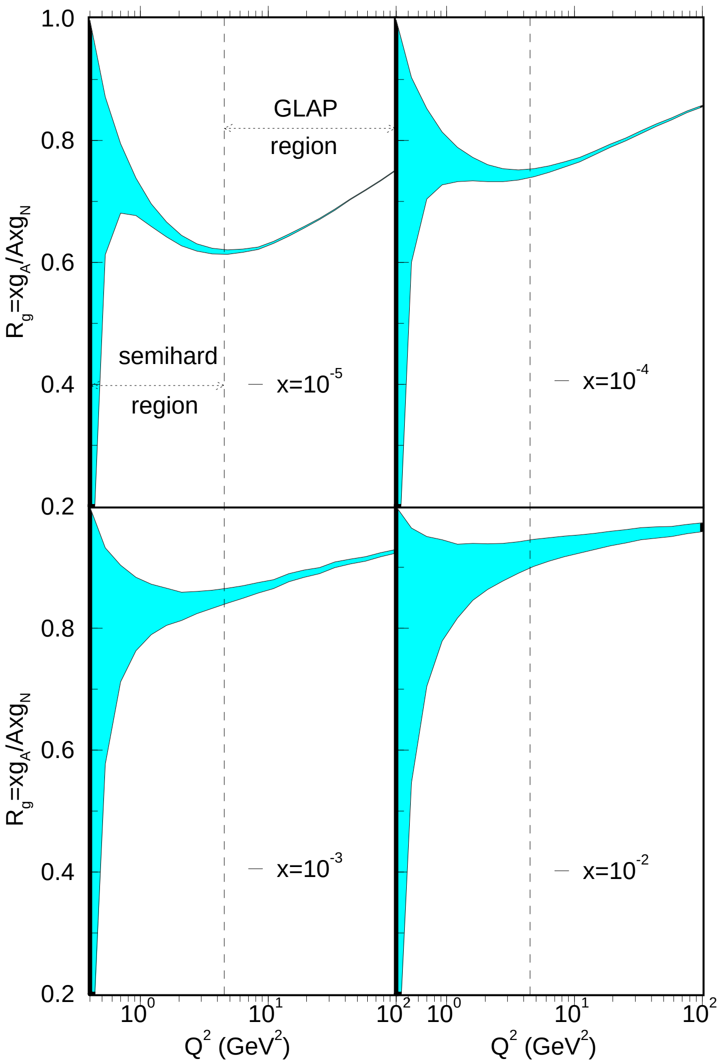

Figure 3: The x-dependence of the gluon shadowing ratio at various Q^2 values. The shaded region indicates the uncertainty due to the initial conditions.

for $Q^2 > 2$ GeV^2. This can be seen in Fig. 3.

The above statement can be made more rigorous by taking a partial derivative of (19) with respect to $\ln Q^2$ at a fixed x

$$\frac{\partial R_g(x,Q^2)}{\partial \ln Q^2} = \gamma(Q^2) \left[R_g^{\rm PT}(x,Q^2) - R_g(x,Q^2) \right] \ , \tag{21}$$

where the anomalous dimension $\gamma(Q^2)$ and the so-called perturbative shadowing ratio $R_g^{\rm PT}$ are defined

$$\begin{aligned} \gamma(Q^2) &= \frac{\partial \ln x g_N(x,Q^2)}{\partial \ln Q^2} \\ R_g^{\rm PT} &= \frac{\partial x g_A(x,Q^2)/\partial \ln Q^2}{A \partial x g_N(x,Q^2)/\partial \ln Q^2} \ . \end{aligned} \tag{22}$$

Note that $R_g^{\rm PT}$ is the ratio of the derivative of xg_A to that of xg_N, which is independent of the initial shadowing ratio and can be calculated perturbatively. In the small-x,

$$R_g^{\rm PT} \simeq \frac{\gamma + \ln \kappa_g + E_1(\kappa_g)}{\kappa_g} = 1 - \frac{\kappa_g}{4} + \frac{\kappa_g^2}{18} - \cdots \; . \tag{23}$$

The interesting feature of (21) is the negative sign in front of R_g on the right hand side such that it is self-stabilizing. If $R_g < R_g^{\rm PT}$ at Q^2 and $\partial R_g/\partial \ln Q^2 > 0$, the shadowing ratio increases with Q^2; while for $R_g < R_g^{\rm PT}$, the shadowing ratio decreases with Q^2. As a result, the Q^2-evolution of R_g is such that it is always in the process of approaching $R_g^{\rm PT}$. Because $R_g^{\rm PT}$ also changes with Q^2, the Q^2-evolution of R_g never stops. The anomalous dimension $\gamma(Q^2)$ determines how fast R_g is approaching $R_g^{\rm PT}$. Introduce an important scale $Q_{\rm SH}^2 = 3$ GeV^2 ("SH" stands for "semihard") where $\gamma(Q_{\rm SH}^2) \simeq$O(1). In the semihard region $Q_0^2 < Q^2 < Q_{\rm SH}^2$, $\gamma(Q^2)$ is large and R_g approaches $R_g^{\rm PT}(Q_{\rm SH}^2)$ fast regardless of what the initial shadowing one has to set at Q_0^2. It is precisely in this region that κ_g is large and (23) gives a large shadowing correction. As $Q^2 > Q_{\rm SH}^2$, the anomalous dimension $\gamma(Q^2)$ gets small and $R_g^{\rm PT}$ approaches 1 fast and the shadowing ratio R_g evolves slowly. Thus, the behavior of the Q^2-evolution of the gluon shadowing can be understood by the interplay between the anomalous dimension of the nucleon gluon structure function and the perturbative shadowing mechanism.

Approximating the perturbative shadowing by $R_g^{\rm PT} = R_g^{\rm PT}(Q_{\rm SH}^2)$ for $Q_0^2 < Q^2 < Q_{\rm SH}^2$ and $R_g^{\rm PT} = 1$ for $Q^2 > Q_{\rm SH}^2$, one obtains the shadowing ratio for $Q^2 > Q_{\rm SH}^2$

$$R_g(t) = 1 - \left[1 - R_g^{\rm PT}(t_{\rm SH})\right] e^{-\int_{t_{\rm SH}}^{t} \gamma(t')dt'} \; . \tag{24}$$

The evolution factor $\exp[-\int]$ no longer falls rapidly and R_g evolves rather slowly. Thus, the Q^2-behavior of gluon shadowing at large Q^2 can be roughly described by an initial condition at $Q_{\rm SH}^2$ followed by a GLAP evolution. The important point is that the initial condition at $Q^2 = Q^2$SH is pre-determined by the perturbative shadowing. Our main conclusion is that even though $R_g^{\rm PT}(Q^2)$ approaches 1 quickly as Q^2 increases beyond $Q_{\rm SH}^2$ (a higher twist effect), the shadowing ratio at large Q^2 is still governed by the perturbative shadowing at the *semihard scale*, namely $R_g^{\rm PT}(Q_{\rm SH}^2)$.

The x-dependence of the gluon shadowing can also be predicted as long as $Q^2 > Q_{\rm SH}^2$ where the influence of the initial condition is minimal. Fig. 3 in Ref. 15 shows the x-dependence of the gluon shadowing ratio at various Q^2 values. The shaded region is bounded by the distributions calculated using two drastically different initial conditions $R_g^0 = 0$ and $R_g^0(x) = 1$. It is clear that the shape of the distribution is quite robust in the small-x region regardless of what initial conditions one may choose. Due to the perturbative nature of the shadowing, these distributions do not exhibit a saturation as x decreases. This is related to the singular behavior of the nucleon gluon distribution at large Q^2 and small x. As long as the nucleon gluon density does not saturates at small x, the shadowing ratio does not saturate either. This is in accordance with the observation by Eskola, Qiu and Wang [7] in the context of the gluon recombination model. The rapid Q^2-evolution of the gluon shadowing ratio in the low Q^2 region found by Eskola [23] can be understood in our approach as the quick approach of the initial shadowing ratio to its perturbative value (see Fig. 7 in

Ref. 15). In Eskola's approach some shadowing persists even at $Q^2 = 100$ GeV^2 which can also be understood in our picture as the region of fully developed GLAP evolution. We note that multiple scatterings inside the nucleon are also possible in the region of very small x, where the eikonalization of the nucleon cross section is needed. However, in this region, the DLA breaks down and a BFKL resummation is necessary.

So far we have confined ourselves to the impact parameter averaged nuclear structure function. However, in the binary approximation of hard scattering processes in pA and AA collisions, one has to calculate the parton cross section at the nucleon-nucleon level at each impact parameter. In addition, to enhance the possible signal of a quark-gluon plasma in heavy-ion collisions, one triggers on central events where the impact parameter is small (e.g. $b < 2$ fm). It is thus necessary to study the impact parameter dependence of the nuclear shadowing effect.

Intuitively, one expects that the nuclear shadowing effect should depend on the local nuclear thickness at a given impact parameter. In the Glauber approach, the effective number of scatterings is a product of the cross section and the nuclear thickness function. Since the shadowing is a non-linear effect in the effective number of scatterings, the impact parameter dependent shadowing ratio cannot be factorized into a product of an average shadowing ratio and the nuclear thickness function, as has been done in previous works [24].

The impact parameter dependent nuclear structure function $x\tilde{g}_A(x, Q^2; \mathbf{b})$ is defined as

$$xg_A(x, Q^2) = \int d^2\mathbf{b}\, x\tilde{g}_A(x, Q^2; \mathbf{b}) \; . \tag{25}$$

where

$$\begin{aligned} x\tilde{g}_A(x, Q^2; \mathbf{b}) \;\; &= \;\; x\tilde{g}_A(x, Q_0^2; \mathbf{b}) + \frac{4}{\pi^3}\int_x^1 \frac{dx'}{x'} \int_{Q_0^2}^{Q^2} dQ'^2 \\ & \qquad 2\left[1 - e^{-\sigma_{ggN} T_A(\mathbf{b})/2}\right] \; , \end{aligned} \tag{26}$$

and $x\tilde{g}_A(x, Q_0^2; \mathbf{b})$ is the initial condition at a fixed impact parameter $\mathbf{b}$. As shown in the previous section, the prediction for gluon shadowing ratio at $Q^2 > 3$GeV^2 does not depend on the initial condition. Thus, as an illustration we take the initial shadowing ratio to be 1 for all $\mathbf{b}$'s. The impact parameter dependent shadowing ratio,

$$R_g(x, Q^2; \mathbf{b}) = \frac{x\tilde{g}_A(x, Q^2; \mathbf{b})}{T_A(\mathbf{b}) x g_N(x, Q^2)} \; . \tag{27}$$

is plotted in Fig. 4.

In summary, the nuclear shadowing phenomenon is a consequence of the parton coherent multiple scatterings. While the quark density shadowing arises from an interplay between "soft" physics and the semihard QCD process, the gluon shadowing is largely driven by a perturbative shadowing mechanism due to the strong scaling violation in the small-x region. The gluon shadowing is thus a robust phenomenon at large Q^2 and can be unambiguously predicted by perturbative QCD.

The scale dependence of the nucleon structure function was used to put a stringent constraint on the gluon density inside the nucleon in the double logarithm approximation. It is shown that the strong scaling violation of the nucleon structure function in the semihard

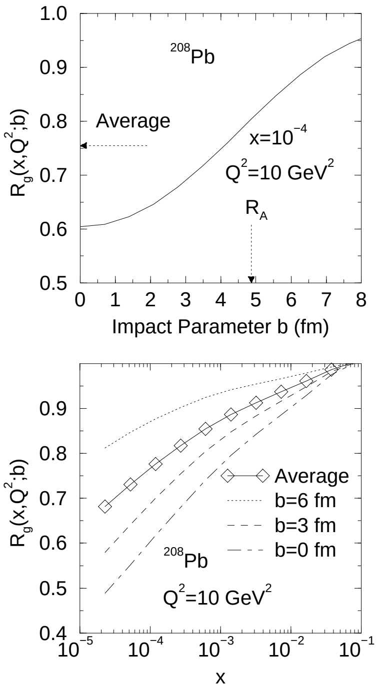

Figure 4: The impact parameter dependent gluon shadowing calculated assuming $R_g^0 = 1$ for any b. The upper panel is the shadowing ratio as function of b at fixed values of $x = 10^{-4}$ and $Q^2 = 10$ GeV^2. Tle lower panel shows the x-dependence of the shadowing ratio at a fixed $Q^2 = 10$ GeV^2 and various values of b.

momentum transfer region $0.8 < Q^2 < 3$ GeV^2 at small x can be reliably described by perturbative QCD and is a central key to the understanding of the scale dependence of the nuclear shadowing effect.

The impact parameter dependence of gluon shadowing is a non-linear effect in the nuclear thickness function. It is important to correctly incorporate the impact parameter dependence of the nuclear structure function when one calculates the QCD processes in the central nucleus collisions.

Future Plans: We plan to re-examine hard processes which are sensitive to the gluon density in a nucleus at small x, such as minijet production and direct photon production at RHIC and LHC energies.

References

[1] NMC Collaboration, P. Amaudruz *et al.*, Z. Phys. C **51**, 387 (1991); Z. Phys.C **53**, 73 (1992); Phys. Lett. B **295**, 195 (1992); NMC Collaboration, M. Arneodo *et al.*, Nucl. Phys. B **441**, 12 (1995).

[2] E665 Collaboration, M.R. Adams *et al.*, Phys. Rev. Lett. **68**, 3266 (1992); Phys. Lett. B **287**, 375 (1992); Z. Phys. C **67**, 403 (1995).

[3] D. Alde *et al.*, Phys. Rev. Lett. **66**, 133 (1991).

[4] S. Gavin and J. Milana, Phys. Rev. Lett. **68**, 1834; C.J. Benesh, J. Qiu and J.P. Vary, Phys. Rev. C **50**, 1015 (1994).

[5] L.V. Gribov, E.M. Levin and M.G. Ryskin, Phys. Rep. **100**, 1 (1983); E. Laenen and E. Levin, Nucl. Phys. B **451**, 207 (1995).

[6] A.H. Mueller and J. Qiu, Nucl. Phys. B **268**, 427 (1986); J. Qiu, Nucl. Phys. B **291**, 746 (1987).

[7] K.J. Eskola, J. Qiu and X.-N. Wang, Phys. Rev. Lett. **72**, 36 (1994).

[8] L. Frankfurt and M. Strikman, Nucl. Phys. B **316**, 340 (1989); L. Frankfurt, M. Strikman and S. Liuti, Phys. Rev. Lett. **65**, 1725 (1990).

[9] S.J. Brodsky and H.J. Lu, Phys. Rev. Lett. **64**, 1342 (1990).

[10] N.N. Nikolaev, Z. Phys. C **32**, 537 (1986); N.N. Nikolaev and B.G. Zakharov, Phys. Lett. B **260**, 414 (1991); Z. Phys. C **49**, 607 (1991).

[11] A.H. Mueller, Nucl. Phys. B **335**, 115 (1990).

[12] A.L. Ayala F, M.B. Gay Ducati and E.M. Levin, Nucl. Phys. B **493**, 305 (1997).

[13] V.N. Gribov and L.N. Lipatov, Sov. J. Nucl. Phys. **15**, 438 (1972); G. Altarelli and G. Parisi, Nucl. Phys. B **126**, 298 (1977); Yu.L. Dokshitser, Sov. Phys. JETP **46**, 641 (1977).

[14] see e.g., G. Piller, W. Ratzka and W. Weise, Z. Phys. A **352**, 427 (1995); T.H. Bauer, R.D. Spital and D.R. Yennie and F.M. Pipkin, Rev. Mod. Phys. **50**, 261 (1978).

[15] Z. Huang, H. J. Lu and I. Sarcevic. AZPH-TH-97-07, hep-ph/9705250, submitted to Nucl. Phys. **A**

[16] R.J. Glauber, in *Lectures in theoretical physics*, ed. W.E. Brittin *et al.* (Interscience Publishers, New York, 1959); R.J. Glauber and G. Matthiae, Nucl. Phys. B **21**, 135 (1970).

[17] A.D. Martin, R.G. Roberts and W.J. Stirling, Phys. Lett. B **387**, 419 (1996); H.L. Lai, J. Huston, S. Kuhlmann, F. Olness, J. Owens, D. Soper, W.K. Tung and H. Weerts, Phys. Rev. D **55**, 1280 (1997); M. Glueck, E. Reya and A. Vogt, Z. Phys. C **67**, 433 (1995).

[18] E.A. Kuraev, L.N. Lipatov and V.S. Fadin, Sov. Phys. JETP **45**, 199 (1977); Ya.Ya. Balitskii and L.V. Lipatov, Sov. J. Nucl. Phys. **28**, 822 (1978); L.N. Lipatov, Sov. Phys. JETP **63**, 904 (1986).

[19] L. McLerran and R. Venugopalan, Phys. Rev. D **49**, 2233 (1994); A. Kovner, L. McLerran and H. Weigert, Phys. Rev. D **52**, 6231 (1995); D **52**, 3809 (1995).

[20] A.J. Brodsky and A.H. Mueller, Phys. Lett. B **206**, 685 (1988); G. Farrar, L. Frankfurt, M. Strikman and H. Liu, Phys. Rev. Lett. **64**, 1996 (1990).

[21] B. Blattel, G. Baym, L. Frankfurt and M. Strikman, Phys. Rev. Lett. **70**, 896 (1993); L. Frankfurt, G. Miller and M. Strikman, Phys. Lett. B **304**, 1 (1993).

[22] B. Kopeliovich and B. Povh, Phys. Lett. B **367**, 329 (1996).

[23] K.J. Eskola, Nucl. Phys. B **400**, 240 (1993).

[24] K.J. Eskola, Z. Phys. C **51**, 633 (1991).

Jet Quenching in High-Energy Heavy-Ion Collisions

(*Ina Sarcevic, Zheng Huang and Xin-Nian Wang*)

Large transverse momentum jets, among many other hard processes in high-energy heavy-ion collisions, have been proposed as effective probes of the transient dense matter. For example, an enhanced acoplanarity and energy imbalance of two back-to-back jets can be used to study multiple scatterings of a parton inside a dense medium [1]. Study of large p_T jets can also probe their energy loss due to inelastic scatterings inside a dense matter or a quark-gluon plasma [2]. Because of the enormous background in high-energy heavy-ion collisions, the conventional calorimetric study cannot measure the jet energy to such an accuracy as required to determine the energy loss. Alternately, single-particle inclusive p_T-spectrum has been shown to be sensitive to the jet energy loss [3]. Since the single-particle spectrum is a convolution of the jet production cross section and the jet fragmentation functions, the suppression of produced hadrons at a fixed p_T results from jet quenching with a wide range of initial transverse energies, thus making it difficult to measure directly the modification of jet fragmentation for a given transverse energy.

We proposed that the jet quenching in high-energy heavy-ion collisions can be studied by measuring the p_T distribution of charged hadrons in the opposite direction of a tagged direct photon [4]. A direct photon is produced by quark-antiquark annihilation or quark(antiquark)-gluon Compton scatterings in which a gluon or quark(antiquark) jet is also produced in the opposite direction of the photon. By tagging a direct photon with a given transverse energy E_T^γ, one can avoid the uncertainties associated with the jet production cross section. One can also determine the initial transverse energy of the produced jet, $E_T \approx E_T^\gamma$, from momentum conservation, modulo calculable corrections from initial state radiations. At collider energies and sufficiently large E_T^γ, the Cronin effect due to multiple scatterings during the initial interaction stage is also negligible [5]. We use perturbative QCD to show that the p_T spectrum of charged hadrons with moderate p_T in the backward direction of a direct photon is a very good approximation of the jet fragmentation function which can thus be reliably extracted. We also study the sensitivity of the modification of the jet fragmentation functions in heavy-ion collisions to the energy loss of jets and the jet interaction mean-free-path inside a dense matter.

Let us consider events with a direct photon in the central rapidity region, $|y| \leq \Delta y/2$, $\Delta y = 1$. For sufficiently large E_T^γ of the photon, the rapidity distribution of the associated jet is also centered around zero rapidity with a comparable width. If the azimuthal angle of the photon is ϕ_γ and $\bar{\phi}_\gamma = \phi_\gamma + \pi$, most of the hadrons from the jet fragmentation will fall into the kinematic region, $(|y| \leq \Delta y/2, |\phi - \bar{\phi}_\gamma| \leq \Delta\phi/2)$, where one can take $\Delta\phi = 2$ according to the jet profile as measured in high-energy $p\bar{p}$ collisions [6]. Given the jet fragmentation functions $D_{h/a}(z)$, with z the fractional momenta of the hadrons, one can calculate the differential p_T distribution of hadrons from the jet fragmentation in the kinematical region $(\Delta y, \Delta\phi)$,

$$\frac{dN_{ch}^{jet}}{dyd^2p_T} = \sum_{a,h} r_a(E_T^\gamma) \frac{D_{h/a}(p_T/E_T)}{p_T E_T} \frac{C(\Delta y, \Delta\phi)}{\Delta y \Delta\phi}, \tag{28}$$

where $C(\Delta y, \Delta\phi) = \int_{|y|\leq\Delta y/2} dy \int_{|\phi-\bar{\phi}_\gamma|\leq\Delta\phi/2} d\phi f(y, \phi - \bar{\phi}_\gamma)$ is an overall factor and $f(y,\phi)$ is the hadron profile around the jet axis. The summation is over both jet (a) and hadron species (h), and $r_a(E_T^\gamma)$ is the fractional production cross section of a-type jet associated with the direct photon. We define $D^\gamma(z) = \sum_{ah} r_a(E_T^\gamma) D_{h/a}(z)$ as the inclusive fragmentation function. $C(\Delta y, \Delta\phi)$ is the acceptance factor for finding the jet fragments in the given kinematic range. We find $C(\Delta y, \Delta\phi) \approx 0.5$ at $\sqrt{s} = 200$ GeV, independent of the photon energy E_T^γ, using HIJING [7] Monte Carlo simulations for the given kinematic cuts.

To calculate the background for the photon-tagged jet fragmentation from particle production in a normal central nucleus-nucleus collision, one convolutes the fragmentation functions with the jet cross sections [8],

$$\frac{dN_{ch}^{AA}}{dyd^2p_T} = K \int d^2r \sum_{abcdh} \int_{x_{amin}}^1 dx_a \int_{x_{bmin}}^1 dx_b f_{a/A}(x_a, r) f_{b/A}(x_b, r) \frac{D_{h/c}(z_c)}{\pi z_c} \frac{d\sigma}{d\hat{t}}(ab \to cd), \tag{29}$$

where $z_c = x_T(e^y/x_a + e^{-y}/x_b)/2$, $x_{bmin} = x_a x_T e^{-y}/(2x_a - x_T e^y)$, $x_{amin} = x_T e^y/(2 - x_T e^{-y})$, and $x_T = 2p_T/\sqrt{s}$. The $K \approx 2$ factor accounts for higher order corrections [9]. The parton distribution density in a nucleus, $f_{a/A}(x,r) = t_A(r) S_{a/A}(x,r) f_{a/N}(x)$, is assumed to be factorizable into the nuclear thickness function $t_A(r)$ (with normalization $\int d^2r t_A(r) = A$), parton distribution in a nucleon $f_{a/N}(x)$ and the parton shadowing factor $S_{a/A}(x,r)$ which we take the parametrization used in HIJING model [7]. In our notation, the scale dependences of the parton distributions $f_{a/N}(x,Q^2)$ and the fragmentation functions $D_{h/a}(z,Q^2)$ are implicit, which we take to be $Q = E_T^\gamma$.

Jet fragmentation functions have been studied extensively in $p\bar{p}$, ep and e^+e^- experiments [10]. We will use the parametrizations of both z and Q^2 dependence of the most recent analysis [11] for the unmodified fragmentation functions $D^0_{h/a}(z)$, in which only pions and kaons are included. We use the MRS D$-'$ parametrization of the parton distributions [12]. Shown in Fig. 5 are the differential p_T distributions from the fragmentation of a photon-tagged jet with E_T^γ =15, 20 GeV and the underlying background of normal central $Au + Au$ collisions at $\sqrt{s} = 200$ GeV. The points are HIJING simulations of 10K events and solid lines are numerical results of Eqs. (28) and (29), in both cases no medium effects have been considered in the fragmentation functions. The background in pp collisions is about 1200 times smaller than $Au + Au$.

In heavy-ion collisions, produced partons will experience secondary scatterings and induced radiation which will drive the system toward equilibrium. As a result, large momentum partons will lose part of their energy before they escape and fragment into hadrons. There have been many studies on the energy loss of a propagating parton inside a medium. It is believed that radiative energy loss dominates even when the Landau-Pomeranchuk-Migdal suppression is taken into account [13, 14]. While a dynamical study of the jet propagation and the modification of the hadronization is more desirable, we will use a phenomenological model here to demonstrate how sensitive our proposed measurement in the photon-tagged events to the interactions and the average energy loss suffered by a parton in a dense medium.

We restrict ourselves to the central rapidity region so that a parton will only propagate in the transverse direction in a cylindrical system. The parton will not hadronize inside a deconfined quark-gluon plasma. In a hadronic medium, we assume that the fragmentation functions can be approximated by their forms in vacuum. We only study the effects of radiative energy loss. Given the inelastic scattering mean-free-path, λ_a, the probability for a parton to scatter n times within a distance ΔL before it escapes the system is assumed to be

$$P_a(n) = \frac{(\Delta L/\lambda_a)^n}{n!} e^{-\Delta L/\lambda_a} . \tag{30}$$

If we assume the average energy loss per scattering suffered by the parton is ϵ_a, the modified fragmentation functions can be approximated as,

$$\begin{aligned} D_{h/a}(z, \Delta L, Q^2) &= \frac{1}{C_N^a} \sum_{n=0}^{N} P_a(n) \frac{z_n^a}{z} D^0_{h/a}(z_n^a, Q^2) \\ &+ \langle n_a \rangle \frac{z_a'}{z} D^0_{h/g}(z_a', Q_0^2), \end{aligned} \tag{31}$$

where $z_n^a = z/(1 - n\epsilon_a/E_T)$, $z_a' = zE_T/\epsilon_a$ and $C_N^a = \sum_{n=0}^N P_a(n)$. We limit the number of inelastic scatterings to $N = E_T/\epsilon_a$ by energy conservation. For large values of N, the average number of scatterings within a distance ΔL is approximately $\langle n_a \rangle \approx \Delta L/\lambda_a$. The first term corresponds to the fragmentation of the leading partons with reduced energy $E_T - n\epsilon_a$ and the second term comes from the emitted gluons each having energy ϵ_a on the average. For simplification, we have neglected the fluctuation in the energy carried by each emitted gluon and its possible rescattering. The inelastic scatterings suffered by the leading parton are normally not hard. Therefore, we also assume the scales in the fragmentation functions of the emitted gluons are given by the initial value $Q_0^2 = 2.0$ GeV^2. Since the emitted gluons will only contribute to hadrons with very small fractional energy, the final modified fragmentation function in the moderately large z region is not sensitive to the actual radiation spectrum and the scale dependence of the fragmentation.

Since the jet production rate is proportional to the number of binary nucleon-nucleon collisions, the averaged inclusive fragmentation function of a photon-tagged jet in a central nucleus-nucleus collision is

$$D^\gamma_{AA}(z) = \int \frac{d^2 r t_A^2(r)}{T_{AA}(0)} \sum_{ah} r_a(E_T^\gamma) D_{h/a}(z, \Delta L) , \tag{32}$$

where $T_{AA}(0) = \int d^2 r t_A^2(r)$ is the overlap function of AA collisions at zero impact-parameter. Neglecting the transverse expansion, $\Delta L(r, \phi - \bar{\phi}_\gamma)$ only depends on the jet production position (r, ϕ). Using Eq. (31) in Eq. (29), we can calculate the single-particle inclusive p_T spectrum of normal central AA collisions taking into account jet quenching.

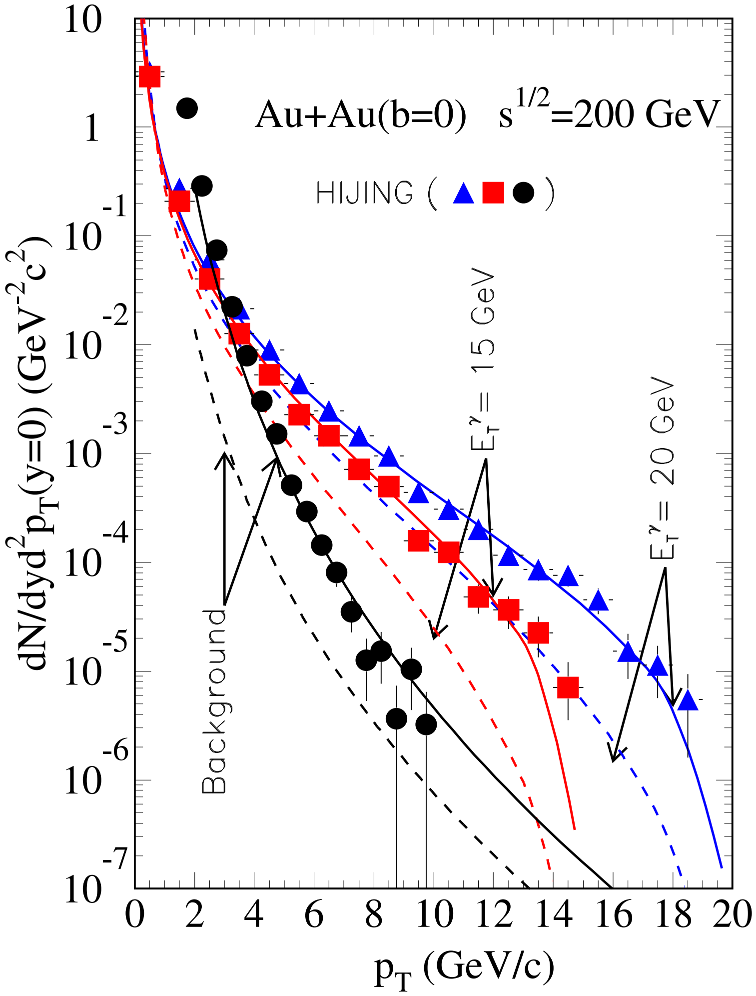

Figure 5: The differential p_T spectrum of charged particles from the fragmentation of a photon-tagged jet with E_T^γ =15, 20 GeV and the underlying background in central $Au + Au$ collisions at $\sqrt{s}$ = 200 GeV [4]. Solid lines are perturbative calculations and points are HIJING simulations. The dashed lines are calculations with jet energy loss, $dE_q/dx = 1$ GeV/fm and the mean-free-path $\lambda_q = 1$ fm. [4].

The dashed lines in Fig. 5 are calculated with the modified fragmentation functions, with $dE_q/dx = 1$ GeV/fm and $\lambda_q = 1$ fm. We have assumed that the mean-free-path of a gluon is half and the energy loss is twice that of a quark. During the parton propagation, multiple scatterings can also change the direction of the parton resulting in a sizable acoplanarity. Such an acoplanarity due to multiple scatterings is probably small as compared to that caused by initial state radiations for a large E_T^γ photon. One observes that there is significant suppression of large p_T particles both from the background and jet fragmentation in the opposite direction of a tagged photon due to jet quenching. Since the number of particles at large $p_T \geq 4$ GeV/c from the underlying background is substantially smaller than from the tagged jet fragmentation with and without jet quenching, one can accurately measure the jet fragmentation function from the p_T distribution of charged particles in the opposite direction of the tagged photons, given enough number of events. Once the background is subtracted, one can push the limit to even smaller $p_T \geq 2$ GeV/c, which corresponds to $z \sim 0.1$. One can then compare the fragmentation functions measured in pp, pA or peripheral AA with central AA collisions to obtain the modification due to jet quenching.

To study the sensitivity of the modified inclusive fragmentation function to the energy loss, and the interaction mean-free-path, λ, we calculate the ratio of the fragmentation functions with and without energy loss for central $Au + Au$ collisions. We find an enhancement of soft particle production due to induced emissions, but only at very small values of z. The fragmentation function is suppressed for large range of z due to energy loss. For fixed $dE_q/dx = 1$ GeV/fm, the suppression is delayed to larger values of z for larger jet energies. The most optimal situation is when the average total energy loss $\langle \Delta E_T \rangle$ is comparable to the initial jet energy so that substantial suppression happens at moderate values of z. From Figs. 2 and 3 in Ref. 4 we can see that there is such a window of opportunity between $E_T^\gamma = 10$ and 20 GeV at $\sqrt{s} = 200$ GeV where the background is small.

For large values of $z > 0.9$, particles from the leading jets, which have suffered at least one inelastic scattering, are completely suppressed. The remaining contribution comes from only those jets that escape the system without a single scattering. The suppression factor is given by $\langle \exp(-\Delta L/\lambda_a) \rangle$, independent of jet energy E_T and the energy loss dE_a/dx. Therefore, one can determine the jet interaction mean-free-path by measuring the suppression factor of the jet fragmentation function at large $z > 0.9$. For intermediate values of $z \sim 0.2$–0.5, particles from the leading partons with reduced energy dominate as far as $\epsilon_a \ll E_T$, a situation we will refer to as the "soft emission" scenario. Since the average total energy loss by the leading parton is $\langle \Delta E_{Ta} \rangle = \langle n_a \rangle \epsilon_a = \langle \Delta L \rangle dE_a/dx$, the suppression factor should scale with dE_a/dx, depending very weakly on the mean-free-path. In Ref. 4 we show the suppression factor at $z = 0.3$ as a function of dE_q/dx for three different values of the mean-free-path. We see that for the soft emission scenario, the suppression factor scales and decreases almost linearly with dE_q/dx. At large values of dE_q/dx and λ_q, the average total energy loss becomes comparable or equal to the initial jet energy E_T. In this "hard emission" scenario, particle production from the emitted gluons and contributions from those jet partons which escape the system without any induced radiation become important. This is why the suppression factor saturates at larger values of dE_q/dx, especially for large values of λ_q. Since the mean-free-path can be determined from the measured suppression factor at large $z > 0.9$ which is independent of dE_q/dx, additional measurements of the suppression at intermediate $z = 0.2$–0.4 will enable one to extract the energy loss.

In summary, we have proposed a way to study jet energy loss in high-energy heavy-ion collisions by measuring the inclusive jet fragmentation function which can be extracted from the differential p_T spectrum of charged particles in the opposite direction of a tagged direct photon. The background to the jet fragmentation is estimated to be small for moderately large p_T. We have also demonstrated that modification of the jet fragmentation function due to jet quenching can be used to obtain the energy loss and the mean-free-path of jet interaction inside the dense matter produced in high-energy heavy-ion collisions.

Our results will be used by the STAR experiment at RHIC to study the effect of jet quenching at RHIC.

References

[1] D. A. Appel, Phys. Rev. D **33**, 717 (1986); J. P. Blaizot and L. D. McLerran, Phys. Rev. D **34**, 2739 (1986); M. Rammerstorfer and U. Heinz, Phys. Rev. D **41**, 306 (1990); S. Gupta, Phys. Lett. **B347**, 381 (1995).

[2] M. Gyulassy and M. Plümer, Phys. Lett. **B243**, 432 (1990); M. Plümer, M. Gyulassy and X.-N. Wang, Nucl. Phys. A 590, 511c (1995).

[3] X.-N. Wang and M. Gyulassy, Phys. Rev. Lett. **68**, 1480 (1992).

[4] X.-N. Wang, Z. Huang and I. Sarcevic, Phys. Rev. Lett. **77**, 23 (1996).

[5] X.-N. Wang, in *Quark-Gluon Plasma II*, R. C. Hwa (ed.) (World Scientific, 1995).

[6] UA1 Collab., G. Arnison *et al.*, Phys. Lett. **B 172**, 461 (1986); C. Albajar et al., Nucl. Phys. **B309**, 405 (1988).

[7] X.-N. Wang and M. Gyulassy, Phys. Rev. D **44**, 3501 (1991); Comp. Phys. Comm. **83**, 307 (1994).

[8] J. F. Owens, Rev. Mod. Phys. **59**, 465 (1987).

[9] K. J. Eskola and X.-N. Wang, Int. J. Mod. Phys. A **10**, 3071 (1995).

[10] P. Mättig, Phys. Rep. **177**, 141 (1989).

[11] J. Binnewies, B. A. Kniehl and G. Kramer, DESY-94-124, hep-ph/9407347.

[12] A. D. Martin, W. J. Stirling and R. G. Roberts, Phys. Lett. **B306**, 145 (1993).

[13] M. Gyulassy and X.-N. Wang, Nucl. Phys. **B420**, 583 (1994); X.-N. Wang, M. Gyulassy and M. Plümer, Phys. Rev. D **51**, 3436 (1995).

[14] R. Baier, Yu. L. Dokshitser, S. Peigne, D. Schiff, Phys. Lett. **B345**, 277 (1995).

Testing for QCD Energy Loss at High x_F

(*Sean Gavin*)

Gavin has had a long interest in parton interactions in nuclei. In addition to their obvious relevance to heavy ion physics, studies of high energy hadron–nucleus and lepton–nucleus collisions provide unique, fundamental spacetime information on QCD [1]. Hard scattering processes such as ψ formation or Drell–Yan dilepton production fleetingly produce high energy quarks and gluons. These partons undergo additional interactions while traversing the nuclear target, gaining transverse momentum [2, 3] and losing energy [4] as they go. Energy loss can lead to a subtle but observable modification of the momentum dependence of the ψ or the DIS jet relative to expectations drawn from standard QCD perturbation theory [5].

To extract quantitative information on these parton interactions from data, it is vital to know the production rates for hard processes in the absence of nuclear effects. In [5], we provide calculations for the Drell–Yan process at next–to–leading order in perturbative QCD for energy and kinematic regimes relevant to nuclear experiments. In [6], we use these results as backgrounds against which signals of thermal dilepton production can be identified. These studies were performed as part of an ongoing Hard Probe Collaboration for RHIC and LHC, a working group patterned after similar groups in the high energy community to provide systematic signal and background computations for RHIC and LHC.

A.H. Mueller, R. Baier, Y. Dokshitser, S. Peigne, and M. Schiff (BDPMS) have calculated the energy loss of high energy partons in nuclear targets [8]. An exciting phenomenological consequence of this calculation is the suggestion that perhaps the total energy loss of a fast quark scales with $A^{2/3}$. This behavior can be understood by estimating the energy loss ΔE of a parton of high energy E as it traverses a nucleus of length $L \propto A^{1/3}$. Emission of a single bremsstrahlung gluon of four-momentum $(\omega, \vec{k}_t, k_z)$ results in an energy loss $\Delta E \sim \omega$. Both the gluon and the parton can undergo further interactions in the nucleus, but only after the gluon travels a transverse distance $r_t \sim 1/k_t$ so that it can be 'resolved' from the parton. In the standard argument [9], one assumes that neither the parton nor the gluon undergo elastic scattering, so that their separation grows as $r_t \sim v_t t$, where $v_t = k_t/\omega$. It then takes a time $t \sim r_t/v_t \sim \omega r_t/k_t \sim \omega/k_t^2$ for the gluon to be resolved. The parton travels a distance Δz in that time. Before that time, any further interactions occur with the gluon-parton system, collectively of energy E. Only after the parton travels a formation length $\Delta z \sim \omega/k_t^2$ can the parton begin it to lose additional energy. Therefore, the parton's energy loss per unit length is limited to a value $dE/dz \sim k_t^2$.

BDPMS observe, however, that before the parton-gluon system is resolved, both the parton and the gluon may suffer *elastic* interactions, which have no formation length [8]. These interactions increase the average $\langle k_t^2 \rangle \propto \Delta z$. Therefore, the energy loss per unit length $dE/dz \sim \langle k_t^2 \rangle$ can grow as $A^{2/3}$. The detailed BDPMS result in a large nucleus is

$$dE/dz = 3\alpha_s \langle k_t^2 \rangle / 8 \tag{33}$$

corresponding to a total energy loss of $\Delta E \approx 15$ GeV for a parton crossing 10 fm of nuclear matter. In contrast, the old estimate $dE/dz \sim 0.3 - 1$ GeV/fm [9] gives $\Delta E \approx 3 - 10$ GeV.

In Ref. [7], we ask whether experimental measures of energy loss reflect a BDPMS $A^{2/3}$ quantum energy loss. To be sure, the leap from the idealized infinite-matter BDPMS calculation to hard-scattering processes in nuclear interactions is not without risk. Nevertheless, there is good experimental evidence that the average transverse momentum in the Drell Yan and other hard processes grows as $A^{1/3}$ [3, 10, 11]. Observe that Huang, Sarcevic and Wang have proposed that photon-hadron jets constitute probe of BDPMS energy loss. Our works are intended to be complementary. They point out that the BDPMS loss leads to strong jet quenching, and ask for future experiments of direct relevance to the jet quenching probe of dense matter. We ask if current pA data are consistent with a BDMPS-type loss.

S. Gavin and J. Milana [4] pointed out that at hard processes near their kinematic extremes are sensitive to parton energy loss. To produce a Drell Yan lepton pair at x_F near the kinematic limit $x_F = 1$, the projectile and target partons must carry momentum fractions $x_p \sim 1$ and $x_t \sim 0$. In a proton-nucleus collision, the projectile parton can lose energy in the nuclear target prior to the hard Drell-Yan process. To produce a lepton pair of x_F, the projectile parton would have to have an $x_p = x_F + x_t + \Delta x > x_F + x_t$. The Drell Yan cross section is proportional to the product of the parton distribution functions f, implying:

$$\frac{\sigma_{pA}}{\sigma_{pp}} \sim \frac{f_p(x_p + \Delta x)}{f_p(x_p)} \sim [1 - \Delta x/(1 - x_F)]^n \tag{34}$$

where the projectile parton distribution is dominated by the quark distribution and varies as $f_p \sim (1-x)^n$ for $n \sim 3$. Even a tiny energy loss corresponding to $\Delta x = \Delta E/E$ can produce a strong effect as x_F, $x_p \rightarrow 1$.

To make the leap from BDPMS to initial-state scattering in proton-nucleus collisions, one must assume that the interactions that occur initial state scattering can lead to energy loss and that BDPMS gives a rough account of these interactions. These assumptions are far from obvious. To properly apply apply these expressions to data, one must also account for shadowing of the target distribution as evident in DIS data.

Energy-loss effects can be stronger in open charm and charmonium production, since interactions can occur in both the final and the initial state. Moreover, interactions of a gluon or a color-octet $c\bar{c}$ are likely stronger than those of color-triplet quarks. For incident partons of sufficient incident energy, the cross section with n initial and m final state scatterings is:

$$\left(\frac{d\sigma}{dx_F}\right)_{pA\rightarrow\psi} = \sum_{n,m} \int d^2b dz \rho(b,z)\ P_n^i(b,z) P_m^f(b,z) \left(\frac{d\sigma}{dx_F}\right)(x_1 + n\Delta x_i, x_2 + m\Delta x_f) \tag{35}$$

where ρ is the nuclear density, $d\sigma/dx_F$ is the relevant QCD cross section at the shifted x_p and x_F. The initial and final state Glauber probabilities, P_n^i and P_m^f, depend on cross sections for initial and final state Bremsstrahlung. To simulate the BDPMS effect we make the ansatz that the initial and final state energy losses per collision are themselves proportional to the number of collisions, $\Delta x_i \propto n$ and $\Delta x_f \propto m$.

To incorporate the effect of shadowing on the target distribution, one can modify that distribution in calculating $d\sigma/dx_F$. To illustrate the extent to which shadowing can affect the pA cross section, we take the rough ansatz that the target sea antiquark distribution have the same nuclear dependences as measured in F_{2A}. Note that it is by no means clear that shadowing and energy loss are independent, as we assume. Some authors view shadowing as yet another manifestation of multiple scattering. We can only hope that phenomenological studies like ours will help to clarify this issue.

We have found that the large BDPMS energy losses are not inconsistent with the available, Drell Yan, charmonium and bottomonium production [7]. In figs. 6 and 7, We show the possible impact of BDPMS energy loss on the x_F in Drell Yan and Υ production in 800 GeV proton–nucleus collisions relative to proton–proton at FNAL.

Inspired by the BDPMS work on energy loss Gavin and Sarcevic plan to address the following interesting questions:

1. Energy loss is relevant to estimating the perturbative contribution to energy deposition and baryon stopping in heavy ion collisions at RHIC and LHC. In particular, the nonlinearities evident in the quantum-mechanical BDPMS result can have striking consequences in A+A collisions. The predicted behavior may be strikingly different from classical cascade codes.

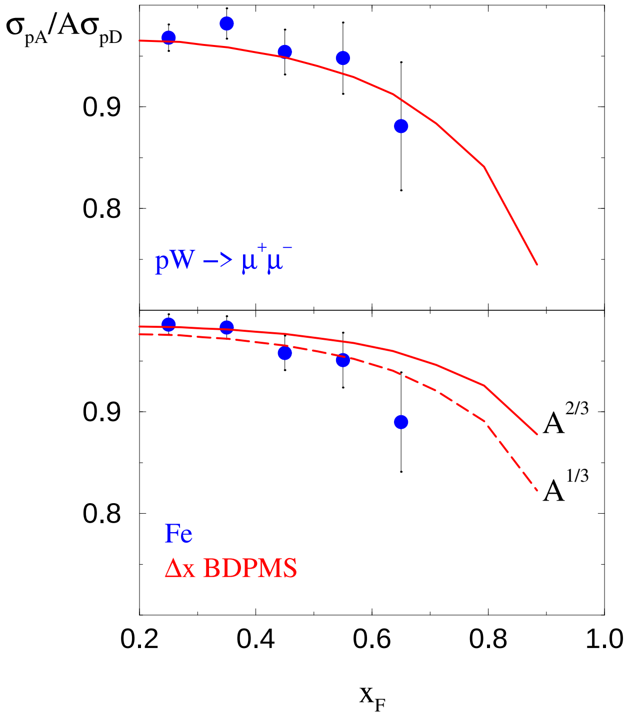

Figure 6: Comparison of Drell Yan in p+W and p+Fe collisions shows the target mass dependence of energy loss.

2. The BDPMS form applies to light partons. What about the heavy charm and bottom quarks? In the regime where interference between successive scattering is unimportant, the QCD Bethe-Heitler dE/dz is valid. This result varies as m^{-2}, which suggests that charm energy loss might be much smaller than BDPMS approach would suggest.

3. Energy loss for charm quarks can have an observable impact on dilepton spectra at RHIC, as pointed out in ref. [12]. However, the BDPMS energy loss (or a variant corrected for the charm mass) is likely different from $dE/dz = 1$ GeV assumed in that work. It is worthwhile reexamining [6] in light of our energy loss results.

4. The Glauber probabilities that enter our calculation depend on parton- nucleon cross sections which were taken as an input parameters. It will be interesting to see whether the parton nucleon cross sections in [13] agree with data in the relevant x regime.

More generally, we hope to understand the interplay between the energy loss described by BDPMS and the parton scatterings [13] in high-energy nuclear collisions.

References

[1] S. Gavin and M. Strikman, eds., “Nuclei At HERA and Heavy Ion Physics,” Proc.

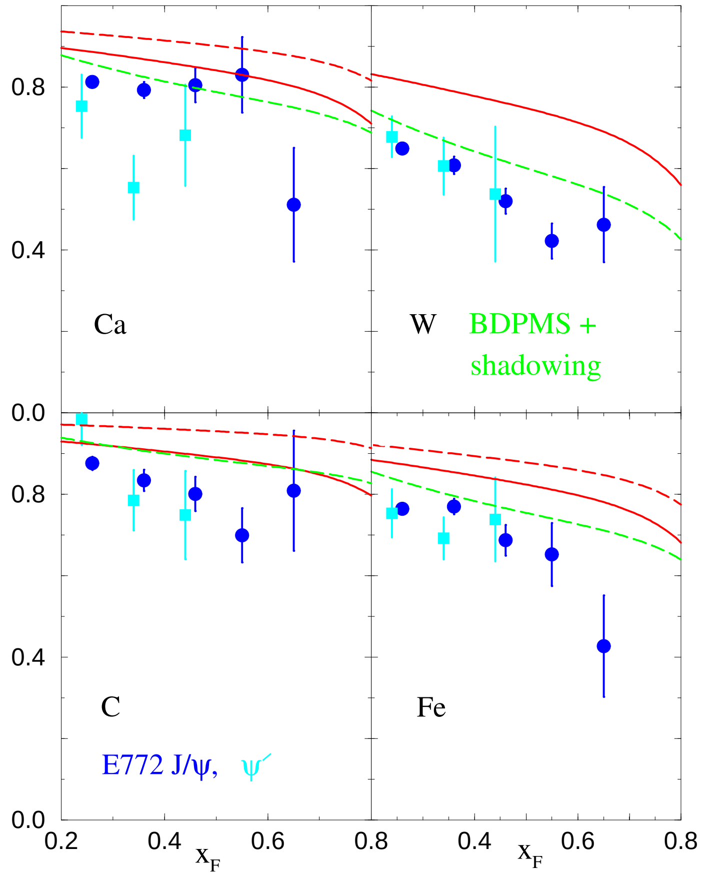

Figure 7: Comparison of charmonium production in four nuclear targets. Calculations include BDPMS-like energy loss and a simple parametrization of shadowing.

Workshop at Brookhaven National Laboratory, 17-18 November 1995, BNL-62634.

[2] Geoffrey T. Bodwin, Stanley J. Brodsky, G.Peter Lepage, Phys. Rev. Lett. **47** 1799, (1981).

[3] S. Gavin and M. Gyulassy, Phys. Lett. **214B**, 241 (1988).

[4] S. Gavin and J. Milana, Phys. Rev. Lett. **68** (1992) 1834.

[5] S. Gavin, R. Kauffman, P.V. Ruuskanen, D.K. Srivastava, and R.L. Thews, Int. J. Mod. Phys. **A10**, 2961 (1995).

[6] David Fein, Zheng Huang, Peter Valerio and Ina Sarcevic Phys. Rev. **C56** 1637 (1997); S. Gavin, P.L. McGaughey, P.V. Ruuskanen and R. Vogt, Phys. Rev. **C54**, 2606 (1996).

[7] S. Gavin and M. Gyulassy, in progress.

[8] R. Baier, Yu.L. Dokshitser, A.H. Mueller, S. Peigne, D. Schiff, Nucl. Phys. **B484** 265 (1997).

[9] S.J. Brodsky and P. Hoyer, Phys. Lett. **B298** 165, (1993); M. Gyulassy and X.-N. Wang, Nucl. Phys. **B420** (1994) 583.

[10] P.L. McGaughey *et al.* (E772 Collab.), Phys. Rev. **D50** 3038 (1994).

[11] See M.H. Schub *et al.* (E789 Collab.) Phys. Rev. **D52** 1307, (1995) and refs. therein.

[12] Zi-wei Lin, Ramona Vogt and Xin-Nian Wang, nucl-th/9705006 (1997).

[13] Zheng Huang, Hung Jung Lu and Ina Sarcevic. AZPH-TH-97-07, hep-ph/9705250 (1997).

Disoriented Chiral Condensate

Ina Sarcevic and Sean Gavin

The primary aim of present and future heavy ion experiments is to establish properties of the QCD phase transition. If the chiral transition is nearly second order, Rajagopal and Wilczek propose that the nonequilibrium dynamics in ion–ion collisions at RHIC can generate transient domains in which a macroscopic pion field develops [1, 2]. These domains are called disoriented chiral condensates (DCC). Bjorken, Kowalski, Taylor and others pointed out that DCC can lead to fluctuations in the charged and neutral pion spectra [3]. In nuclear collisions, the ability of experimenters to identify DCC amidst the background due to conventionally produced particles critically depends on the size and energy content of the domains.

Equilibrium high temperature QCD manifests a chiral symmetry if the light up and down quarks are taken to be massless. However, a phase transition occurs at a critical temperature $T_c \sim 150$ MeV in which chiral symmetry is broken by the formation of a scalar $\langle \overline{q}q \rangle$ condensate. In the real world chiral symmetry is explicitly broken at all temperatures by the few–MeV current quark masses. In that case, the nature of the transition has yet to be established.

Rajagopal and Wilczek pointed out that the chiral condensate can become temporarily *disoriented* in the nonequilibrium conditions encountered in heavy ion collisions [1]. As the temperature drops below T_c, the symmetry can begin to break by developing domains in which the condensate is misaligned in the isospin space. The misaligned condensate has the same quark content and quantum numbers as do pions, and essentially constitutes a macroscopic pion field. In a heavy ion system the evolving domains can radiate pions preferentially according to their isospin content. The excitation of a pion field over a substantial fraction of the collision volume can then result in novel fluctuations in the number of neutral and charged pions. If the pion field produced in nuclear collision were uniform over the collision volume, then the fraction of neutral pions f radiated from a series of such collisions would satisfy the probability distribution

$$P(f) \sim 1/\sqrt{f}. \tag{36}$$

On the other hand, if the pion field is not uniform, the nuclear collision instead produces many uncorrelated small domains, the spectrum of fluctuations would be gaussian, as expected, *e.g.*, if the pions were produced independently.

To develop a concrete picture of how the chiral condensate evolves in a nuclear collision, most authors have used the linear sigma model [1]. In this model, the pion field is coupled to a scalar σ field that characterizes the scalar condensate. These fields interact through a potential

$$V = \lambda(\vec{\pi}^2 + \sigma^2 - v^2)^2/4 - H\sigma. \tag{37}$$

Chiral symmetry transformations correspond to O(4) rotations of the vector field $\vec{\Phi} = (\sigma, \vec{\pi})$.

For $H = 0$ this symmetry is spontaneously broken at zero temperature, with $|\langle\vec{\Phi}\rangle| = v$. As the temperature is increased, this symmetry is restored in a second order phase transition in the same universality class as the O(4) Heisenberg model and QCD. The mean–field estimate for the critical temperature of this transition is $T_c \sim \sqrt{2}v$. Aspects of the equilibrium statistical mechanics of this model are treated in refs. [4]. For $H \neq 0$, the symmetry is explicitly broken at all temperatures and there is no phase transition in the strict thermodynamic sense; this may well be the case in QCD also. However, for a sufficiently small H, the thermal–equilibrium value of the condensate is reduced from $\approx v$ to a value $\langle\sigma\rangle \sim (H/\lambda)^{1/3}$ at $T = \sqrt{2}v$ (again in the mean–field approximation).

In the 'quench' scenario proposed by Rajagopal and Wilczek, one assumes that the system initially has $\Phi = 0$, as appropriate at high temperature, and follows the development of the system using $T = 0$ equations of motion derived from V. The initial state of the system is clearly unstable. The system "rolls down" from the unstable local maximum of $V(\Phi)$ towards the nearly stable values with $|\Phi| = v$ (the symmetry breaking term $-H\sigma$ is relatively small). Field configurations with $\vec{\pi} \neq 0$ develop during the roll–down period. The field will eventually settle into stable oscillations about the unique vacuum $(f_\pi, \vec{0})$ for $H \neq 0$, but oscillations continue until interactions eventually damp the motion.

Gavin, Gocksch and Pisarski studied the size and f distributions of domains using numerical simulations of the linear sigma model equations of motion. Linearized equations of motion imply that the average domain size is roughly [5]

$$R_D \sim 2\tau_R \propto m_\sigma^{-1}. \tag{38}$$

For $m_\sigma = 600$ MeV, the pion field in simulations exhibit structure that grow to a size of order $2 - 4$ fm the quench scenario [5, 6, 7, 9]. Observe that the notion of domains of a fixed 'size' is not rigorously defined in this system – the pion field is inhomogeneous and the scale of inhomogeneities are on average $\sim 2 - 4$ fm.

In ref. [5] we studied the distribution of the fraction of neutral pions with fields $\vec{\pi}$ obtained by simulating the fully nonlinear classical field equations in 3+1 dimensions. Our simulations were performed on a lattice of a volume relevant to a heavy ion collision, $40 \times 10 \times 10$ fm^3. To study the dependence of the results on the sigma mass, calculations were performed for both the normal free–space mass, $m_\sigma = 600$ MeV, and for a very light mass, 2 MeV. In [5], as in [1], a 1 fm lattice spacing was used to simulate the fact that short–wavelength fluctuations are stable.

The lesson drawn from the quench scenario is that large nucleus–sized domains can occur if the sigma mass is small. It is quite possible that the effective m_σ is reduced from the 600 MeV free space value in the high energy density heavy ion environment [6, 7]. In fact, at a truly second order phase transition one expects m_σ — the inverse correlation length — to vanish! In that case, the parameters of the effective potential for our model cannot be *naively* taken from the zero temperature Gell–Mann—Levy model as we have done.

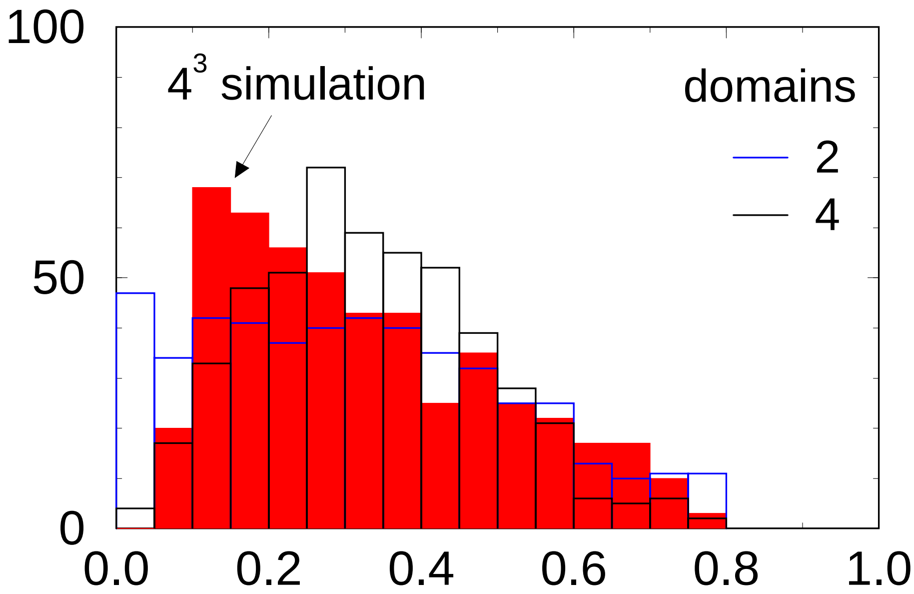

Figure 8: The probability distribution for the fraction of neutral pions f calculated in the linear sigma model.

To explore the role of the medium in domain formation, Gavin and Müller studied the dynamical evolution of the condensate in the presence of a nonequilibrium bath of quasiparticles [8]. The three-dimensional expansion of the heat bath changed the effective potential rapidly enough to create a quench-like condition. The size scale was for domains was found to be somewhat larger, perhaps $\sim 3-6$ fm, compared to fixed-geometry quench simulations [5] and one-dimensional Bjorken-scaling expansion [9]. This result has been verified by simulations by Randrup [10]. [This use of the term "annealing" in ref. [8] is misleading. Annealing simulations in [9] simulate true annealing, where both the order parameter and quasiparticles are essentially in thermal equilibrium. In ref. [8], the order parameter is assumed to be out of equilibrium while the quasiparticles are in equilibrium.]

The properties of strongly-interacting matter can change drastically as the temperature is raised above a value $T_c \approx 150$ MeV, perhaps undergoing a phase transition. The light up and down quarks have masses of about 7.5 MeV, much smaller than this temperature. On the other hand, the strange quark has a mass of about $m_s \sim 150$ MeV, coincidentally very close to T_c. In the chiral limit with massless light quarks, the phase transition would be second order if the strange quark mass were much larger than T_c, or first order if the mass were much smaller. If this regime describes real world QCD, then disoriented chiral condensates are likely to be observed at RHIC.

How well does the O(4) linear sigma model describe high temperature QCD? Gavin, with Gocksch and Pisarski, pointed out that, if we could vary m_s as a parameter, we would eventually reach a critical point, analogous to that in the liquid-gas phase transition. Specifically, they addressed the nature of the chiral transition in [14], studying the dependence of QCD on m_s in the SU(3) linear sigma model. Increasing the quark masses but keeping the strange-to-light-quark fixed at the natural value ~ 20 decreases the strength of this first order transition until a second order chiral critical point is reached. We find that a scalar

$\sigma_{\eta'}$ meson — the parity partner of the η' — becomes massless at that point. Together with recent lattice simulations, these results provide the first indication that QCD in the real world can be near a Z(2) critical point in the universality class of the liquid-gas system. Whether or not the real world is near the chiral critical point remains an issue of current debate in the lattice QCD community. It is not clear from lattice results which side of the critical line we are on.

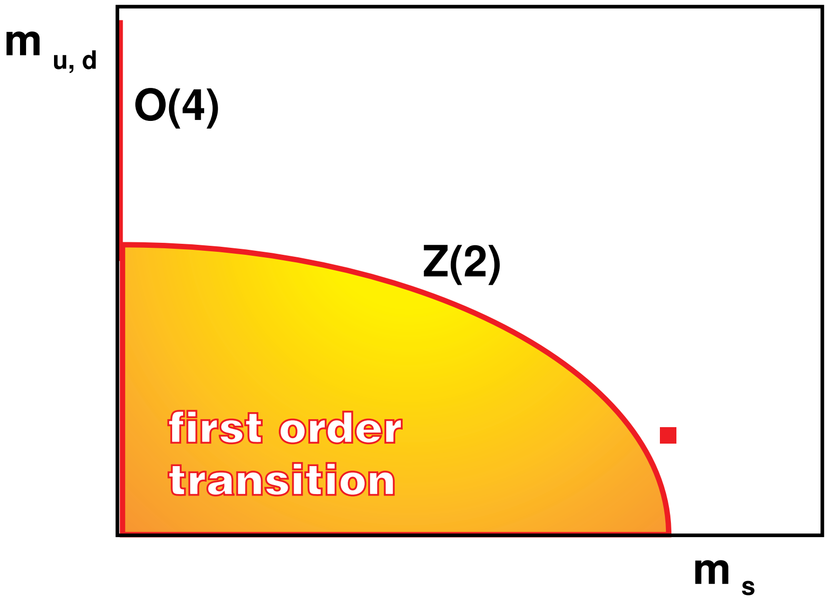

Figure 9: Columbia plot [16] showing the order of the QCD phase transition as a function of the light and strange quark masses. The shaded area denotes values for which the phase transition is first order. The phase transition is second order along the red lines. The red square indicates the likely mass values in the real world.

We start at zero temperature by fitting the scalar and pseudoscalar mass spectrum in QCD to that found in a linear sigma model. For three quark flavors we introduce the field Φ ($\sim \overline{q}_{left}\, q_{right}$), as a complex valued, three by three matrix, $\Phi = \sum_{a=0}^{8}(\sigma_a + i\,\pi_a)t^a$; $t_{1\ldots8}$ are the generators of the $SU(3)$ algebra in the fundamental representation, and t_0 is proportional to the unit matrix. The effective lagrangian for the Φ field is taken to be [15]

$$\mathcal{L} \;=\; tr\,|\partial_\mu \Phi|^2 \;-\; tr\left(H(\Phi+\Phi^\dagger)\right) \;+\; \mu^2\, tr\left(\Phi^\dagger\Phi\right) \qquad (39)$$

$$-\;\sqrt{6}\,c\left(det(\Phi)\;+\;det(\Phi^\dagger)\right) \;+\; (g_1-g_2)\left(tr\Phi^\dagger\Phi\right)^2 \;+\; 3\,g_2\,tr\left(\Phi^\dagger\Phi\right)^2$$

The parameters of the linear sigma model are the background field H, a mass parameter μ^2, an "instanton" coupling constant c, and two quartic couplings, g_1 and g_2. Neglecting effects from $m_u \neq m_d$, for the background field H we take $H = h_0\,t_0 - \sqrt{2}\,h_8\,t_8$. The current quark masses are then related to the background field as $m_u = m_d \sim h_0 - h_8$ and $m_s \sim h_0 + 2\,h_8$. Our $T = 0$ results agree with those of Chan and Haymaker [15].

We then explore the nature of the phase diagram as a function of the quark masses $m_u = m_d$ versus m_s [16]. We find that along the entire line of chiral critical points, only the

$\sigma_{\eta'}$ is massless, but that the singlet/octet ratio in the $\sigma_{\eta'}$ changes. At the $SU(3)$ symmetric point, $m_u = m_d = m_s$, the $\sigma_{\eta'}$ is an $SU(3)$ singlet. Decreasing m_s to the critical point where $m_s = 0$ and $m_u = m_d \neq 0$, the $\sigma_{\eta'}$ becomes entirely strange, $\sigma_{\eta'} \sim \bar{s}s$.

The opposite limit of $SU(2)$ chiral symmetry, $m_u = m_d = 0$, is more familiar. Assume, as in ref. [16], that the chiral phase transition with two massless flavors is of second order, with the universality class that of an $O(4)$ critical point. There is then a special value of $m_{strange} = m_{strange}^{crit}$, with a line of $O(4)$ critical points for $m_s > m_s^{\rm crit}$, and a line of first order transitions when $m_s < m_s^{\rm crit}$.

At the time [14] was written, parameters for the linear sigma model were fit by identifying the mass of the $\sigma_{\eta'}$ with that of the $a_0(980)$. However, since then the Particle Data Group has recently added a $\sigma(600)$ to its list of particles. This meson may possibly correspond to Rajagopal and Wilczek's SU(2) symmetric sigma meson, *i.e.* the chiral partner of the pion. Certainly, feeding that identification into our analysis will change the results, and can have important implications regarding whether the real world is closer to O(4) or Z(2) behavior.

Suppose now that we make a DCC — how can we tell? Let us focus on the O(4) case. Disoriented chiral condensate production results in a fluctuation of the number of charged and neutral pions at low transverse momentum, perhaps $< 100 - 200$ MeV. The signature of this phenomenon is a probability distribution of the fraction of of neutral pions that is broader than a gaussian. The task of discovering DCC therefore amounts to determining charged and neutral pion distributions at low p_T either in individual events or in event classes (superevents).

Gavin obtained the estimate of the magnitude of the DCC signal in heavy ion collisions by supposing that each collision is dominated by a single large domain [11]. In this case, the number of pions is determined by the amount of energy available for pion production per unit volume, which is essentially the potential difference $\Delta V \sim 60$ MeV fm^{-3} between $\Phi = 0$ and $\Phi = (f_\pi, \vec{0})$. If all of the energy in a domain of size $\xi \sim 3$ – 4 fm goes into pion production, one expects $N_{\rm DCC} \sim \Delta V \xi^3/m_\pi \sim 30$ – 100 pions. In comparison, conventional production mechanisms in a central Au+Au collision at RHIC can produce ~ 350 neutral pions per unit rapidity; this constitutes a background to the DCC signal.

The source of pions from this domain is coherent and, therefore, concentrated at low transverse momenta. Pions are radiated from the coherent state [12] describing such a domain give rise to a distribution:

$$E\left(\frac{dN}{d^3p}\right)_{\rm DCC} \propto {\rm e}^{-r^2/R^2}, \tag{40}$$

where R is the size scale of the domain. Coherent production from the domain adds to incoherent production from the underlying event (the "heat bath"), so that the total distribution is

$$E\left(\frac{dN}{d^3p}\right)_{\rm tot} = E\left(\frac{dN}{d^3p}\right)_{\rm background} + E\left(\frac{dN}{d^3p}\right)_{\rm DCC}. \tag{41}$$

For a background distribution taken from the HIJING event generator [13], the calculated distribution is shown in Fig. 10.

Gavin has distributed a monte carlo event generator that produces charged an neutral pions from a single large DCC to aid RHIC experimenters in testing their event-by-event

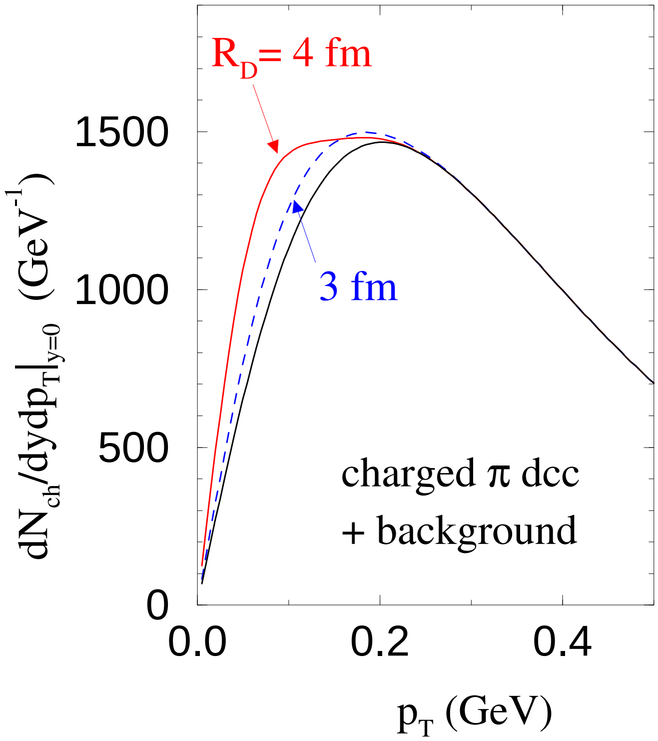

Figure 10: The distribution of charged pions from a single large DCC of sizes 3 fm (dashed curve) and 4 fm (solid curve) in Au+Au at RHIC. The background (heavy solid curve) is estimated using HIJING.

sensitivity to low momentum pions. This generator has been used by RHIC PHENIX, STAR and PHOBOS, CERN WA98 and AGS E864 and E866, to name a few.

New excitement surrounds the possibility of looking for event structure, whether by wavelet analysis or by lego plots. Generally, a collision can form many domains with a range of sizes, rather than a single dominant structure. The distribution that gives rise to EdN/d^3p is then broader and without the bump at low p_T. This is not a "bug" as first feared, but a "feature" — a feature that one can search for. Specifically, the spatial structure of DCC events can translate into momentum space structure that experiments can probe for.

Future work:

To help experimenters develop the more sophisticated analysis tools needed to search for this structure, Rajagopal and Gavin are developing an event generator that generates the DCC signal pions using occupation numbers generated from classical field simulations. These are then added to a background from HIJING. This prescription shares much of the ad hoc nature of my earlier generator. However, there remain many obstacles to building a theoretically well founded event generator for RHIC experiments, and the time for beam at RHIC is coming closer.

How would an approximate Z(2) transition differ from an approximate O(4) transition? What are the phenomenological implications for heavy ion collisions? If the real world is near the chiral critical point, heavy ion collisions can result in nonequilibrium behavior of the $\sigma_{\eta'}$ field. Because this field has $s\overline{s}$ as well as light-quark content, its fluctuations can result in both kaon and pion fluctuations. This behavior is different from the 'familiar' disoriented chiral condensates, which correspond to a world in which QCD has O(4) chiral phase transition. The formation of O(4) DCC affects only pion production. Moreover, nonequilbrium behavior near a Z(2) critical point will shift the masses of the η and the η', leading to enhanced photon production [17]. We intend to investigate the phenomena in the context of the linear sigma model.

References

[1] K. Rajagopal and F. Wilczek, Nucl. Phys. B379 (1993) 395; B404 (1993) 577.

[2] K. Rajagopal, HUTP-95-A013 (1995), to appear in Quark Gluon Plasma, 2nd edition, R. Hwa ed., World Scientific.

[3] J.D. Bjorken, K.L. Kowalski and C.C. Taylor, SLAC-PUB-6109 (1993); K.L. Kowalski and C.C. Taylor, CWRUTH-92-6 (1992), hep-ph/9211282; A.A. Anselm and M.G. Ryskin, Phys. Lett. B266 (1989) 482; J.-P. Blaizot and A. Krzywicki, Phys. Rev. D46 (1992) 246.

[4] G. Baym and G. Grinstein, Phys. Rev. D15 (1977) 2897; H. E. Haber and H. A. Weldon, Phys. Rev. D25 (1982) 502; K. M. Benson, J. Bernstein, and S. Dodelson, Phys. Rev. D44 (1991) 2480.

[5] S. Gavin, A. Gocksch and R.D. Pisarski, Phys. Rev. Lett. 72 (1994) 2143.

[6] D. Boyanovsky, H.J. de Vega and R. Holman, Phys. Rev. **D51**, 734, (1995).

[7] F. Cooper, Y. Kluger, E. Mottola and J.P. Paz, Phys. Rev. **D51**, 2377 (1995).

[8] S. Gavin and B. Müller, Phys. Lett. B329 (1994) 486.

[9] M. Asakawa, Z. Huang, X.-N. Wang, Phys. Rev. Lett. **74**, 3126 (1995).

[10] J. Randrup, Phys. Rev. Lett. **77**, 1226, (1996).

[11] S. Gavin, Nucl. Phys. **A590**, 163c, (1995).

[12] D. Horn and R. Silver, Ann. Phys. (N.Y.) 66 (1971) 509; M. Gyulassy, S.K. Kauffmann, L.W. Wilson, Phys. Rev. C20 (1979) 2267; R.D. Amado , F. Cannata, J.P. Dedonder, M.P. Locher, Bin Shao, Phys. Rev. Lett. 72 (1994) 970.

[13] X.-N. Wang and M. Gyulassy, Comput. Phys. Commun. **83**, 307, (1994),

[14] S. Gavin, A. Gocksch and R.D. Pisarski, Phys. Rev. D49 R3079 (1994).

[15] L.-H. Chan and R. W. Haymaker, Phys. Rev. **D7**, 402 (1973).

[16] F. R. Brown *et al.*, Phys. Rev. Lett. **65**, 2491 (1990).

[17] Z. Huang and X.-N. Wang, Phys. Rev. **D53**, 5034 (1996).

Wavelet Analysis of the DCC in Heavy-Ion Collisions

(*Ina Sarcevic, Zheng Huang, Xin-Nian Wang and R.L. Thews*)

Detection of DCC [1], would provide valuable information on the vacuum structure of the strong interaction and the nature of the chiral phase transition. Preliminary theoretical investigations on non-equilibrium dynamics using the classical linear σ-model have found some evidence for the growth of long wavelength pion modes, which may indeed lead to domain structure or cluster formation [2, 3]. If there are many uncorrelated small domains, the integrated probability distribution of the neutral pion fraction f emitted from a disoriented region, predicted to be $P(f) = 1/2\sqrt{f}$, [1] would become Gaussian. This makes the experimental search for the DCC signal a rather difficult task. In order to disentangle the DCC domain structure in high energy heavy-ion collisions, we propose a new method which emphasizes not only the behavior of the probability distribution in the full phase space region but also its fluctuation in rapidity η or azimuthal angle ϕ. In other words, one needs to study the "local" properties of the distribution in phase space if the DCC clusters are "localized" objects in phase space.

A novel method is a multi-resolution analysis performed by a discrete wavelet transformation (DWT) [4] which has been found effective in systematically detecting structures of various scales in turbulence, and multiparticle production.[5, 6] For any one-dimensional sample of a point distribution $f(x)$, such as the rapidity distribution of the neutral pion fraction in the interval $[0, 1]$ with resolution Δx, can be represented as a histogram of 2^J bins where $J = \mathrm{mod}(|\mathrm{ln}\Delta x|/\mathrm{ln}2) + 1$

$$f(x) \equiv f^{(J)}(x) = \sum_{k=0}^{2^J-1} f_{Jk}\phi_{Jk}(x), \tag{42}$$

where $\phi_{Jk}(x)$ are the piecewise constant functions called the mother functions. The histogram function at the next finer resolution is the average of adjacent bins at the finest scale. Evidently some detail is lost compared to (42). The difference between (42) and $f^{(J-1)}$ can be fully expressed in terms of the difference functions $\psi_{J-1,k}(x)$ which are stairwell functions called father functions. The difference amplitudes or one defines the DWT coefficients

$$\tilde{f}_{jk} = 2^j \int f(x)\psi_{jk}(x)dx, \tag{43}$$

where the basis functions $\psi_{jk}(x)$ have a unique property: they are related to each other by scaling and translation: $\psi_{jk}(x) = \psi(2^j x - k)$. The index j denotes the resolution scale and k the position at each scale. The idea of multiresolution analysis is to find representations of the sample function $f(x)$ at various scales. Unlike the Fourier transformation which requires the information in whole physical space, the wavelet SSD requires only the local information in space. Roughly speaking, the multiresolution analysis is a journey down (or up) a hierarchy of scales and to view the "world" in different "eyes" with magnifying or reducing glasses.

The central idea of using the wavelet analysis is to attempt an unbiased separation of the DCC physics from the various "backgrounds" which cannot be otherwise easily eliminated.

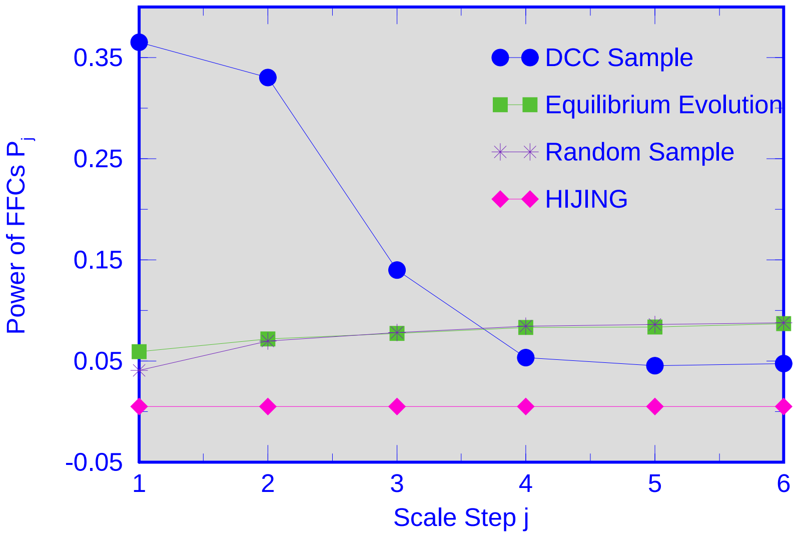

Figure 11: The power spectra of the wavelet coefficients for different dynamical scenarios.

The usual correlation method is not so effective here because the different scale correlations are mixed together in the same phase space. The discrete wavelet transformation (DWT), on the other hand, has an extra dimension – the scale which can be used to separate these correlations. The main source of the "backgrounds" is the fluctuations at small correlation scale due to pion radiation from the uncorrelated regions in space-time, which can coexist with a DCC domain. The background can also come from the partial thermalization of the system leading to thermal correlations.

We have calculated the wavelet power spectrum for rapidity distribution of the neutral pion fraction simulated using the classical linear σ model [3]. One defines the power spectrum with respect to the wavelet basis at each j as

$$P_j = \frac{1}{2^j} \sum_{k=0}^{2^j-1} |\tilde{f}_{jk}|^2 \ . \tag{44}$$

P_j is then the power of fluctuations on length scale $L/2^j$. It is also the mean square of the probability distributions of the wavelet coefficients defined in (43). The result is shown in Fig. 11. For the random samples and the equilibrium evolution of the classical field where there is no DCC production mechanism, the wavelet power is flat indicating there is no sensitivity on the change of the scale. For the DCC samples, the power starts to build up as j goes down below $j_d \sim 4$ and rises rather quickly, departing distinctively from the equilibrium and the random cases. This suggests the existence of the DCC clustering with a typical size of $\Delta\eta_d = 2\eta_{\max}/2^{j_d} \simeq 0.8$ units in rapidity. Also plotted is the power spectrum from HIJING Monte Carlo data which also features a flat distribution.

Our wavelet analysis has attracted a lot of attention and has been already used by WA98 Collaboration for studying DCC formation in Pb+Pb collisions at CERN [7]. Wavelet analysis will also be used by the STAR Collaboration at RHIC, whose preliminary studies are shown in Fig. 12 below.

References

[1] J. -P. Blaizot and A. Krzywcki, Phys. Rev. D**46**, 246 (1992); J. D. Bjorken *et al.*, SLAC preprint SLAC-PUB-6109.

[2] K. Rajagopal and F. Wilczek, Nucl. Phys. **B404**, 577 (1993).

[3] Z. Huang and X.-N. Wang, Phys. Rev. **D49**, R4339 (1994); M. Asakawa, Z. Huang, and X.-N. Wang, Phys. Rev. Lett. **74**, 3126 (1995)

[4] Z. Huang, I. Sarcevic, R. Thews and X.-N. Wang, Phys. Rev. **D54**, 750 (1996).

[5] M. Farge, Ann. Rev. Fluid. Mech. **24**, 395 (1992).

[6] M. Greiner, P. Lipa and P. Carruthers, Phys. Rev. **E51**, 1948 (1995)

[7] T. Nayak, plenary talk at Quark Matter '97, Tsukuba, Japan, December, 1997.

Event Structure of DCC

(*Sean Gavin)*

Gavin with R. Bellwied and T. Humanic, collaborators at RHIC experiment STAR, are now exploring the effect of collective flow and final state scattering on DCC signals [1]. We can see the importance of flow by considering the following illustration. At midrapidity in a central symmetric heavy ion collision, the matter tends to flow radially outward from the origin. Suppose that as the system cools below T_c, a DCC forms with a field configuration such that it will radiate only charged pions for $x > 0$ and only neutral pions for $x < 0$. At each point the DCC will have the same average radial velocity as the underlying matter (in the matter's local rest frame, the pion field has no preferred direction). Therefore, the charged pions exhibit a net flow towards $x > 0$. An appropriate experiment would detect directed flow towards $+x$. Such flow is entirely unexpected because the collision system is symmetric, *i.e.* the impact parameter is zero. More generally, radiation from DCC can produce pions that reflect the velocity field of the underlying fluid, thereby resulting in an apparent azimuthal anisotropy.

To study the effect of flow in a realistic setting in which pion scattering can occur, Bellweid, Gavin and Humanic combine Gavin's monte carlo DCC generator [2] with Humanic's hadronic cascade code [3]. The cascade assumes an initial distribution of mesons with a Bjorken geometry, but then allows them to scatter with cross sections taken from phenomenology. Scattering tends to absorb or thermalize pions from DCC domains produced in the interior of the collision volume. The following figure shows the effect of scattering

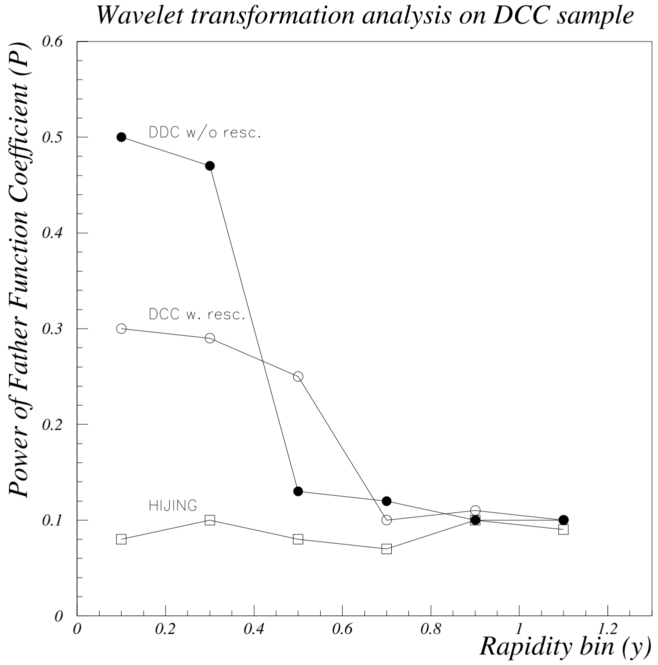

Figure 12: Wavelet analysis from Bellwied, Gavin and Humanic for a DCC in the center of a simulated Au+Au collision at RHIC with cascading included.

on DCC centered at the origin as seen in a wavelet analysis. The STAR acceptance is assumed. For a DCC in the center of a collision volume, none of the flow effects are present. Nevertheless, the wavelet analysis still picks out a signal.

In contrast, we expect that the anisotropy resulting from a moving, off-center domain to actually be *enhanced* by the scattering of DCC pions. Pions with momenta oriented towards the center of the collision region have a greater chance of scattering than outbound pions. Inbound pions are likely to rescatter, while outbound DCC pions have a good chance of escaping without scattering.

References

[1] R. Bellwied, S. Gavin and T.J. Humanic, in preparation.

[2] S. Gavin, Nucl. Phys. **A590**, 163c, (1995).

[3] T.J. Humanic, Phys. Rev. **C53**, 901, (1996).

HBT from DCC

(*Sean Gavin and and Ina Sarcevic)*

We plan to study the question of how DCC influences the Bose correlations of pairs of identical pions (see [1] for a preliminary analysis). Pions produced by conventional scattering mechanisms are largely incoherent, and exhibit an intensity interference that is analogous to the Hanbury–Brown—Twiss effect for photons [2, 3]. Measurements of $\pi\pi$ correlations are typically used to study information on the size of the interaction volume in nuclear collisions, much as the HBT effect is used to measure the size of stars (although interpretation of experiments is highly nontrivial). In contrast, a fully coherent source of pions exhibits interference at the amplitude level. Consequently, the single particle spectrum from an isolated domain depends on the size of the domain, while the pair distribution is simply the product of single particle spectra.

The formation of DCC will therefore suppress the HBT effect in a nuclear collision if a large domain forms. However, the HBT effect does not completely disappear, since intensity interference can occur when a pion from the DCC has a similar momentum to a background pion. In general, the four point function determines the normalized two pion rate

$$C(p_1, p_2) \propto \sum_{i,j,k,l} \mathrm{e}^{-ip_1\cdot(x_i-x_k)-ip_2\cdot(x_j-x_l)} \langle \pi^0(x_i)\pi^0(x_j)\pi^0(x_k)\pi^0(x_l)\rangle \tag{45}$$

The HBT signal from a single DCC is

$$\begin{aligned} C(p_1, p_2) &= 1 + (1 - D(p_1))(1 - D(p_2))\tilde{\rho}(q)^2 \\ &+ 2\{D(p_1)D(p_2)(1 - D(p_1))(1 - D(p_2))\}^{1/2}\tilde{\rho}(q), \end{aligned} \tag{46}$$

where $q = p_1 - p_1$ is the relative momentum of the pair and $\tilde{\rho}$ is the Fourier transform of the space–time density of the background pions. This result depends strongly on the fraction of coherent pions $D = (dN/d^3p)_{\rm DCC}/(dN/d^3p)_{\rm tot}$.

The possible impact of a DCC on $\pi^-\pi^-$ correlations is illustrated in fig. as a function of domain size, assuming that the domain produces only charged pions and that the transverse source size for the HIJING background is 7 fm. A combination of one– and two–particle measurements can allow one to disentangle the DCC signal from the background.

This estimate is derived assuming that the quantum state of the DCC is a simple type of coherent state that only conserves isospin on the average. Coherent states that strictly enforce isospin conservation have also been proposed [4]; see also the paper by Horn and Silver in ref. [2]. Kogan has proposed that the DCC may be a novel squeezed state [5]. Amado and Kogan have shown that the fluctuations of neutral and charged particles differ for these different states [5], and it is plausible that the four point function differs as well.

References

[1] S. Gavin, Nucl. Phys. **A590**, 163c, (1995).

[2] D. Horn and R. Silver, Ann. Phys. (N.Y.) 66 (1971) 509; M. Gyulassy, S.K. Kauffmann, L.W. Wilson, Phys. Rev. C20 (1979) 2267; R.D. Amado , F. Cannata, J.P. Dedonder, M.P. Locher, Bin Shao, Phys. Rev. Lett. 72 (1994) 970.

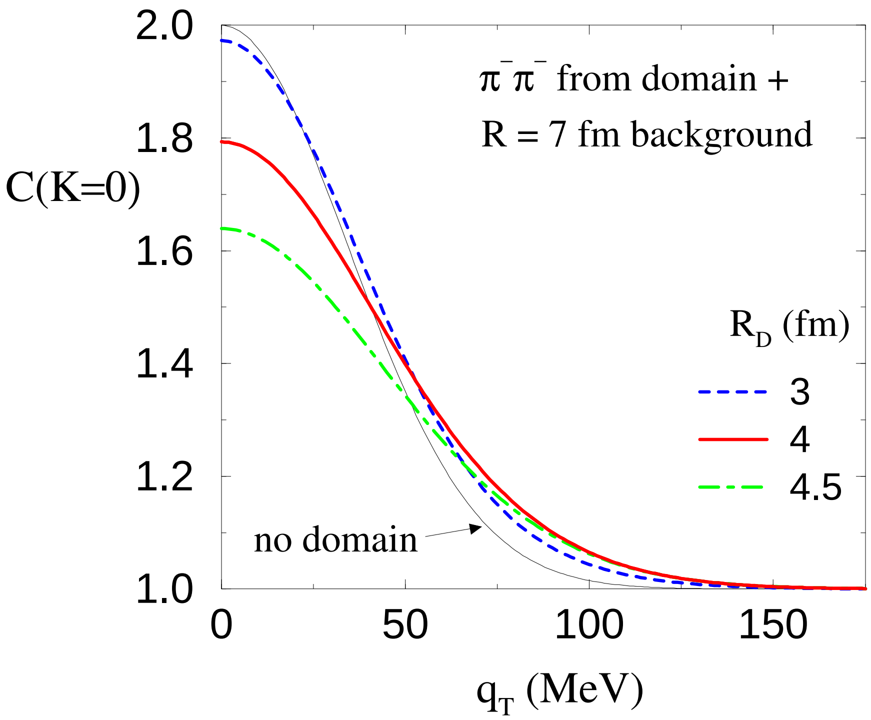

Figure 13: $\pi^-\pi^-$ correlations as a function of $q_T = p_{T1} - p_{T2}$ from a single large DCC plus a background of incoherent pions in Au+Au at RHIC. The total momentum of the pair is taken to be $K = (p_{T1} + p_{T2})/2 \equiv 0$.

[3] W. Zajc, in NATO Workshop on Particle Production in Highly Excited Matter, H. H. Gutbrod and J. Rafelski eds., (Plenum, 1993), p. 427.

[4] T.D. Cohen, M.K. Banerjee, M. Nielsen, X.-M. Jin Phys. Lett. B333 (1994) 166.

[5] R.D. Amado and I.I. Kogan, Phys. Rev. D51 (1995) 190; I.I. Kogan, JETP Lett. 59 (1994) 307.

Dynamics of Chiral Condensate Formation

(Sean Gavin)

Gerd Welke and I plan to study the dynamics of DCC formation in nuclear collisions. Nuclear collisions produce a distribution of pions that, in general, bears no relation to the equilibrium distribution of pions in a "box" the size of the collision volume. Collisions and expansion then tend to drive these particles towards equilibrium. Gavin and Ruuskanen and Welke *et al.* [1] observed that SPS S+A collisions can produce pions in a larger number than the thermal equilibrium number given the energy and volume of the collision region. If a large enough number of pions were produced, a fraction of these pions would tend to form a Bose condensate as in an ideal Bose gas. Whether or not a condensate forms will depend on how rapidly the system expands compared to the time scale for condensate formation. Gavin and Ruuskanen found that the density was not high enough for condensation of an ideal Bose gas.

However, the pion fluid is not an ideal gas but a strongly interacting system, with interactions described approximately by the linear sigma model. Even if the system is in thermal thermal equilibrium at temperatures above T_c, a condensate – the sigma condensate – must form as the temperature drops. Haber and Weldon have shown that the phase diagram of the linear sigma model is very different from that of an ideal pion gas [2]. Earlier studies [1] must then be reexamined.

If the initial density is above equilibrium for that temperature and volume, then the σ and π condensate will be enriched as T drops. The time scale for condensation to occur is m_σ^{-1}, and as we know this time can be rapid in the real world where $m_\pi \neq 0$. Condensed matter physicists have made great advances in understanding the dynamics of Bose condensation. Gavin and Welke plan to apply techniques developed by Kagan et al. [3] to the study of dynamic chiral condensation at RHIC and SPS energies.

References

[1] S. Gavin and P.V. Ruuskanen "Low-p_T Pion Enhancement from Partial Thermalization," Phys. Lett. **262B**, 326 (1991); G.M. Welke and G.F. Bertsch, Phys. Rev. **C45**, 1405, (1992)

[2] H. E. Haber and H. A. Weldon, Phys. Rev. D25 (1982) 502.

[3] See Yu. Kagan, B.V. Svistunov, to be published in Phys. Rev. Lett., cond-mat/9709032 (1997), and refs. therein.

Dilepton and Photon Production from a Coherent Pion Oscillation

(*Z. Huang and X.-N. Wang*)

Preliminary studies of DCC [1] have suggested that there may be a coherent pion field oscillation following a nonequilibrium second order phase transition which may lead to characteristic soft pion production [2, 3]. According to a "Baked Alaska" scenario suggested by Bjorken, Kowalski and Taylor [1], the collision debris in a high energy central event form a "hot" source on the light front and move outward while emitting quasi-goldstone bosons in the cool interior of light cone. These pions are not assumed to reach a thermal equilibrium, rather, they behave collectively and a coherent field description is more relevant. The space-time evolution of the condensate field is mainly determined by the classical equation of motion for a low energy effective theory such as a linear or nonlinear σ model. Eventually, the "disoriented vacuum" relaxes back to normal vacuum by emitting physical pions. The final hadrons, however, are emitted from on the freeze-out hyper surface and the information on the space-time evolution of the coherent field is partially lost.

In contrast, the electromagnetic signature is known to be an ideal probe of a dense hadronic matter [4] owing to the fact that it escapes the strong interaction region once produced without further final state interactions and thus carries the information on the early dynamical evolution. We study the dilepton and direct photon production from the classical pion field in the context of a disoriented chiral condensate (DCC) or most generally a nonequilibrium pion cloud. We develop a general formalism for the dilepton and photon emissions in the presence of a classical electromagnetic current. Since the electromagnetic current coincides with the third component of the isovector current, the isospin angular oscillation of the condensate field can be a significant source for the electromagnetic emission in the low mass (transverse momentum) region. As an example, we calculate the dilepton and photon spectra in an analytical solvable model where a general class of solutions are obtained by Blaizot and Krzywicki [5] and by Huang and Suzuki [6]. Although our formalism for the emission rate is quite general, the model for the classical field evolution is clearly an oversimplified version of a more realistic situation. Nevertheless, it may capture the essential features of soft pion production such as the light cone singularity, the boost invariance and the longitudinal expansion. The results obtained should only be taken as indicative, and a detailed comparison with the experimental data is only possible when a more realistic study is available. Fortunately, such an approach is already in progress [7].

The pionic part of electromagnetic interactions is introduced by replacing (we neglect the anomalous electromagnetic coupling) $\partial_\mu \boldsymbol{\pi}$ by $\partial_\mu \boldsymbol{\pi} + \frac{ie}{\sqrt{2}}[\boldsymbol{\pi}, Q]\mathcal{A}_\mu$ in the kinetic part of lagrangian

$$\mathcal{L}^{\rm em}(x) = ie[\pi^-(x)\partial_\mu \pi^+(x) - \pi^+(x)\partial_\mu \pi^-(x)]\mathcal{A}^\mu(x) = -eJ^{\rm cl}_\mu(x)\mathcal{A}^\mu(x) \ , \tag{47}$$

where $\mathcal{A}_\mu$ is the photon field and $J^{\rm cl}_\mu$ is the third component of the classical isospin current $J^{\rm cl}_\mu(x) = (\boldsymbol{\pi}(x) \times \partial_\mu \boldsymbol{\pi}(x))_3$. To $O(e^2)$, the matrix element for the dilepton emission from the classical field [8, 9, 10, 11] is

$$\mathcal{M} = \langle \ell^+\ell^-|S^{(2)}|0\rangle = e^2\bar{u}(p_1)\gamma_\nu v(p_2)D^{\nu\mu}(p_1+p_2)J^{\rm cl}_\mu(p_1+p_2) \ , \tag{48}$$

where $J^{\rm cl}_\mu(p_1+p_2)$ is the Fourier transformation of $J^{\rm cl}_\mu(x)$, u and v are the Dirac spinors for the electron and positron, $D^{\nu\mu}$ is the photon propagator. The number of dileptons produced per final state phase space is

$$\begin{aligned} dN_{\ell^+\ell^-} &= \sum_{\rm spin} |\mathcal{M}|^2 \frac{d^3p_1}{(2\pi)^3 2E_1}\frac{d^3p_2}{(2\pi)^3 2E_2} \\ &= \int d^4q\,\delta^4(q-p_1-p_2)\sum_{\rm spin}|\mathcal{M}|^2\frac{d^3p_1}{(2\pi)^3 2E_1}\frac{d^3p_2}{(2\pi)^3 2E_2} \ . \end{aligned} \tag{49}$$

The dilepton differential distribution with respect to the lepton pair 4-momentum q is then

$$\frac{dN_{\ell^+\ell^-}}{d^4q} = \frac{\alpha^2}{6\pi^3}\frac{B}{q^4}[q^\mu q^\nu - q^2 g^{\mu\nu}]J^{\rm cl}_\mu(q)J^{\rm cl*}_\nu(q) \ , \tag{50}$$

where $B = [1 + 2m_\ell^2/q^2][1 - 4m_\ell^2/q^2]^{1/2}$ and m_ℓ is the lepton mass. Similarly, the direct photon momentum distribution is calculated

$$\frac{dN_\gamma}{d^3\boldsymbol{q}/\omega_q} = -\frac{\alpha}{(2\pi)^2}J^{{\rm cl}\mu}(q)J^{\rm cl*}_\mu(q) \ , \tag{51}$$

where q stands for the photon 4-momentum. Moreover, splitting the current into parts parallel and orthogonal to q_μ: $J^{\rm cl}_\mu(q) = q_\mu J^{\rm para}(q) + J^{\rm tr}_\mu(q)$, one finds that only the orthogonal part contributes to the emissions. The dependence of the electromagnetic spectra on the space-time history is entirely contained in the Fourier transformation of the isospin current.

We present the idea by examining some simple scaling solutions in the 1+1 boost invariant model which are first obtained by Blaizot and Krzywicki [5]. Since the calculation is fully analytical, we hope to understand some qualitative features of dilepton production from the classical field. The lagrangian for the nonlinear σ model is

$$\mathcal{L} = \frac{f_\pi^2}{4}\mathrm{tr}\Big[\partial_\mu \Sigma^\dagger(x)\partial^\mu \Sigma(x)\Big] + \frac{m_\pi^2 f_\pi^2}{4}\mathrm{tr}\Big[\Sigma^\dagger(x) + \Sigma(x)\Big], \tag{52}$$

where one defines the pion field by $\sigma + i\boldsymbol{\tau}\cdot\boldsymbol{\pi} = f_\pi \Sigma$ with the constraint $\sigma = \sqrt{f_\pi^2 - \boldsymbol{\pi}^2}$. Σ transforms like $\Sigma \to U_L \Sigma U_R^\dagger$ under $SU(2)_L \times SU(2)_R$ rotations. We are interested in an idealized boost-invariant case [12] where the field $\boldsymbol{\pi} = \boldsymbol{n}(\tau)\pi(\tau, \boldsymbol{x}_\perp)$, i.e. the orientation $\boldsymbol{n}$ of the pion field is only function of the proper time τ defined by $\tau = \sqrt{t^2 - z^2}$ and uniform in spatial rapidity and transverse coordinates $\boldsymbol{x}_\perp$. This would correspond to a single DCC domain in the transverse dimension. The transverse profile of the field amplitude π^2 is determined by the shape and size of the DCC domain, which we take a Gaussian form as suggested in numerical simulations [3]

$$g(\boldsymbol{x}_\perp) = \exp[-|\boldsymbol{x}_\perp|^2/R_D^2] \ , \tag{53}$$

where R_D is the size of a DCC domain (typically $R_D = 1 \sim 2$ fm [3]). Such a class of solutions are well known to predict a distinctive neutral pion probability distribution

$$\frac{dP}{df} = \frac{1}{2\sqrt{f}} \ , \tag{54}$$

where P is the probability of find a neutral pion fraction $f = N_{\pi^0}/(N_{\pi^0} + N_{\pi^\pm})$. However, if there exists more than one DCC domain, as it is likely the case especially in heavy-ion collisions where the transverse dimension R_A of the interaction volume is much larger than the size of a DCC domain R_D, the field orientation $\boldsymbol{n}$ could depend on the transverse coordinates $\boldsymbol{x}_\perp$. In this case, the prediction (54) in general no longer holds. Such a possibility can only be studied in detail in numerical simulations. We confine ourselves to the case when the single domain dominates and only comment on how our result might change in a multi-domain case.

According to the "Baked Alaska" scenario [1], the boundary conditions for the solutions are imposed such that the classical waves propagate forward in proper time, starting at an initial time τ_0.In other words, we are interested in a retarded wave that vanishes when $\tau < \tau_0$ and $t < \tau_0$. Such a solution only exists when there is a source located on the hyperbola of equal $\tau = \tau_0$. The "hot" source can be regarded as the summation of the degrees of freedom other than pion modes. Away from the source located near the surface of the light cone, the field propagates freely and one should have the (partial) conservation of (axial) isovector currents

$$\begin{aligned} \partial_\mu \boldsymbol{V}^\mu &= \partial_\mu(\boldsymbol{\pi} \times \partial^\mu \boldsymbol{\pi}) = 0 \ , \qquad (\tau > \tau_0) & (55)\\ \partial_\mu \boldsymbol{A}^\mu &= \partial_\mu(\sigma\partial^\mu\boldsymbol{\pi} - \boldsymbol{\pi}\partial^\mu\sigma) = -m_\pi^2 f_\pi \boldsymbol{\pi} \ . \qquad (\tau > \tau_0) & (56) \end{aligned}$$

For a function only of τ, a partial derivative $\partial_\mu f(\tau)$ is equal to $(\tilde{x}_\mu/\tau) df/d\tau$ where $\tilde{x}_\mu = (t, z, 0, 0)$. Eq.(55) yields the integration

$$\boldsymbol{\pi} \times \partial^\mu \boldsymbol{\pi} = f_\pi^2 \boldsymbol{a} \frac{\tilde{x}_\mu}{\tau^2} g(\boldsymbol{x}_\perp) , \tag{57}$$

where $\boldsymbol{a}$ is a dimensionless constant vector in isospin space. In the chiral limit, the axial current is also conserved, which defines another constant vector $\boldsymbol{b}$ in isospin space with a constraint $\boldsymbol{a} \cdot \boldsymbol{b} = 0$ [5]

$$\boldsymbol{\pi} \partial^\mu \sigma - \sigma \partial_\mu \boldsymbol{\pi} = f_\pi^2 \boldsymbol{b} \frac{\tilde{x}_\mu}{\tau^2} g(\boldsymbol{x}_\perp) . \tag{58}$$

The pion field orientation vector $\boldsymbol{n}(\tau)$ precesses with proper time τ around $\boldsymbol{a}$ in the plane perpendicular to $\boldsymbol{a}$ [6].

The dilepton and photon emissions probe the nature of the source using time-like momenta $q = (q_0, q_{||}, \boldsymbol{q}_T)$ with $q^2 = M^2$ and $q^2 = 0$ respectively. The Fourier transformation of the electromagnetic current can be readily calculated in the light cone variables

$$\begin{aligned} J_\mu^{\rm cl}(q) &= f_\pi^2 a_3 \int d^4x e^{iqx} \frac{\tilde{x}_\mu}{\tau^2} \theta(\tau - \tau_0) g(\boldsymbol{x}_\perp) \\ &= -i f_\pi^2 a_3 \frac{\tilde{q}_\mu}{M_\perp} \frac{\partial}{\partial M_\perp} \int_{\tau_0} \frac{d\tau}{\tau} \int d\eta e^{iM_\perp \tau \cosh(\eta - y)} \int d^2\boldsymbol{x}_\perp g(\boldsymbol{x}_\perp) e^{-i\boldsymbol{q}_T \cdot \boldsymbol{x}_\perp} \\ &= -\frac{\pi^2 R_D^2}{2} f_\pi^2 a_3 \frac{\tilde{q}_\mu}{M_\perp^2} \exp[-q_T^2 R_D^2/4][J_0(M_\perp \tau_0) - i N_0(M_\perp \tau_0)] , \end{aligned} \tag{59}$$

where $\tilde{q}_\mu = (q_0, q_{||}, 0, 0)$, $M_\perp = \sqrt{q_0^2 - q_{||}^2}$ and J_0 and N_0 are the Bessel functions. For a direct photon, $M_\perp = q_T$. In deriving (59), we have performed the τ-integration from τ_0 to infinity. Since the electromagnetic current density decreases rapidly with the proper time, the integrated current turns out to be finite and the emission is most effective in the early evolution of the classical field. It is clear from (59) that due to the singular behavior of the Neumann function for small argument, the emission spectra are sensitive to the initial time scale τ_0. The exponential factor $\exp[-q_T^2 R_D^2/4]$ provides a strong q_T cutoff so that the emission is only significant in low momentum region. The constant a_3 can be estimated using the symmetry argument. The important assumption in the disoriented chiral condensate scenario is the equal probability of all internal orientations. The energy density due to the internal chiral oscillations should be equally distributed among all components of vectors $\boldsymbol{a}$ and $\boldsymbol{b}$. One thus has

$$\langle a_i^2 \rangle = \langle b_i^2 \rangle = \frac{1}{6} \frac{\epsilon_0 \tau_0^2}{2 f_\pi^2} \qquad (i = 1, 2, 3) . \tag{60}$$

where ϵ_0 is the initial energy density carried by the internal chiral oscillation at $\tau = \tau_0$, which may be roughly estimated assuming that it is comparable to the thermal energy density (in order for the DCC to have any physical significance). For some typical values $\epsilon_0 \sim 0.5 T_c^4 \sim 0.1$ GeV/fm^3 and $\tau_0 = 5$ fm/c, the average value of a_3^2 is about 4.8.

In Fig. 14 we numerically integrate over $M_\perp$ and plot the dilepton invariant mass spectrum for different values of $\tau_0 = 5, 10$ fm/c and $R_D = 1, 2$ fm. The a_3 is calculated from (60) assuming that the initial energy density for the internal chiral oscillations is 0.1 GeV/fm^3. Also plotted in Fig. 14 is the typical thermal spectrum of dilepton production mainly from

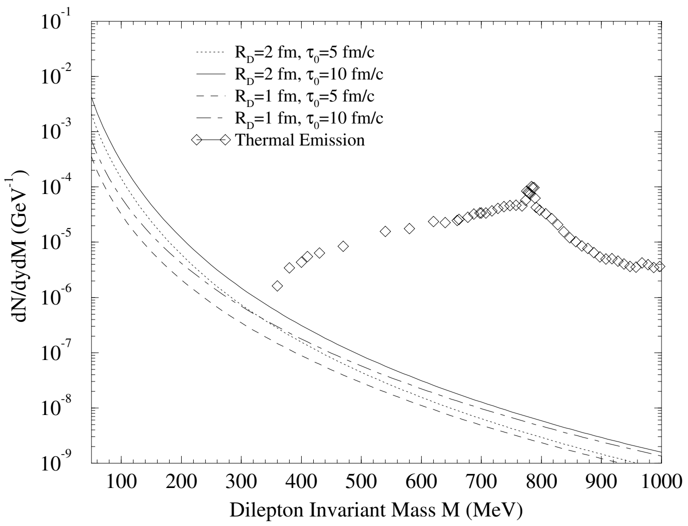

Figure 14: The dilepton invariant mass spectrum for different choices of initial time scale τ_0 and the coherent field domain size R_D. The initial energy density is assumed to be $\epsilon_0 = 0.1$ GeV/fm^3. The typical thermal spectrum due to the π-π annihilation is also plotted for a comparison.

π-π annihilation, which is taken from Ref.[11], where we have assumed the initial temperature of 160 MeV, the freeze-out temperature of 130 MeV, and the transverse size of system $R_A = 5$ fm suitable for heavy-ion collisions. Most notably, there does not exist a pion mass threshold for the dilepton production from the coherent field: the spectrum rises even below $M = 2m_\pi$. The finite pion mass plays no roles in the conserved isovector current whose third component directly couples to the photon. Therefore, the coherent field is most effective in producing lepton pairs in the low mass region $M < 2m_\pi$.

We have also studied the direct photon transverse momentum spectrum for different choices of τ_0 and R_D. The outstanding feature in the spectrum is the sensitivity on the domain size parameter R_D. The measurement of direct photon spectrum at very small transverse momentum can thus provide a sensitive probe of the spatial extension of the DCC domain.

In conclusion, we have demonstrated that the electromagnetic emission from a disoriented chiral condensate can be calculated using the space-time evolution of the classical field. The emissions due to the coherent isospin oscillation can be an important additional source to the electromagnetic signals from a dense hadronic matter, especially in low mass (momentum) region. Our results are based on an oversimplified model on classical field evolution and should only be taken as a qualitative estimation. Once a more realistic calculation is available, it would be very interesting to see whether or not the idea suggested may indeed provide some mechanism for the observed low mass dilepton enhancement by the CERES and HELIOS collaborations at CERN SPS experiments [13].

References

[1] J.D. Bjorken, K.L. Kowalski, C.C. Taylor, "Baked Alaska", SLAC-PUB-6109, 7th Les Rencontres de Physique de la Vallee d'Aoste: Results and Perspectives in Particle Physics, La Thuile, Italy, 7-13 March, 1993; A. A. Anselm and M. G. Ryskin, Phys. Lett. B **266**, 482 (1991); K. Rajagopal and F. Wilczek, Nucl. Phys. **B404**, 577 (1993).

[2] S. Gavin and B. Müller, Phys. Lett. **B329**, 486 (1994).

[3] S. Gavin, A. Gocksch, and R. D. Pisarski, Phys. Rev. Lett. **72**, 2143 (1994);M. Asakawa, Z. Huang, and X.-N. Wang, Phys. Rev. Lett. **74**, 3126 (1995);F. Cooper, Y. Kluger, E. Mottola, and J. P. Paz, Phys. Rev.**D51**, 2377 (1995); J. Randrup, LBL Preprint LBL-38125 (1996).

[4] E. Shuryak, Phys. Lett. **B79**, 135 (1978); K. Kajantie and H.I. Miettenen, Z. Phys. **C9**, 341(1981); K. Kajantie, J. Kapusta, L. McLerran and A. Mekjian, Phys. Rev. **D34**, 2476 (1986).

[5] J. -P. Blaizot and A. Krzywcki, Phys. Rev. D **46**, 246 (1992).

[6] Z. Huang and M. Suzuki, Phys. Rev. **D53**, 891 (1996).

[7] Y. Kluger and F. Cooper, Private communications.

[8] L. McLerran and T. Toimela, Phys. Rev. **D31**, 545(1985).

[9] P.V. Ruuskanen, in *Particle Production in Highly Excited Matter*, edited by H. Gutbrod (Plenum, New York, 1993).

[10] H. Weldon, Phys. Rev. **D42**, 2384 (1990).

[11] Z. Huang, Phys. Lett. **B361**, 131 (1995).

[12] J. Bjorken, Phys. Rev. **D27**, 140 (1983).

[13] G. Agakichiev, *et al.*, Phys. Rev. Lett. 75, 1272 (1995).

Charmonium Suppression

(*Sean Gavin and Ina Sarcevic*)

Charmonium suppression remains among the most exciting and tantalizing problems in relativistic heavy ion physics. At the Quark Matter '96 meeting, CERN Collaboration NA50 reported the first measurement of ψ and ψ' production in Pb+Pb collisions. Controversy developed as many asked if the data signaled quark gluon plasma formation [1]. At the meeting, Gavin and Vogt showed that the data agreed with predictions based on their comover model of charmonium suppression in nuclear collisions [2]. However, at the Quark Matter '97 meeting, NA50 reported results from a much more extensive data set. While the overall trend of this data is consistent with the '96 data, the new data may show one or perhaps two

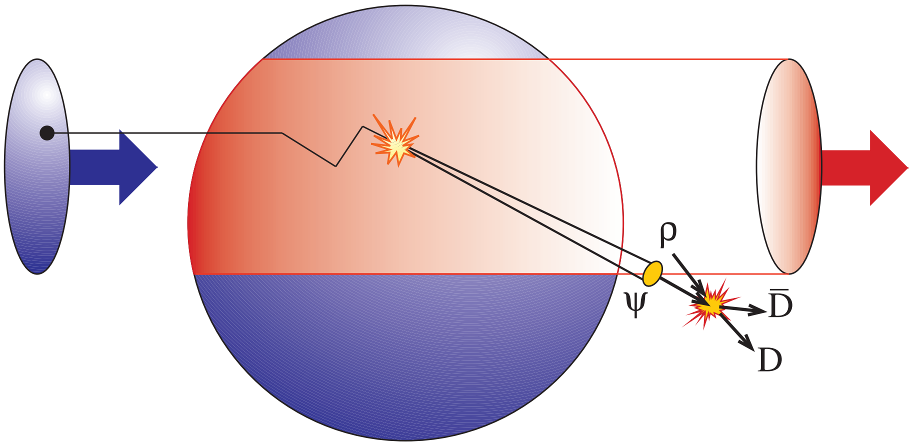

Figure 15: Conventional wisdom on charmonium suppression is summarized in this figure. The charm-anticharm pair is produced in a hard process as the projectile nucleus crashes through the target. Before that process, initial state scattering can occur broadening transverse momentum and possibly leading to energy loss. After formation, the pair can scatter in the nucleus or with comovers.

abrupt changes in the suppression. While data is as yet preliminary, even one such feature would be inconsistent with a model in which comovers are treated as hadrons.

Charmonium production provides a probe of the densities achieved in nucleus–nucleus collisions that is also sensitive to quark gluon plasma production. However, Gavin, Gyulassy, and Jackson [7] were the first to point out that scattering with hadronic comovers can explain data with light nuclear projectiles, $A < 32$. We know know that the plasma suppression occurs amid a host of background effects: initial state parton scattering, nucleon absorption, comover scattering, and nuclear dependence of the parton distributions (shadowing and EMC effects). Careful systematic studies of hadron–nucleus, hA, and nucleus–nucleus, AA, data are needed to distinguish these effects. Using with the latest hA and AA data on ψ and ψ' production from CERN, the comover model implies that Pb+Pb collisions achieve densities greater than ten times that of ordinary nuclear matter – if we ignore the discontinuities. Conventional nucleon–absorption alone cannot consistently describe the Pb data, constituting evidence of an additional high–density suppression mechanism such as scattering with co–moving mesons.

Agreement with Pb data would support our hadronic explanation, but would not rule out a contribution from plasma formation. The possible appearance of discontinuous behavior is exciting. Nevertheless, it is worthwhile to look for other systematic discrepancies with hadronic models. In [6] we predict the transverse momentum dependence of charmonium and Drell–Yan dimuon production. Deviations from these predictions, if any, can reveal plasma contributions to the suppression. However, we expect this contribution to be small at the low SPS energy, ~ 20 GeV per nucleon in the center of mass. More likely, the answer to the fundamental question — what gave rise to the suppression — awaits the completion of RHIC at 200 GeV per nucleon.

The hadronic contribution to the suppression arises from scattering of the nascent ψ with produced particles – the comovers – and nucleons [9, 10]. To determine the suppression from nucleon absorption of the ψ, we calculate the probability that a $c\overline{c}$ pair produced at a point (b, z) in a nucleus survives scattering with nucleons to form a ψ. The standard [10] result is

$$S_A = \exp\{-\int_z^{\infty} dz\, \rho_A(b, z)\sigma_{\psi N}\} \tag{61}$$

where ρ_A is the nuclear density, b the impact parameter and $\sigma_{\psi N}$ the absorption cross section for ψ–nucleon interactions. Suppression can also be caused by scattering with mesons that happen to travel along with the $c\overline{c}$ pair (see refs. in [9]). The corresponding survival probability is

$$S_{\rm co} = \exp\{-\int d\tau n\, \sigma_{\rm co} v_{\rm rel}\}, \tag{62}$$

where n is the comover density and τ is the time in the ψ rest frame.

For collisions at a fixed b, the ψ–production cross section is

$$\sigma_{\psi}^{AB}(b) = \sigma_{\psi}^{NN} \int d^2s dz dz'\, \rho_A(s, z)\rho_B(b - s, z')\, S, \tag{63}$$

where $S \equiv S_A S_B S_{\rm co}$ is the product of the survival probabilities in the projectile A, target B and comover matter. The continuum cross section is

$$\sigma_{\mu^+\mu^-}^{AB}(b) = \sigma_{\mu^+\mu^-}^{NN} \int d^2s dz dz'\, \rho_A(s, z)\rho_B(b - s, z'). \tag{64}$$

We calculate σ_{ψ}^{NN} using the phenomenologically–successful color evaporation model [11]. The continuum in the mass range used by NA50, $2.9 < M < 4.5$ GeV, is described by the Drell–Yan process. To confront NA50 and NA38 data in the appropriate kinematic regime, we compute these cross sections at leading order following [11, 12] using GRV LO parton distributions with a charm K–factor $K_c = 2.7$ and a color evaporation coefficient $F_{\psi} = 2.54\%$ and a Drell–Yan K–factor $K_{DY} = 2.4$. Observe that these choices were fixed by fitting pp data at all available energies [11].

To obtain E_T dependent cross sections, we write

$$\sigma^{AB}(E_T) = \int d^2b\, P(E_T, b)\sigma^{AB}(b). \tag{65}$$

The probability $P(E_T, b)$ that a collision at impact parameter b produces transverse energy E_T is related to the minimum–bias distribution by

$$\sigma_{\rm min}(E_T) = \int d^2b\; P(E_T, b). \tag{66}$$

We parametrize $P(E_T, b) = C\exp\{-(E_T - \overline{E}_T)^2/2\Delta\}$, where $\overline{E}_T(b) = \epsilon\mathcal{N}(b)$, $\Delta(b) = \omega\epsilon\overline{E}_T(b)$, $C(b) = (2\pi\Delta(b))^{-1}$ and $\mathcal{N}(b)$ is the number of participants (see, *e.g.*, Ref. [9]). We take ϵ and ω to be phenomenological calorimeter–dependent constants.

We now calculate charmonium suppression in Pb+Pb collisions. To determine nucleon absorption, we used pA data to fix $\sigma_{\psi N} \approx 4.8$ mb in Ref. [10]. This choice is in accord with the latest NA38 and NA51 pA data. A value of $\sigma_{\psi N} \approx 7.2$ mb yields better agreement with

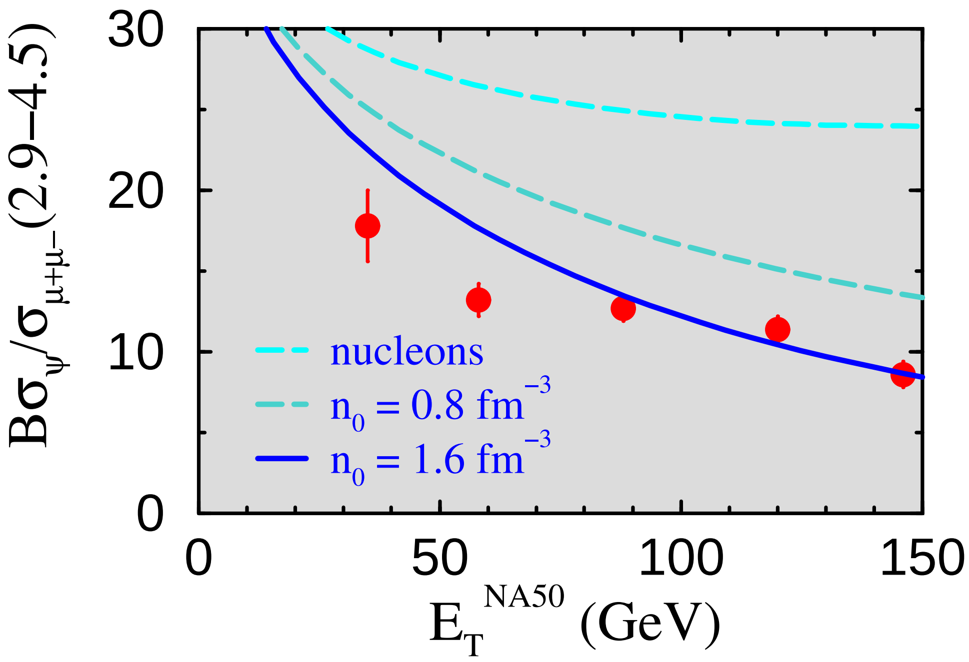

Figure 16: Suppression in Pb+Pb after changing normalization [5] and doubling the density. Data is from QM '96.

peripheral data in both S+U and Pb+Pb. The survival probability for comover scattering is

$$S_{\rm co} = \exp\{-\sigma_{\rm co} v_{\rm rel} n_0 \tau_0 \ln(\tau_F/\tau_0)\} \tag{67}$$

where $\sigma_{\rm co} \approx 2\sigma_{\psi N}/3$ and n_0 is the initial density of sufficiently massive ρ, ω and η mesons; we take $\tau_0 \sim 2$ fm, $\tau_F \sim R_T/v_{\rm rel}$ and $v_{\rm rel} \sim 0.6$ as in [9].

We expect the comover contribution to the suppression to increase in Pb+Pb relative to S+U for central collisions because both the initial density and lifetime of the system can increase. To be conservative, we assumed in [2] that Pb and S beams achieve the *same* mean initial density. With the information then in hand, we found agreement with data. However, Vogt has recently computed the Drell Yan cross section at NNLO in QCD, incorporating detailed knowledge of the NA50 muon acceptance [5]. She now finds results that fall above the data for the S+U density[2]. To bring the comover model into agreement, we must increase the value of $\beta = \sigma_{\rm co} v_{\rm rel} n_0 \tau_0 \ln(\tau_F/\tau_0)$ by a factor of two in Pb+Pb relative to S+U. We can achieve this by one or all of the following:

- Increase the initial comover density. A value of n_0 for Pb+Pb that is the same as S+U is in fact too small to explain NA49 Pb+Pb data.

- Increase the fraction of resonances to prompt pions in the hadron gas. One would expect the ρ abundance to increase due to $\pi\pi$ scattering in the comover gas.

- Increase the system lifetime τ_F to a value larger than R/v to allow for collective transverse flow.

Any combination of these adjustments that increases β by a factor of two would bring the model into better agreement. I show the effect of varying β in the figure below.

References

[1] See, *e.g.*, G. Taubes, *Science,* **273**, 13 September 1996, 1492.

[2] S. Gavin and R. Vogt, Phys. Rev. Lett. **78**, 1006 (1997).

[3] S. Gavin and R. Vogt, Nucl. Phys. **A610**, 442c (1996).

[4] D. Kharzeev, C. Lourenco, M. Nardi and H. Satz Z. Phys. **C74**, 307, (1997).

[5] R. Vogt, hep-ph/9708294.

[6] S. Gavin and R. Vogt, CU-TP-791, hep-ph/9609470.

[7] S. Gavin, M. Gyulassy, and A. Jackson, Phys. Lett. **207B**, 257, (1988).

[8] M. Gonin *et al.* (NA50), Proc. Quark Matter '96, Heidelberg, Germany, P. Braun-Munzinger *et al.*, eds. (1996).

[9] S. Gavin and R. Vogt, Nucl. Phys. B345 (1990) 104.

[10] S. Gavin, H. Satz, R. L. Thews, and R. Vogt, Z. Phys. C61 (1994) 351; S. Gavin, Nucl. Phys. A566 (1994) 383c.

[11] R. Gavai *et al.*, Int. J. Mod. Phys. A10 (1995) 3043.

[12] S. Gavin *et al.*, Int. J. Mod. Phys. A10 (1995) 2961.

[13] N. Armesto and A. Capella, hep-ph/9706452.

Interpreting SPS and RHIC J/ψ Experiments

(*Sean Gavin and Ina Sarcevic)*

Much detailed work is needed to understand the very precise new data reported by NA50 and to make high-quality predictions for RHIC. It is sobering to observe that all of the analyses [1, 2, 4, 3] are based on work in ref. [5], a paper that is seven years old. We have learned a lot about heavy ion collisions since then.

There is currently a dispute over whether or not one can tune parameters to obtain further agreement [1, 2]. We find the agreement with peripheral data can be improved compared to the accompanying figure (and also for S+U) by using a value $\sigma_{\psi N} = 7.2$ mb following ref. [4]. For these parameters, however, we would have to take the comover density to be zero in S+U and over 1 fm^{-3} in Pb+Pb. This is unreasonable in the context of hadronic comovers. However, there are many nuclear effects mandated by pA, eA, and AB data that are omitted in current models [3, 4]. These features are:

1. Nuclear parton-distribution effects, such as shadowing, EMC and fermi smearing. These effects vary with impact parameter and, consequently transverse energy, and can be different for gluon and quark distributions (see, *e.g.*, Huang, Lu and Sarcevic in this proposal).

2. Baryon stopping, measured at CERN but ignored by Glauber approximations, can add to the suppression. Slow baryons contribute to comover suppression with a low threshold via $\rho N \to \overline{D}\Lambda_c$.

3. Transverse flow of the comover fluid.

4. Different absorption of color-singlet and color-octet $c\overline{c}$ pairs.

5. Elastic scattering of the J/ψ by pions at energies below the threshold for $\pi\psi \to D\overline{D}$.

6. Chemical reactions such as $\rho\psi \to \chi\pi$.

7. Quantum effects in J/ψ formation from the $c\overline{c}$ boundstate.

8. Charm contribution to the continuum, which complicates the fitting procedure used by NA50 to extract the "Drell Yan" cross section.

9. Puzzling behavior of CERES and NA50 dilepton data may indicate that there are additional affects of unknown origin that enhance the continuum below – and perhaps *underneath* – the J/ψ.

Any of these effects can alter the pattern of suppression at the $\sim 10\%$ level in AB collisions relative to pA. In sum, these effects could account for the rather minute discrepancies between calculations and data.

The more important question is how seriously one should take the rapid shift in transverse energy shown by the latest QM '97 data. If one interprets the abrupt change at $E_T = 50$ GeV, then there is no point in tuning a hadronic model. While we will be in a better position to assess the need for further work when details concerning the new data are published, it is interesting to consider the possibility that novel behavior has been seen.

We observe that a sharp discontinuity in transverse energy is difficult to understand on the basis of a bulk [6], local equilibrium phase transition in a system where finite-size effects are appreciable. In addition to the obvious effect of dispersion in the relation between impact parameter and E_T, any post-transition effects tend to obscure the relationship between E_T and the local energy density within an inhomogeneous collision volume [7]. Perhaps a two dimensional dynamical percolation transition of color strings into flux tubes is a more plausible alternative [8], since the order parameter for such a transition is the number of strings per unit transverse area. This variable is more closely related to E_T than the energy density. Such a transition would have broad implications for many observables. For example, flux tube or 'color rope' formation has been proposed to account for the measured production of strange hyperons and anti-hyperons. The figure shows the relation between the E_T distributions for NA49, which measures hyperons, and NA50. We intend to estimate the change in other observables such as Strangeness and HBT that would accompany flux tube percolation [10].

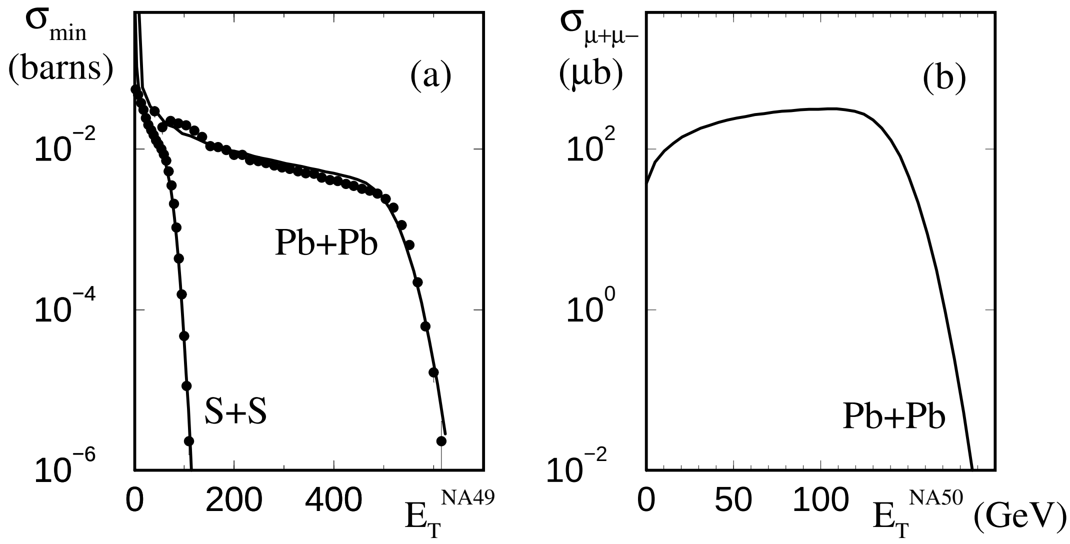

Figure 17: Where to look for plasma – comparison of transverse energy distributions for a) NA49 and b) NA50. NA50 sees a rapid drop in J/ψ production at $E_T \sim 50$ GeV.

References

[1] N. Armesto and A. Capella, hep-ph/9706452.

[2] R. Vogt, hep-ph/9708294.

[3] S. Gavin and R. Vogt, Phys. Rev. Lett. **78**, 1006 (1997).

[4] D. Kharzeev, C. Lourenco, M. Nardi and H. Satz Z. Phys. **C74**, 307, (1997).

[5] S. Gavin and R. Vogt, Nucl. Phys. B345 (1990) 104.

[6] D. Kharzeev, M. Nardi and H. Satz, hep-ph/9707308.

[7] Gordon Baym, Gerald Friedman and Ina Sarcevic, Phys. Lett. **B219**, 205, (1989)

[8] N. Armesto, M. A. Braun, E. G. Ferreiro and C. Pajares, hep-ph/9607239

[9] See, *e.g.* H. Sorge, nucl-th/9707021 and refs. therein.

[10] Sean Gavin, in progress.

Perturbative Contribution to J/ψ Suppression

(*Sean Gavin and Ina Sarcevic*)

J/ψ production is a complex process that begins with the hard production of a $c\overline{c}$ pair, predominantly through gluon fusion. Gluon fusion is a hard process, with momentum transfer $Q \sim M_\psi \sim 3$ GeV and can be described using perturbative QCD. The $c\overline{c}$ can then form a

3^S_1 J/ψ bound state in two ways: a) if the $c\bar{c}$ is color singlet, it can form a P-wave χ meson, which can emit a photon and become a J/ψ, or b) if the $c\bar{c}$ is color octet, it can radiate gluons and become a J/ψ. Data at the SPS shows production through χ decay accounts for 30% of the production. In J/ψ *suppression*, much of the discussion has focused on the octet channel. There, most authors regard the $c\bar{c}$ as a strongly interacting object that can be absorbed in nucleon interactions with a cross section perhaps as large as 7 mb. However, the question of the singlet contribution has not been addressed.

In this work we use perturbative QCD to explore the production and absorption of the singlet channel for J/ψ in high-energy γA and pA collisions in the region of high x_F. This channel can be probed experimentally by measuring the associated photon from the $\chi \to \gamma + J/\psi$ decay. For photoproduction at high x_F, two nuclear effects are possible:

- Gluon shadowing of the target gluon distribution,
- Nucleon absorption of the J/ψ.

We apply the partonic picture developed by Huang, Lu and Sarcevic to estimate both of these effects. That shadowing is important at high x_F is well known — HLS simply gives us a model that can be used to calculate gluon shadowing. That absorption can have a role is a surprising consequence of the HLS picture, and violates the conventional wisdom CW [3, 2] for J/ψ suppression.

This work can also have implications for J/ψ suppression at SPS energy, where very precise new data for S+U and Pb+Pb collisions is soon to be published. Various authors confront these data with models that ignore shadowing and absorption of the color singlet component, because these effects are small. Some find discrepancies at the 30-40% level. Before one draws conclusions from such small discrepancies, one must have a very precise understanding of all contributions.

In the CW picture of J/ψ suppression [3, 2], the absorption of a high energy color singlet $c\bar{c}$ pair as it traverses the nucleus is taken to be negligible. The reason for this is that the pair is regarded as pointlike at the point of its creation, with a spatial extent on the order of $\sim 1/M_{c\bar{c}}$. In the rest frame of the pair, it then takes a time $\tau_F \sim 1$ fm for the pair to expand to the size of a χ meson. But in the nuclear frame, this formation time is dilated to $\sim E\tau_F/M_{c\bar{c}}$, where E is the energy of the pair. A pair with energy $E \gg M_{c\bar{c}}R_A/\tau_F \sim 18$ GeV will barely have time to reach its bound state radius before it escapes a lead-sized nucleus of $R_A = 6$ fm. If we then follow CW and take the absorption cross section to scale as the classical geometrical size of the pair, then this cross section can be very small for high energy pairs.

To see how CW breaks down in the large x_F region, we use perturbative QCD to calculate the interaction of a nucleon with a $q\bar{q}$ pair of transverse separation r_t in the double logarithm approximation [7]:

$$\sigma_{q\bar{q}N} \propto r_t^2 \alpha_s x g_{DLA}(x, r_t^{-2}) \tag{68}$$

where g_{DLA} is the gluon distribution inside the nucleon for gluons of scale $Q \sim r_t^{-1}$ and momentum fraction x. Observe that for x_F large, the target x is small; E772 measured J/ψ production in 800 GeV pA for up to $x_F \sim 0.64$ and down to $x \sim 10^{-2}$ [8]. For large Q and moderate x, the cross section indeed vanishes roughly as $Q^{-2} \sim r_t^2$.

At small $x < 10^{-2}$ the nucleon structure function exhibits a strong scaling violation in the semihard region 0.9 GeV$< Q < 3$ GeV^2. In general, scaling violations cause the gluon density to grow $xg \propto (Q^2)^\gamma$ as Q increases for fixed x, where γ is the anomalous dimension. At small x, γ can exceed unity, so that the growth of the parton density can compensate the smallness of r_t^2. We write

$$\sigma_{q\overline{q}N} \propto r_t^{2(1-\gamma)}. \tag{69}$$

This effect has been used by Huang, Lu, and Sarcevic to describe shadowing. Here, we see that scaling violations can compensate for the smallness of the size of the $c\overline{c}$ pair.

Future plans: We intend to apply the lessons learned from this analysis to calculate the perturbative contribution to J/ψ suppression at RHIC and LHC energies. At high energies a substantial fraction of the $c\overline{c}$ interactions may occur at hard scales where we can apply perturbative QCD. The expected dominance of hard scales at high energies has driven attempts to apply parton cascade models to describe RHIC and LHC phenomenology. When the predominant interactions occur at the parton level, the picture of spacetime evolution differs strongly from that at SPS energy. It is not meaningful to distinguish between nucleon absorption and comover scattering – all interactions of the $c\overline{c}$ are essentially with comoving quarks and gluons produced as minijets, starting from a very early time $\tau_0 \sim 0.1$ fm. These interactions may then be calculated using perturbation theory. At RHIC and particularly LHC, typical midrapidity partons are formed from interactions at very small x. If we are phenomenologically successful in describing the high x_F region at FNAL, we will be able to apply our techniques to describe the major contributions to charmonium production and suppression at higher energies:

- Primary production of $c\overline{c}$ through hard scattering.
- Gluon shadowing of the target gluon distribution takes place.
- Secondary production of $c\overline{c}$ can now occur through semihard parton-parton scattering.
- Interactions of the $c\overline{c}$ with semihard comover partons can now be described using perturbative QCD.

We remark that the interactions of octet $c\overline{c}$ in the medium at high energies are also perturbative. Reactions with surrounding gluons can easily change octet pairs into singlet pairs without resolving the individual c and $\overline{c}$. We suspect that even for an octet pair, the gluon must resolve either the quark or antiquark to dissociate the pair. Therefore, the cross section for dissociation of an octet may also depend on size as above, albeit with a larger charge.

References

[1] Zheng Huang, Hung Jung Lu and Ina Sarcevic, hep-ph/9705250

[2] S. Gavin and R. Vogt, Nucl. Phys. B345 (1990) 104.

[3] Stanley J. Brodsky and A.H. Mueller, Phys. Lett. **206B**, 685, (1988); J.P. Blaizot and J.Y. Ollitrault, Phys. Lett. **B217**, 386, (1989).

[4] S. Gavin and R. Vogt, Phys. Rev. Lett. **78**, 1006 (1997).

[5] D. Kharzeev, C. Lourenco, M. Nardi and H. Satz Z. Phys. **C74**, 307, (1997).

[6] R. Vogt, hep-ph/9708294.

[7] Gordon Baym, B. Blättel, L. L. Frankfurt, and M. Strikman, Phys. Rev. Lett. **70**, 869, (1993), and references therein.

[8] See M.H. Schub *et al.* (E789 Collab.) Phys. Rev. **D52** 1307, (1995) and refs. therein.

Correlating Signals: Antiproton and Deuteron Production in Nuclear Collisions

(*Sean Gavin*)

Antiproton production [1] and deuteron production [2] can provide independent measures of the spacetime evolution of baryons in relativistic heavy ion collisions. In both cases, however, this information has been difficult to extract from data owing to the complexity of the dynamics [3, 4, 5]. We propose that a 'superevent' analysis [6] combining antiproton and deuteron measurements with suitable centrality information can help to extract this spacetime information. In addition, such an analysis can be used to identify rare events that produce quark gluon plasma droplets.

This study has two goals. First, we point out for the first time the added information that can be obtained by measuring deuteron and antiproton production simultaneously. To reach this goal we use analytic calculations to illustrate the principles and RQMD cascade-model simulations to build in realism. Second, we develop the analysis tools needed to extract this information – this will be done with RQMD simulations in the context of AGS experiment E864. The heart of this analysis is the grouping of like events into classes. These classes, called superevents, can then be used to obtain statistically meaningful distributions of antiprotons and deuterons.

We emphasize while we focus on AGS data, the methods that we develop will have important implications for RHIC as well. Experimental information on the baryon spacetime distribution can provide significant leverage in testing parton-cascade and hadronic models.

Prior to the first AGS and SPS antiproton measurements, we had predicted that annihilation with baryons suppresses $\overline{p}$ production [1]. Specifically, an increase in the spacetime extent of baryons of the collision system for a fixed initial baryon density leads to a decrease in the antiproton-to-proton ratio,

$$R_{\overline{p}} \equiv \frac{EdN(\overline{p})/d^3p}{EdN(p)/d^3p}, \tag{70}$$

compared to that measured in proton-proton collisions. While suppression has been observed [7, 8], the measured reduction at AGS energy is significantly smaller than calculations based on free-space $\overline{p}$ production and annihilation cross sections. To remedy this disagreement, authors have introduced various effects such as screening [4, 5], enhanced production [3] and additional $\overline{p}$ from strange antibaryon decay together with enhanced strangeness [8]. At present, there is little objective information to indicate how much each effect contributes to $\overline{p}$ production – the spacetime information remains hidden.

The deuteron story is similar: Remler and others [2] suggested that deuteron production depends on the correlation of neutrons and protons and, correspondingly, provides information on the spacetime distribution of baryons. An increase of the system's spatial size or lifetime tends to a reduce the deuteron coalescence parameter:

$$B_2 \equiv \frac{EdN(d)/d^3p}{[EdN(p)/d^3p]^2}. \tag{71}$$

Again, AGS deuteron results defied straightforward efforts to combine Remler's phase-space coalescence with cascade calculations. Isospin effects [10] and a quantum coalescence model [11] have remedied the disagreement, but complicate the initial objective of extracting spacetime information.

We suggest that combined measurement of antiproton and deuteron can be used to isolate to the different nuclear effects in these systems. We seek to establish a correlation between B_2 and $R_{\overline{p}}$ as the size of the system and the baryon density vary from event-to-event. To cope with the fact that deuterons and antiprotons are rare particles at AGS energy, it is necessary to divide data into event classes in order to map out this correlation. To illustrate these correlations, we use the Boltzmann equation to derive the schematic expressions:

$$R_{\overline{p}}^{AA} = R_{\overline{p}}^{pp} \exp\{-(\pi/8)^{1/2} \sigma_{_{N\overline{N}}}\, \rho_B(0) R\} \tag{72}$$

and

$$B_2^{AA} = 2\pi g m^{-1} (R^2 + d^2/4)^{-3/2}, \tag{73}$$

where R is the rms spatial size of the collision volume, $\rho_B(0)$ is the initial baryon density at the center of the collision volume, $\sigma_{N\overline{N}}$ is the annihilation cross section, $g = 3/4$ is the spin-degeneracy factor for d relative to the n–p system, m is the nucleon mass and $d \approx 1.7$ fm is the deuteron size parameter. Note that (3) and (4) are valid only for symmetric nucleus-nucleus collisions and assume that antiprotons are produced only in first NN collisions. Observe that (3) is essentially the AGS-energy analog of eq. (1) in ref. [1], while eq. (4), which characterizes the expectations of refs. [2], is derived using the same formulation.

It is straightforward to see from (3) and (4) how medium effects obscure the R dependence of these quantities individually. For example, to describe deuteron data using RQMD, authors [10] augment the spin-degeneracy factor $g = 3/4$ (see, *e.g.* [2]) with an additional isospin degeneracy factor 1/2. This complicates the interpretation of data, since one cannot tell from deuterons alone whether a change in B_2^{AA} with A arises from a change in the coalescence mechanism or from an increase in R. Nevertheless, we are aware of no connection between the proposed modification of d-coalescence [10, 11] and $\overline{p}$-annihilation [3, 4, 5]. We expect an increase in R to systematically modify both d and $\overline{p}$.

The aim of our superevent analysis is to measure the event-by-event *correlation* of the antiproton-to-proton ratio and the deuteron coalescence parameter as a function of the pion multiplicity, a centrality parameter related to system size. Since $\overline{p}$ and d are rare particles at AGS energy, one must develop event-by-event criteria that pick out similar events. These events can then be combined into event classes – the superevents – for further analysis.

System size, lifetime, baryon number and energy density likely fluctuate from event to event, leading to fluctuations in B_2 and $R_{\overline{p}}$. However, data in real experiments also fluctuate due to instrumental effects. By constructing superevents using RQMD-simulated data, we have begun to establish selection criteria that preserve the interesting fluctuations while minimizing the uninteresting ones.

Our first analysis of RQMD data seem to reflect the systematic B_2 and $R_{\overline{p}}$ expected for hadronic systems, as well they should. But superevents from real experiments may prove much more interesting!

Beyond the hadronic framework, both antiproton and deuteron distributions can vary from our hadronic expectations if quark gluon plasma forms. A variety of mechanisms from chiral restoration in a plasma to disoriented chiral condensate formation [14, 15, 16] can enhance antibaryon production. Model calculations typically yield values of $R_{\overline{p}}$ approaching unity – well above values seen in $pp \to \overline{p}X$ at AGS energies. On the other hand, plasma formation can reduce the deuteron coalescence parameter, e.g., if a first order phase transition leads to the dramatic increase of the collision-system lifetime and size. If seen, a trend with larger systems producing more antiprotons relative to protons, i.e., smaller B_2 and larger $R_{\overline{p}}$, runs counter to hadronic expectations.

While this trend is not seen in typical central Au+Au collisions at the AGS, it may appear in rare events. Kapusta and Vischer [13] have discussed the possibility that plasma can form in rare events, perhaps at the $0.1 - 1\%$ level. To determine the level at which our analysis can pick out such events, we combine an 'afterburner code' to modify RQMD output to simulate the production of rare plasma droplets.

References

[1] S. Gavin, M. Gyulassy, M. Plümer, and R. Venugopalan, Phys. Lett. **234B**, 175 (1990).

[2] H. Sato and K. Yazaki, Phys. Lett. **98B**, 153 (1981), E. A. Remler, Ann. Phys. **136,** 293 (1981); M. Gyulassy, K. Frankel and E. A. Remler, Nucl. Phys. **A402**, 596 (1983).

[3] A. Jahns, H. Stoecker, W. Greiner and H. Sorge, Phys. Rev. Lett. **68** 2895, (1992); A. Jahns, C. Spieles, R. Mattiello, H. Stoecker, W. Greiner and H. Sorge, Phys. Lett. **B308** 11, (1993); Erratum-ibid. **B314**, 482, (1993).

[4] S.H. Kahana, Y. Pang, T. Schlagel, C.B. Dover, Phys. Rev. **C47** 1356, (1993); Y. Pang, D.E. Kahana, S.H. Kahana, H. Crawford, Phys. Rev. Lett. **78**, 3418 (1997).

[5] C. Spieles, *et al.*, Phys. Rev. **C53**, 2011 (1996).

[6] J. Sandweiss, private communication.

[7] M.J. Bennett et al. (E878 Collab.) Phys. Rev. C56 1521, (1997); Y. Akiba et al. (E866 Collab.), Nucl. Phys. **A610**, 139c, (1996).

[8] T.A. Armstrong et al. (E864 Collab.) Phys. Rev. Lett. **79**, 3351 (1997); J. Nagle, Yale University Ph. D. thesis (1997); B. A. Cole, private communications.

[9] J.L. Nagle, B.S. Kumar, M.J. Bennett, G.E. Diebold, J.K. Pope (Yale U.), H. Sorge, J.P. Sullivan, Phys. Rev. Lett. **73** 1219, (1994).

[10] J.L. Nagle, B.S. Kumar, D. Kusnezov, H. Sorge and R. Mattiello, Phys. Rev. **C53**, 367, (1996).

[11] D.E. Kahana, S.H. Kahana, Y. Pang, A.J. Baltz, C.B. Dover, E. Schnedermann, T.J. Schlagel, Phys. Rev. **C54**, 338, (1996).

[12] M. Bleicher, C. Spieles, A. Jahns, R. Mattiello, H. Sorge, H. Stocker, W. Greiner, Phys. Lett. **B361**, 10, (1995).

[13] Joseph I. Kapusta, Axel P. Vischer, Phys. Rev. **C52**, 2725 (1995).

[14] T.A. DeGrand, Phys. Rev. **D30** 2001, (1984).

[15] Ulrich Heinz, P.R. Subramanian, Walter Greiner, Z. Phys. **A318**, 247 (1984); P. Koch, B. Müller, H. Stocker and W. Greiner, Mod. Phys. Lett. **A3**, 737 (1988).

[16] John Ellis, Ulrich Heinz and Henryk Kowalski, Phys. Lett. B233, 223 (1989); Joseph I. Kapusta and Ajit M. Srivastava, Phys. Rev. **D52**, 2977 (1995).

Superevent Analyses in Relativistic Heavy Ion Collisions

(*Sean Gavin*)

The antiproton–deuteron analysis of the previous section is only a special case of a superevent analysis. If that study is successful, S.V. Greene, T. Miller and I plan to address a wide range of problems at RHIC where the information contained in event-by-event correlations is desirable. The large experiments PHENIX and STAR are being built with the potential of measuring several distinct signals of interesting phenomena in *combination.* For example, PHENIX can measure J/ψ suppression, continuum-dilepton production and strangeness enhancement, to name a few signals [1]. At the very least, PHENIX can measure these signals for the same conditions of centrality, minimizing the usual systematic uncertainties met when one tries to compare different experiments.

We point out that much more information can be had if *e.g.*, charmonium, strangeness and dilepton production cab be known in each event. The obstacle to overcome in obtaining such information is that an experiment may not store – or even detect – enough information to construct sufficiently detailed spectra from a single event. [One average, a J/ψ is produced only in rare collisions!] However, an experiment may cull enough information from each event to group events into superevent classes with similar properties. It may then be possible to construct desired spectra for these particles from each event class. The challenge is both experimental and theoretical – one must find superevents that are a) interesting and b) realistic.

We hope to apply superevent techniques to the following measurements:

- By correlating the kaon abundance with the identical-pion Hanbury-Brown Twiss correlations (HBT) on an event-by-event basis, one can look for events with both enhanced lifetime and enhanced strangeness. This measurement can help determine if the deconfinement phase transition is first order.

- The real signature of disoriented chiral condensate is event-by-event fluctuations in low-p_T charged and neutral pions.

- Event-by-event correlation of dilepton production with HBT can determine if long lifetime events undergo a long period of expansion at constant temperature. Such a measurement may reveal the value of the QCD critical temperature.

We focus on the PHENIX collaboration in which we are members, although the techniques we develop will be applicable elsewhere.

References

[1] S. Aronson *et al.*, Nucl. Phys. **A566**, 383c (1994).

Collins-Soper-Sterman Approach to the Drell Yan $p_{\rm T}$ Distribution in Nuclear Collisions

Gavin P.V. Ruuskanen, D.K. Srivastava and R.L. Thews, are addressing Drell Yan $p_{\rm T}$ distributions in hadron–nucleus and nucleus–nucleus, applying techniques adapted from proton–proton collisions [1]. This work is part of the ongoing efforts of the 'hard probes collaboration' The HPC is group of theorists convened to provide benchmark estimates for hard processes at RHIC and LHC. Previously, this group provided calculations for nucleon-nucleon rates at RHIC and LHC ion-ion energies [2]. In turning to nuclear collisions, they now must consider how the nuclear target affects these rates. Possible effects that modify hadron-nucleus collisions are:

- *Initial state scattering*, which modifies transverse momentum distributions in Drell Yan [3].

- *shadowing*, which effects parton distributions in the target and, consequently, the overall rate [4].

- *energy loss*, which can effect distributions at kinematic extremes [5].

- final state scattering, which alters momentum distributions and rates of processes with hadronic final states [6].

All of these topics have been studied extensively by Gavin and Sarcevic, as reported in this proposal.

Gavin and coworkers were the first to apply phenomenological models of initial state scattering to Drell Yan and ψ production [3]. This new work is an attempt to develop a more microscopic and theoretically-justified model to confront detailed questions, such as the shapes and rapidity dependence of transverse momentum distributions at RHIC.

To begin, Gavin *et al.* will develop a microscopic formulation of elastic initial state scattering in the Drell Yan process in hadron-nucleus collisions. This formulation is similar in spirit to an earlier one developed by Chiappetta and Pirner [7]. The novel feature of the new formulation is that it incorporates the empirical result that initial state scattering is essentially a soft process, while the Drell Yan process is hard. The distinction between soft, resummed and hard contributions to the Drell Yan transverse momentum distribution is clearest in the Collins-Soper-Sterman formulation [12].

The transverse momentum dependence of the Drell Yan process has always been of interest in nucleon-nucleon collisions. Experiments show that the net transverse momenta of lepton pairs produced by the Drell-Yan process are of the order of 1 GeV for a dimuon mass $M = 10$ GeV. Such values are substantially smaller than the transverse momenta $\sim M/2$ carried by each of the leptons individually. On the other hand, the $p_{\rm T}$ of a Drell-Yan pair is much larger than the few-hundred MeV typical of soft QCD. If we neglect the transverse momentum of the incoming partons, then the lowest order process $q\bar{q} \rightarrow \gamma^* \rightarrow e^+e^-$ produces a final state with net $p_{\rm T} = 0$. While any spread in the initial momentum will increase the final $p_{\rm T}$ on average, the intrinsic width of the parton distribution is rather small, $\langle p_{\rm T}^2 \rangle_{\rm soft} \sim (0.3~{\rm GeV})^2$. This scale is determined by the inverse hadron size, since the target and projectile partons cannot be localized within their parent hadrons. Therefore, we can attribute part of the measured $p_{\rm T}$ to the parton's intrinsic $p_{\rm T}$, but not all.

The dimuon pair acquires additional transverse momentum from production mechanisms that occur beyond leading order in perturbation theory [8, 9]. For example, the Compton and annihilation processes

$$qg \rightarrow q\gamma^* \quad \text{and} \quad \bar{q}q \rightarrow \gamma^* g \tag{74}$$

occur in which the dimuon's $p_{\rm T}$ can be balanced by the recoil of the final state quark or gluon. One can compute the $p_{\rm T}$ distribution perturbatively from these processes and their radiative corrections. The perturbation expansion is well behaved for $p_{\rm T} \sim M$. However, at low $p_{\rm T}$ the perturbation expansion breaks down and a resummation of the perturbation series is required.

To see why this resummation is necessary, observe that the cross section in the region $p_{\rm T}^2 << M^2$ is dominated by the leading-logarithm contributions:

$$\frac{{\rm d}\sigma}{{\rm d}p_{\rm T}^2} \sim \frac{\alpha_{\rm w}\alpha_{\rm s}}{p_{\rm T}^2} \ln\left(\frac{Q^2}{p_{\rm T}^2}\right)\left[v_1 + v_2\alpha_{\rm s}\ln^2\left(\frac{Q^2}{p_{\rm T}^2}\right) + v_3\alpha_{\rm s}^2\ln^4\left(\frac{Q^2}{p_{\rm T}^2}\right) + \cdots\right], \tag{75}$$

where $\alpha_{\rm s}$ is evaluated at the scale Q^2. This series is effectively an expansion in $\alpha_{\rm s}\ln^2(Q^2/p_{\rm T}^2)$, rather than $\alpha_{\rm s}$ alone. The effective expansion parameter can be large at low $p_{\rm T}$ even if $\alpha_{\rm s}(Q^2)$ is small. The leading-logarithm series (75) describes the effect of soft gluon radiation from the initial state q and $\bar{q}$ prior to their annihilation. Specifically, these logarithms are remnants of the mass and collinear singularities arising from the radiated gluons. The annihilation process in (74) contributes the term $\propto \alpha_{\rm s}\ln(Q^2/p_{\rm T}^2)/p_{\rm T}^2$ and, in general, $q\bar{q} \rightarrow \gamma^* + n$ gluons produces the term of order $\alpha_{\rm s}^n$. Fortunately, the coefficients v_i of Eq. (75) are not independent and it is possible to sum the series exactly so that it applies even when $\alpha_{\rm s}\ln^2(Q^2/p_{\rm T}^2)$ is large.[10, 11, 12] In addition, 'subleading' logarithm contributions, though smaller, can also be important.

The formalism needed to sum the leading and subleading logarithms was developed by [12] by Collins, Soper and Sterman. For each species of colliding partons, one finds

$$\frac{{\rm d}\sigma}{{\rm d}p_{\rm T}^2\,{\rm d}y}({\rm resum}) = \frac{4\pi^3\alpha_{\rm w}}{3s}\int\frac{{\rm d}^2b}{(2\pi)^2}e^{i\mathbf{b}\cdot\mathbf{p}_{\rm T}}W(b), \tag{76}$$

$$
\begin{aligned}
W(b) &= \exp\left\{-\int_{\beta/b^2}^{Q^2}\frac{\mathrm{d}q^2}{q^2}\left[\ln\left(\frac{Q^2}{q^2}\right)A(\alpha_{\mathrm{s}}(q^2))+B(\alpha_{\mathrm{s}}(q^2))\right]\right\} \\
&\quad \times (C\circ f_A)(x_A;\beta^2/b^2)\ \times\ (C\circ f_B)(x_B;\beta^2/b^2). \qquad (77)
\end{aligned}
$$

where s is the total hadronic center-of-mass energy, f_{A} and f_{B} are the parton structure functions of the two colliding particles, and

$$
x_{\mathrm{A}} = e^{+y}\sqrt{Q^2/s}, \qquad x_{\mathrm{B}} = e^{-y}\sqrt{Q^2/s} \qquad (78)
$$

are the dominant values of x as $p_{\mathrm{T}} \to 0$. The integration variable b is the impact parameter, the variable conjugate to p_{T}, and $\beta \equiv 2\,\mathrm{e}^{-\gamma_{\mathrm{E}}}$, where γ_{E} is Euler's constant. The function C is a coefficient function that converts the structure functions f into distributions $C\circ f$ specific to the process at hand. The functions A, B, and $C(x)$ have perturbative expansions in α_{s}, with A and B starting at order α_{s}. The expansion for C begins at order 1 for quarks and order α_{s} for gluons. These functions can be extracted to a given order from the perturbative result, and have been determined for the Drell Yan process at next-to-leading order by Davies *et al.*

The resummed result (76) applies only when $p_{\mathrm{T}}^2 \ll Q^2$ because it includes only those terms that diverge as $1/p_{\mathrm{T}}^2$ as $p_{\mathrm{T}} \to 0$. The nonsingular contributions to the p_{T} distribution omitted in (76) become important at large p_{T} because they fall off less rapidly. On the other hand, conventional perturbation theory works well at large p_{T}, describing the complete p_{T} dependence to a given order in α_{s}. Bridging the two regions is accomplished by adding in the terms that are not resummed, the so-called remainder or non-singular terms. Arnold and Kauffman developed a prescription for calculating the remainder terms that explicitly matches the high and low p_{T} results.

The Arnold and Kauffman prescription proceeds as follows. One first expands the resummed result (76) in powers of α_{s}. This series, $\mathrm{d}\sigma/\mathrm{d}p_{\mathrm{T}}^2\,\mathrm{d}y(\mathrm{asym})$, contains the singular 'asymptotic' $1/p_{\mathrm{T}}^2$ part of complete perturbation series $\mathrm{d}\sigma/\mathrm{d}p_{\mathrm{T}}^2\,\mathrm{d}y(\mathrm{pert})$. The asymptotic result in Ref. [16] is expressed as convolutions of structure functions with the coefficient functions of (76) and with Altarelli-Parisi splitting functions arising from the scale dependence of the structure functions. With the singular terms isolated in the asymptotic result, the remainder is the difference between the perturbative result and the asymptotic result, $R = \mathrm{d}\sigma/\mathrm{d}p_{\mathrm{T}}^2\,\mathrm{d}y(\mathrm{pert}) - \mathrm{d}\sigma/\mathrm{d}p_{\mathrm{T}}^2\,\mathrm{d}y(\mathrm{asym})$. The perturbation series for the p_{T} distribution — and therefore R — has been computed to 2nd order Ref. [9]. The total cross section is then written

$$
\frac{\mathrm{d}\sigma}{\mathrm{d}p_{\mathrm{T}}^2\,\mathrm{d}y}(\mathrm{total}) = \frac{\mathrm{d}\sigma}{\mathrm{d}p_{\mathrm{T}}^2\,\mathrm{d}y}(\mathrm{resum}) + \frac{\mathrm{d}\sigma}{\mathrm{d}p_{\mathrm{T}}^2\,\mathrm{d}y}(\mathrm{pert}) - \frac{\mathrm{d}\sigma}{\mathrm{d}p_{\mathrm{T}}^2\,\mathrm{d}y}(\mathrm{asym}). \qquad (79)
$$

The "matching" is now manifest: at low p_{T} the perturbative and asymptotic pieces cancel, leaving the resummed; at high p_{T} the resummed and asymptotic pieces cancel to 2nd order, leaving the perturbative contribution. The relative error is explicitly of order α_{s}^2, see Ref. [16].

At very high p_{T} the matching prescription breaks down and one must switch back to the perturbative result. This breakdown occurs because R is only known to 2nd order, while $\mathrm{d}\sigma/\mathrm{d}p_{\mathrm{T}}^2\,\mathrm{d}y(\mathrm{resum})$ in effect contains all orders in α_{s}. For example, $\mathrm{d}\sigma/\mathrm{d}p_{\mathrm{T}}^2\,\mathrm{d}y(\mathrm{resum})$ introduces terms $\propto \alpha_{\mathrm{s}}^3(\ln p_{\mathrm{T}})^5/p_{\mathrm{T}}^2$ that will not be canceled in the 2nd order expression for R. Such terms are important at large p_{T} when $\mathrm{d}\sigma/\mathrm{d}p_{\mathrm{T}}^2\,\mathrm{d}y$ has fallen off to the extent that R

is comparable to the total. From that point on, the perturbative prediction is more reliable than (79). The switch is done at sufficiently high $p_{\rm T}$ so that the error incurred is free of large logarithms.

The form factor $W(b)$ contains $\alpha_{\rm s}$ and parton distributions evaluated at the scale $1/b$, and its evaluation is problematic for $b > 1$ GeV^{-1}. Moreover, one wishes to include the effect of the intrinsic $p_{\rm T}$ of the partons. Both of these ends are met by replacing

$$W(b) \to W(b_*) {\rm e}^{-S_{\rm np}(b)} \tag{80}$$

where $b_* = b/\sqrt{1+(b/b_{\rm max})^2}$ and $b_{\rm max} = 0.5$ GeV^{-1}. The Collins-Soper-Sterman formalism specifies that $S_{\rm np}$ have a term which depends on $\ln Q$ and a term which does not and that the $\ln Q$ term does not depend on the colliding hadrons or on the parton x's. However, beyond these constraints $S_{\rm np}$ is arbitrary and must be extracted from experiment. Ladinsky and Yuan parametrize

$$S_{\rm np} = g_1 b \left[b + g_3 \ln\left(\tau/\tau_1\right)\right] + g_2 b^2 \ln\left(Q/2Q_1\right), \tag{81}$$

where $\tau = x_A x_B$ [17]. To fit the ISR $p_{\rm T}$ distribution from R209, they take $g_1 = 0.11$ GeV^2, $g_2 = 0.58$ GeV^2, $g_3 = -1.5$ GeV^2, $\tau_1 = 0.01$ and $Q_1 = 1.6$ GeV. Note that these parameter choices are somewhat different from those in Ref. [15, 16].

Momentum distributions presented in [1] were computed using a code adapted from Ref. [16]. Values of the nonperturbative parameters in $S_{\rm np}$ were taken from earlier studies of $W^\pm$ and Z production at high Q^2. Agreement with Drell Yan data at much lower Q^2 was fair. As a first step in our new work, we intend to refit the nonperturbative parameters in $S_{\rm np}$.

Data suggests that multiple initial state parton scattering increases the square of the transverse momentum in accord with

$$\langle p_{\rm T}^2 \rangle_{pA} = \langle p_{\rm T}^2 \rangle_{pp} + \kappa^2(\langle n \rangle - 1)/2, \tag{82}$$

where $\langle n \rangle$ is the average number of initial state scatterings. Observe that recent Drell Yan data imply that the momentum transferred in each initial state scattering, κ, roughly is on the order of soft scales, ~ 200 MeV [18]. In the Collins-Soper-Sterman formalism, the effect of soft scales is parametrized by the nonperturbative form factor $S_{\rm np}$. In describing hA interactions, Gavin *et al.* introduce a form factor $S_{\rm np}(n)$ that depends on the number of scatterings and reproduces the random walk formula. The hA cross section is then:

$$\left(\frac{d\sigma}{dp_{\rm T}}\right)_{pA} = \sum_n \int d^2b dz \rho(b,z) P_n^i(b,z) \left(\frac{d\sigma}{dp_{\rm T}}\right)(n), \tag{83}$$

where P_n^i is the Glauber probability for a NN collision prior to the hard Drell Yan process, and $(d\sigma/dp_{\rm T})(n)$ is the same as in pp collisions but with $S_{\rm np}$ replaced by $S_{\rm np}(n)$. This approach is formally similar to ref. [7], except that, here, initial state scattering is taken to contribute to the soft part of S, while in [7] it contributes to the resummed part. In addition, experimental knowledge of Drell Yan in pA collisions has improved considerably since [7]. First results will be reported to the hard probes collaboration at the next meeting at INT/Seattle this spring.

References

[1] S. Gavin, R. Kauffman, P.V. Ruuskanen, D.K. Srivastava, and R.L. Thews, Int. J. Mod. Phys. **A10**, 2961 (1995).

[2] Volume of Int. J. Mod. Phys. **A10** (1995) starting pg. 2881; see also similar work in David Fein, Zheng Huang, Peter Valerio and Ina Sarcevic, Phys. Rev. **C56** 1637 (1997).

[3] S. Gavin and M. Gyulassy, Phys. Lett. **214B**, 241 (1988).

[4] Zheng Huang, Hung Jung Lu and Ina Sarcevic. AZPH-TH-97-07, hep-ph/9705250 (1997).

[5] S. Gavin and J. Milana, Phys. Rev. Lett. **68** (1992) 1834.

[6] S. Gavin and R. Vogt, Phys. Rev. Lett. **78**, 1006 (1997).

[7] P. Chiappetta and H.J. Pirner, Nucl. Phys. **B291**, 765, (1987).

[8] K. Kajantie and R. Raitio, Nucl. Phys. **B139**, 72 (1978); R. K. Ellis, G. Martinelli and R. Petronzio, Phys. Lett. **104B**, 45 (1981); R. K. Ellis, G. Martinelli and R. Petronzio, Nucl. Phys. **B211**, 106 (1983).

[9] P. Arnold and M. H. Reno, Nucl. Phys. **B319**; 37 (1989); [Erratum **B330**, 284 (1990)]; P. Arnold, R. K. Ellis and M. H. Reno, Phys. Rev. **D40**, 912 (1989); R. Gonsalves, J. Pawlovski, and C.-F. Wai, Phys. Rev. **D40**, 2245 (1989).

[10] Yu. L. Dokshitser, D. I. Dyakonov and S. I. Troyan, Phys. Reports **58**, 269 (1980).

[11] J.C. Collins, D.E. Soper, Nucl. Phys. **B193**, 381 (1981); B197 (1982) 446; [Erratum **B213**, 545 (1983)].

[12] J. Collins, D. Soper and G. Sterman, Nucl. Phys. **B250**, 199 (1985).

[13] G. Altarelli, G. Parisi and R. Petronzio, Phys. Lett. **76B**, 351 (1978).

[14] G. Altarelli, R.K. Ellis, M. Greco and G. Martinelli, Nucl. Phys. **B246**, 12 (1984).

[15] C. Davies and W. J. Stirling, Nucl. Phys. **B244**, 337 (1984); C. Davies, B. Webber and W. J. Stirling, Nucl. Phys. **B256**, 413 (1985).

[16] P. Arnold and R. Kauffman, Nucl. Phys. **B349**, 381 (1991).

[17] G. A. Ladinsky and C. P. Yuan, Phys. Rev. **D50**, R4239 (1994); C. Balazs and C.-P. Yuan, Phys. Rev. **D56**, 5558 (1997).

[18] S. Gavin and R. Vogt, CU-TP-791, hep-ph/9609470.

PHENIX Experiment at RHIC

(*Sean Gavin*)

I have been a member of the PHENIX experimental collaboration at RHIC. As such I have had two roles, as a theoretical consultant and as leader of the THINC collaboration.

My role as theoretical consultant has been to provide PHENIX with calculations and other theoretical guidance to help in the design of the experiment. I have had major impact in the three major areas where my expertise overlaps with PHENIX capability, J/ψ, open charm and disoriented chiral condensate. My interest in PHENIX was sparked by my desire to ensure that J/ψ suppression is measured at RHIC. At that time – Fall of 1991 – SPS J/ψ results appeared ambiguous and interest in measuring J/ψ was low. Discussion with PHENIX members made it clear to me that a J/ψ measurement adequate to test theory would require the addition of a muon spectrometer to their baseline electron and photon capability. Through seminars, calculations and lobbying with PHENIX members, I helped to promote the muon spectrometer to an important part of the baseline. Since then, the controversy and excitement over the recent SPS Pb results has stimulated a new interest in J/ψ measurements.

Contact with PHENIX members has stimulated my interest in open charm [2], disoriented chiral condensates [3] and, most recently, superevents. Much of this work has been discussed elsewhere in this proposal. Calculations provided in [2] helped in testing whether muon-electron coincidence measurements could be used by PHENIX to distinguish between charm and Drell Yan contributions to the dilepton continuum. Estimates in [3], together with a DCC event generator that I constructed have helped in learning whether PHENIX can be run at low magnetic field to increase its acceptance for low transverse momentum charged pions.

As leader of the THeory INterface Committee, THINC, I have worked to bring theory work other than my own to the attention of PHENIX collaborators and to promote interest in PHENIX among outside theorists. I organized a number of theory workshops over the years as part of PHENIX collaboration meetings. I also provided a webpage with detailed references on topics of interest in PHENIX.

References

[1] S. Aronson *et al.*, Nucl. Phys. **A566**, 383c (1994).

[2] S. Gavin, P.L. McGaughey, P.V. Ruuskanen and R. Vogt, Phys. Rev. **C54**, 2606 (1996).

[3] S. Gavin, Nucl. Phys. **A590**, 163c, (1995).

Budget Explanation

In this renewal we request one month summer support for Professor Sarcevic and funding for the Senior Research Scientist, Dr. Gavin and one graduate student (half-time support, i.e. 0.25 FTE).

Our budget requests $\$1,500$ for travel for Dr. Gavin and \$500 for Prof. Sarcevic.

The computer maintenance item covers the cost of maintenance contracts on our workstations and membership in the Campus Site License Group (CSLG) which allows us to use nearly all the Sun and DEC software. Costs for these contracts are negotiated by the university on a yearly basis and billed in July, so these estimates for 1998 expenses are based on the costs in 1997.

The publications item covers costs of publications in refereed journals that require publication charges. The budget line for materials and supplies includes telephone charges, duplicating charges, and office supplies. It also covers computer repair expenses not included in the maintenance contracts, such as repair of printers and terminals and possible repairs to equipment obtained from the SSC labs.